UNCLASSIFIED

AD 416786

DEFENSE DOCUMENTATION CENTER

FOR

SCIENTIFIC AND TECHNICAL INFORMATION

CAMERON STATION, ALEXANDRIA, VIRGINIA

UNCLASSIFIED

DISCLAIMER NOTICE

THIS DOCUMENT IS BEST QUALITY PRACTICABLE. THE COPY FURNISHED TO DTIC CONTAINED A SIGNIFICANT NUMBER OF PAGES WHICH DO NOT REPRODUCE LEGIBLY.

NOTICE: When government or other drawings, specifications or other data are used for any purpose other than in connection with a definitely related government procurement operation, the U. S. Government thereby incurs no responsibility, nor any obligation whatsoever; and the fact that the Government may have formulated, furnished, or in any way supplied the said drawings, specifications, or other data is not to be regarded by implication or otherwise as in any manner licensing the holder or any other person or corporation, or conveying any rights or permission to manufacture, use or sell any patented invention that may in any way be related thereto.

BENDIX-PACIFIC DIVISION • THE BENDIX CORPORATION

416786

CATALOGED BY DDC
AS AD No. 416786

Breadboard Feasibility Study Of The

416786 DERRINGER WEAPON GUIDANCE SYSTEM

DDC
SEP 18 1963
TISIA B

Final Report Under Contract DA-04-495-ORD-3554

23 May 1963 Report 91-109-2

BREADBOARD FEASIBILITY STUDY OF THE DERRINGER WEAPON GUIDANCE SYSTEM

FINAL REPORT

CONTRACT DA-04-495-ORD-3554

Prepared for

BALLISTIC RESEARCH LABORATORIES
ABERDEEN PROVING GROUND
ABERDEEN, MARYLAND

THE BENDIX CORPORATION
Bendix-Pacific Division
North Hollywood, California

ABSTRACT

The content of this report covers tests designed to determine the feasibility of the beam rider technique for a high speed missile utilizing controlled propagation techniques. At a frequency of 13.5 gc the use of circularly polarized r.f. energy did not eliminate the multipath reflection in the region of the grazing angles examined. (Four degrees or less.)

The use of a narrow beam missile antenna provided angular discrimination which was found to be more significant in the reduction of the multipath interference than the polarization factor. The application of these techniques to high speed missile guidance is discussed in the Analytical Section of this report.

PREFACE

In late summer of 1961, Bendix sponsored tests were performed to determine boresight shift utilizing circular polarization in Ku band (16.5 kmc) microwave transmissions at low grazing angles. These tests were performed specifically to determine the feasibility of utilizing the referenced microwave transmissions applied to the guidance of a small, high velocity missile identified in this report as the "Derringer."

The results of these tests were encouraging in that scatter was within a 0.5 milliradian centered on optical boresight in the elevation plane. These tests were reported in Bendix-Pacific Division Report ENL-556-1, dated 1 September 1961. The results of this series of tests applied to Derringer evolved the Bendix-Pacific Division Proposal 9-813R "Proposed Breadboard Feasibility Study of the Derringer Weapon Guidance Concept." This proposal resulted in the study now being reported.

TABLE OF CONTENTS

LIST OF ILLUSTRATIONS

LIST OF ILLUSTRATIONS (Cont'd.)

LIST OF ILLUSTRATIONS (Cont'd.)

Section 1

INTRODUCTION

This report covers tests designed to examine the feasibility of the r.f. beam rider technique employing controlled polarization of the propagated energy.

When an r.f. system is operated in a manner which allows the illumination of the ground between the propagating source and the target, reflected signals are present which cause angular pointing errors. The magnitude and direction of these errors is dependent on the magnitude and phase of the reflected signal relative to the normal free space operating signal. The rate of occurrence of these errors is a function of propagation frequency, rate of change of path length as related to that frequency, and the velocity with which the receiving system travels along the nominal beam path (Figure 1).

The data covers wide beam tests intended to provide multipath discrimination by utilizing the concept of reversal of the circularly polarized wave upon reflection, and also narrow beam tests intended to discriminate the multipath energy by utilizing controlled beam patterns.

Section 2

PROGRAM SCOPE

2.1 TEST OBJECTIVE

The purpose of the Derringer Study program was to determine the characteristics of circularly polarized radio frequencies below the Brewster angle and to resolve the basic guidance parameters necessary for proper application of the Derringer guidance system. The frequency used was Ku band (approximately 13.5 gc). The program was conducted in a flexible manner enabling the contractor to delete, add or substitute as indicated by the results obtained and mutually agreed upon by the contractor and Project Office within the financial scope of the contract. The tests were conducted within the scope of the work statement established for Army Contract DA-04-495-ORD-3554.

2.2 TEST CONDITIONS

To conduct the tests under reasonable control of the reflective surface, three specific conditions were selected. These were:

1. Smooth earth
2. Canyon wall (deleted)
3. Smooth grass (deleted)

The sites selected consistent with these requirements were the Bendix Sylmar antenna range (Figure 2) and the Bendix-Pacific engineering antenna range. The range area at Sylmar was graded and compacted to establish the smooth earth condition.

2.3 EQUIPMENT SETUP AND CALIBRATION

The following procedures were evolved and implemented to qualify the range for use:

1. Calibrate Receiving and Transmitting Systems

   Signal strength versus frequency
   Signal strength versus deflection
   Modulation level versus deflection

2. Between Test Point No. 1 and Test Point No. 3

   Plot boresight shift versus frequency
   Plot boresight shift versus temperature (ambient)

3. Plot Test Point No. 2 Drift and Control Characteristics

   Time of day versus temperature, versus frequency
   Plot E1 versus frequency (E1 = Beam Voltage)

4. Plot Test Point No. 3 Drift and Control Characteristics

   Time of day versus temperature, versus frequency

2.4 BORESIGHT TESTS, CONDITION NO. 1 - SMOOTH EARTH (dry compacted earth)

1. With the nutating receiver at the upper Test Point No. 1 station, and the polarizer adjusted to within one db axial ratio, the boresight error versus target height was plotted. The target height was varied to the full range of Test Point No. 2 tower.
2. With the nutating receiver at the upper Test Point No. 1 station, and the receiver polarizer adjusted to three db axial ratio with the major axis of the polarization ellipse oriented vertically, boresight error versus target height was plotted. The points of maximum deviation over the full range of the Test Point No. 2 tower elevations were noted.
3. With the nutating receiver at the upper Test Point No. 1 station, and the receiver polarizer adjusted to six db axial ratio with the major axis of the polarization ellipse oriented vertically, boresight error versus target height was plotted. The points of maximum deviation over the full range of the Test Point No. 2 tower elevations were noted.
4. With the nutating receiver at the upper Test Point No. 1 station, and the receiver polarizer adjusted to 12 db axial ratio with the major axis of the polarization ellipse oriented vertically, boresight error versus target height

was plotted. The points of maximum deviation over the full range of the Test Point No. 2 tower elevations were noted.

5. With the nutating receiver at the upper Test Point No. 1 station, and the receiver polarizer adjusted to 12 db ellipticity horizontal, boresight error versus target height was plotted. The points of maximum deviation over the full range of the Test Point No. 2 tower elevations were noted.
6. With the nutating receiver at the lower Test Point No. 1 station (concrete platform at the base of the tower) and the receiver polarizer adjusted to one db axial ratio with the major axis of the polarization ellipse oriented vertically, boresight error versus target height was plotted. The points of maximum deviation over the full range of the Test Point No. 2 tower elevations were noted.
7. With the nutating receiver at the lower Test Point No. 1 station (concrete platform at the base of the tower) and the receiver polarizer adjusted to 12 db axial ratio with the major axis of the polarization ellipse oriented vertically, boresight error versus target height was plotted. The points of maximum deviation over the full range of the Test Point No. 2 tower elevations were noted.
8. With the nutating receiver at the lower Test Point No. 1 station (concrete platform at the base of the tower) and the receiver polarizer adjusted to 12 db ellipticity horizontal, boresight error versus target height was plotted. The points of maximum deviation over the full range of the Test Point No. 2 tower elevations were noted.

A calibration run against Test Point No. 3 before and after each test was conducted until equipment performance was firmly established.

2.5 SYSTEM TEST BREADBOARD MODELS

All breadboard models were constructed for use at the field test site on either Test Point No. 1, Test Point No. 2, or Test Point No. 3.

1. Test Point No. 1

The breadboard for Test Point No. 1 consisted of an antenna assembly and a stand with an indexing head. The antenna assembly contained a parabolic reflector, nutation motor, polarizer, and transition, an offset feed, and their associated mounting brackets.

The indexing head was mounted on a steel stand constructed at Bendix. Affixed to the indexing head were a pair of aluminum channels to which the antenna assembly and the optical sight (Figures 3 and 4) were attached.

2. Test Point No. 2

The breadboard for Test Point No. 2 consisted of an antenna assembly and an r.f. power source. The cooling system for the r.f. was mounted on an existing 20 foot tower (Figures 5 and 6).

The antenna assembly contained a circular horn, polarizer, transition, and engineering test equipment (directional couplers and detector mount).

The r.f. power source was modified to include a Klystron cooling system.

The 20 foot tower was furnished by the microwave laboratory and several mounting plates were fabricated to hold the antenna assembly, cooling system, and optical sight.

3. Test Point No. 3

The breadboard for Test Point No. 3 consisted of an antenna assembly, an r.f. source, cooling fan, and associated mounting fixtures (Figure 7).

The antenna assembly contained a parabolic reflector, polarizer, transition, and a feed (constructed by the engineering model shop). The r.f. power source and cooling fan were furnished by the microwave laboratory and the mounting fixtures were constructed in the Bendix model shop.

Section 3

TEST FACILITIES

A total of three antenna pattern measurement ranges were chosen for the purpose of conducting the tests.

The microwave laboratory range located on the roof of Bendix Pacific Division's Plant 3 in North Hollywood, California (Figure 8) was used for initial breadboard calibration.

To comply with condition 1, smooth earth, and condition 3, smooth grass, the open area on the Bendix-Pacific Division Electronic Center property in Sylmar, California (Figure 9) was modified:

1. A 1,250 foot long area which required the least amount of grading and fill to produce a reasonably smooth flat plane surface was selected.
2. An elevation study was made and sites selected (Figure 10).
3. A 52 foot tower was constructed for Test Point No. 1, a portable 20 foot adjustable tower was located on Test Point No. 2, and a 15 foot fixed tower was located at Test Point No. 3 (Figure 11).
4. The area between Test Point No. 1 (Figure 12) and Test Point No. 2 (Figure 13) was graded and compacted to represent a flat plane (Figure 14). The ground level difference between test points was established as 55 feet.

3.1 EQUIPMENT FURNISHED

The equipment used, other than items specifically constructed for the tests, were:

1.	Cross Guide Coupler	Demoronay Bonardi DBF 234
2.	Directional Coupler	PRD 405

3.	Detector Mounts (2)	FxR Y205B
4.	Transition (CP)	Demoronay Bonardi DBF 030
5.	Polarizer	Demoronay Bonardi DBF 930
6.	Klystron	Varian X 12
7.	Klystron	Varian VA-504B
8.	Model Tower	Scientific Atlantic SA 411
9.	Broad Band Receiver	Scientific Atlantic SA 402
10.	Recorder	Scientific Atlantic SA 121B
11.	Signal Monitor	Scientific Atlantic SM 1
12.	Precision Attenuator	Hewlett Packard P 382A
13.	4 Ku Aupply	4K-100B
14.	Field Klystron Supply	Microline 555
15.	Lab Klystron Supply	Cubic 701
16.	SWR Amplifier	Hewlett Packard 415B
17.	Wave Analyzer	Hewlett Packard 300A
18.	Scope	
19.	Scope Pre-Amplifier	
20.	Bendix Crystal Amplifier	Bendix Microwave Lab Equipment
21.	Bendix Control Panel	Bendix Microwave Lab Equipment
22.	(Decade) DC Amplifier	Ballentine 220
23.	400 Cycle 3 Phase Supply	
24.	Signal Generator	Hewlett Packard 687A
25.	Slotted Section	Hewlett Packard P810B
26.	Frequency Meter	Hewlett Packard P530A
27.	Nutation Motor	Bendix Microwave Lab Equipment

All of the above equipment listed and furnished as capital equipment was calibrated by the Bendix Calibration Laboratory using reference standards qualified by the U. S. Bureau of Standards, Pomona, California.

3.2 LABORATORY CALIBRATION OF BREADBOARDS

The Bendix-Pacific Division's Plant 3 roof range of the microwave laboratory was used to qualify the breadboard system devised to conduct the necessary field tests.

Figures 15 through 31 present in block diagram form the assemblage of equipments used to conduct the qualifying tests and to obtain the test patterns and curves from these tests.

Section 4

TEST PROGRAM

4.1 LABORATORY CALIBRATION OF EQUIPMENT

1. Test Point No. 1 Equipment (Receiver)

a. The E & H plane profile patterns were plotted with the optimized feed f_o and $f_o \pm 50$ mc with both linear and CP illumination 0 degree -180 degree and 90 degree -270 degree positions.

b. The cp at the nutation axis was optimized.

c. The system was excited with CP using Test Point No. 3 dish and a plot of modulation signal versus look angle with the feed nutating was made.

d. The boresight versus frequency $f_o \pm 50$ mc was plotted.

e. The cp phase shifter was set for optimum ellipticity, 3, 6, and 12 db at the null axis and a plot for each setting of db versus look angle and modulation versus look angle and ellipticity versus look angle was made.

f. The pattern and modulation versus look angle with one of the antennas reverse circularly polarized was plotted.

g. The VSWR versus frequency $f_o \pm 250$ mc was plotted.

h. The absolute antenna gain was calibrated.

2. Test Point No. 2 Equipment (High Power Transmitter)

a. The antenna pattern in E & H plane profiles with linear polarization was plotted.

b. The cp at the peak of the main lobe was optimized.

c. The system was excited with CP and plot plane profiles in two planes at f_o and $f_o \pm 50$ mc were made.

d. The VSWR versus frequency over the range of $f_o \pm 250$ mc was plotted.

e. The ellipticity versus look angle at f_o and $f_o \pm 50$ mc at peak of beam and at ± 5 degrees, ± 10 degrees, and ± 15 degrees in two planes was plotted mechanically.

f. The Test Point No. 3 antenna was used as a source for No. 3 and No. 5.

g. The absolute antenna gain was calibrated.

3. Test Point No. 3 Equipment (Calibration Transmitter)

a. The antenna pattern in E & H plane profiles was plotted.

b. The VSWR versus frequency $f_o \pm 250$ mc was plotted.

c. The antenna patterns at f_o +50 mc and f_o -50 mc with cp illumination were plotted.

d. The absolute antenna gain was calibrated.

4.2 SYLMAR TEST SITE INSTALLATIONS

The field test site installations underwent six basic variations during different height and power level tests.

1. Test Point No. 3 was a fixed installation comprised of a circularly polarized 4 degree antenna assembly and a low power klystron. The klystron (Test Point No. 3) was controlled remotely from Test Point No. 1 (Figure 32).
2. Test Point No. 3 was used as a reference calibration point to show the variations which occurred at Test Point No. 1 and Test Point No. 2 for the high level, high power; high level, low power; low level, high power; low level, low power; low level, low power displaced; and intermediate level, low power runs.

a. High Level, High Power Installation: The circularly polarized 4 degree nutating antenna assembly and the boresight null detecting equipment were located on the 52 foot tower (Test Point No. 1). The high power klystron and the calibrated circularly polarized 20 degree antenna assembly were located on the 20 foot adjustable tower (Test Point No. 2) (Figure 32).

b. High Level, Low Power Installation: The circularly polarized 4 degree nutating antenna assembly and the low power klystron were located on the 52 foot tower (Test Point No. 1). The calibrated circularly polarized 4 degree antenna assembly and the boresight null detection equipment were located on the 20 foot adjustable tower (Test Point No. 2) (Figure 33).

c. Low Level, High Power Installation: The circularly polarized 4 degree nutating antenna assembly and boresight null detecting equipment were located on the ground level cement pad (Test Point No. 1). The high power klystron and the calibrated circularly polarized 20 degree antenna assembly were located on the 20 foot adjustable tower (Test Point No. 2) (Figure 34).

d. Low Level, Low Power Installation: The circularly polarized 4 degree nutating antenna assembly and the low power klystron were located on the ground level cement pad (Test Point No. 1). The calibrated circularly polarized 4 degree antenna assembly and the boresight null detection equipment were located on the 20 foot adjustable tower (Test Point No. 2) (Figure 35).

e. Low Level, Low Power Displaced Installation: The circularly polarized 4 degree nutating antenna assembly and the low power klystron were located on the ground level displaced down range 130 feet (Test Point No. 1). The calibrated circularly polarized 4 degree antenna assembly and the boresight null detection equipment were located on the 20 foot adjustable tower (Test Point No. 2) (Figure 36).

f. Intermediate Level, Low Power Installation: The circularly polarized 4 degree nutating antenna assembly and the boresight null detection equipment were located on a scaffold 10 feet above the ground level cement pad (Test Point No. 1). The calibrated circularly polarized 4 degree antenna assembly and the low power klystron were located on the 20 foot adjustable tower (Test Point No. 2) (Figure 37).

4.3 OPERATIONS

The test program conducted on the Derringer guidance study was divided into two phases. Phase I was initially directed to investigate the following areas:

1. Circular polarization rejection at grazing angles below Brewster's angle.
2. The effects of reflected ellipticity upon this circular polarization rejection.
3. Meteorological effects in terms of boresight instability.
4. Propagation characteristics through canyon or trough terrain.
5. A comparison of smooth grass terrain to a graded specular earth surface.

Field tests were commenced in October 1962. Test results indicated that no circular polarization sense reversal was occurring for grazing angles below the pseudo-Brewster's angle. The ground reflected wave was not rejected at the receiving antenna.

Testing was continued and data records were obtained for vertical, horizontal and circular polarization boresight error as a function of grazing angle. This test data was very consistent and displayed the periodic error maxima and minima associated with conically-scanned wave propagation experiencing ground interference. A qualitative treatment of error magnitude and spacing has been discussed by Kerr[1]. An analysis of the data indicates horizontal polarization suffers the greatest error excursions. Except for other important system considerations, circular and vertical reflection characteristics are essentially comparable when reflected at angles sufficiently below the pseudo-Brewster's angle by a smooth surface.

Test Site characteristics were investigated to determine the effects of cross-range wires. An interfering obstacle (car) was also positioned about the range. The wires had no effect on boresight, when swung through a one foot displacement. Only the center three-fifths of the range width appeared sensitive to the presence of the automobile. These measurements were made using 4 degree beamwidth transmitting and receiving antennas.

No indication was obtained of data shift due to meteorological changes. Neither nonstandard refraction or varying ground reflection properties were noted. To a certain extent, the relatively short microwave transmission path precluded such observations.

As a result of the test findings, a conference was held at BRL in November, 1962 and it was decided to reorient the original test program. The guidelines and data requests established for Phase II were:

1. Discontinue canyon and grass terrain tests.
2. Verify boresight stability with time.
3. Check reversal of circular polarization upon reflection.
4. Determine the shift in boresight for improved antenna side-lobe characteristics.
5. Investigate boresight distortion due to low level sighting in terms of boresight shift.
6. Recheck existing data as necessary.

Electrical boresight stability was checked consistently throughout the test program. Repeatable results were obtained for measurements above and below the pseudo-Brewster's angle, even after extensive field testing.

Comparative measurements between a metal reflecting surface and a fibreglass roof covering verified that no reversal occurred at grazing angles below the pseudo-Brewster's angle for a poor conducting medium.

Phase I Tests: The initial series of tests were performed at the Sylmar Test Site, described in Part 3. Boresight error as a function of grazing angle was recorded for vertical, horizontal, and circular polarization. In each case, interference patterns were noted.

Interpretation of these data should be based on an assessment of the useability of the information for guidance purposes. This requires that the maximum and minimum boresight errors give way to the consideration of the bias that will be residual after suitable processing techniques are employed.

4.4 TEST DATA SUMMARY

1. Upper Test Site (Test Point No. 1) - 20 Degree System

   Pitch Error - Figures 38, 39, 40

   The same position of maximum and minimum occurred for horizontal polarization, vertical polarization, and circular polarization as a function of grazing angle. The residual bias which would result from signal processing appears to be similar in all polarizations.

2. Lower Test Site (Test Point No. 1) - 20 Degree System

   Pitch Error - Figures 41, 42, 43

   Similar characteristics to A were observed. The period of maximum and minimum excursion was increased at these lower grazing angles, compatible with Kerr's observations[1].

3. Lower Test Site (Test Point No. 1) - 4 Degree System

   Pitch Error - Figures 44, 45, 46

   The lower test site exhibited the same position of maxima and minima for horizontal polarization, vertical polarization, and circular polarization. Peak excursions were comparable to the 20 degree system. A similarity of bias again appears to be common in all polarizations.

4. Upper Test Site (Test Point No. 1) - 4 Degree System

   Pitch Error - Figures 47, 48, 49

   The position of maximum and minimum of the circular polarization error corresponds to that of the 20 degree system A. Vertical polarization, horizontal

polarization, and circular polarization error excursions are in order of magnitude smaller than the 20 degree system. The vertical polarization and circular polarization errors coincide in position of maximum and minimum.

The horizontal polarization errors occur at the same position as the circular polarization errors but have a cyclical in-and-out of phase relationship. The circular polarization errors appear to have a somewhat reduced inherent residual bias as compared to either the horizontal or vertical case.

5. Yaw Error for Lower 20 Degree System

Figures 56, 57, 58

Too random to plot trend.

6. Yaw Error for Lower 4 Degree System

Figures 59, 60, 61

The horizontal and circular polarization cases indicate that their bias under suitable signal processing would be somewhat lower than that experienced in the vertical case. It is to be noted, however, that the major discontinuities are essentially the same in all cases.

4.5 PHASE II TESTS

In view of the interference effects noted during the Phase I tests, the program was reoriented. The test equipment was transferred from the Sylmar test site to the engineering antenna range. Confidence tests were performed to determine the effect of field testing on equipment calibration.

Axial ratios, measured by the rotating linear horn technique, were less than 1.5 db at zero degrees look angle. It is noted that this measurement technique always resulted in a higher axial ratio compared to the value obtained from the E and H primary

patterns; at zero degrees look angle. The variation in axial ratio for the Test Point No. 1 assembly was less than 1/2 db across a 200 mc bandwidth as shown in Figure 62. It was concluded that field testing did not degrade the antenna system performance.

Measurements of the sense of circularly polarized waves upon reflection were made using the limited geometry of the engineering test site. The equipment used is shown in Figure 63.

Grazing angles of approximately 9 degrees and 16 degrees were readily available using the standard equipment.

The roof reflecting surface is composed of a combination cement, fiberglass batting, and tar paper to a thickness of 1-5/16 inches over a metal decking. It is estimated that the surface has a relative dielectric constant of five and is a lossy medium.

Roof surface reflection measurements at a grazing angle of 16 degrees were not conclusive in determining circular polarization sense reversal. They did, however, indicate that horizontal polarization was substantially greater upon reflection than vertical polarization. It was concluded that the grazing angle was in the vicinity of the pseudo-Brewster's angle for this hybrid surface.

Reflection measurements at a grazing angle of approximately 9 degrees indicate that circular polarization does not reverse sense, when incident at grazing angles less than the pseudo-Brewster's angle. A sequence of measurements to support this statement are shown in Figures 64, 65, 66, and 67.

A comparison of the dielectric roof surface is made to a four foot by eight foot metal screen. The predictable sense reversal for all combinations is noted.

It is seen that incomplete circular polarization rejection occurs in Figure 67. This is due to the limited (4 foot by 8 foot) metal reflecting surface. The spill-over reflecting from the roof reduces the normal rejection. This effect is not evident in Figure 65, because the roof contribution is now in a reverse sense to the receiving antenna and is not accepted.

The boresight shift, as a function of side-lobe level and at a low height site was not independently measured. Figure 68 was recorded at the Sylmar test site. The height of the Test Point No. 1 assembly was increased by 10 feet and the side-lobes of Test Point No. 3 assembly were reduced by more than five db for this test as indicated in Figure 69. The same general characteristics; i. e., positive and negative boresight errors increasing in frequency as the grazing angle increases, are evident.

Data Review: The conclusions to be drawn from the abbreviated Phase II program are:

1. Circular Polarization incident below the pseudo-Brewster's angle does not reverse sense, when reflected from a non-conducting surface.
2. Field testing has been accomplished without degradation in equipment calibration.

Section 5

REVIEW OF TEST PROGRAM DATA

Field test data was obtained for horizontal polarization, vertical polarization, and circular polarization waves reflected at low grazing angles from the ground.

The test program has experimentally shown that circular polarization does not reverse sense for energy which is incident at the grazing examined angles (in the region of four degrees or less). This fact was also apparent in the field test results in the terms of the boresight error encountered.

The boresight error data indicates that horizontal polarization probably causes the largest error magnitudes. Circular and vertical polarization errors are quite comparable, with the vertical polarization perhaps having some advantage.

The general data trend indicates that in many cases these boresight error magnitudes can be substantially reduced by the proper application of signal processing techniques to the actual dynamic case. The suitability of these processed signals in providing guidance with a specific accuracy would require analysis beyond the intended scope of this particular program.

It is expected that, while the magnitude of error should decrease for irregular ground characteristics, the periodicity of the errors should be predictable for general types of terrain.

Some deviations in data have been noted in terms of yaw displacements. An ambiguity in phase relations between vertical and horizontal polarization upon reflection has been observed with the 4 degree system. Further analysis must be carried out to explain these characteristics.

Boresight stability with time has been very good. Data has been consistently repeatable. Equipment calibration has been maintained throughout the field test series.

No meteorological effects have been observed. The short microwave transmission path and constant weather conditions may account for little change due to these effects.

Horizontal Polarization - ⌒
Vertical Polarization - —
Maximum - X
Minimum - O

BORESIGHT ERROR - MINIMUM AND MAXIMUM COINCIDENCE OF VERTICAL POLARIZATION AND HORIZONTAL POLARIZATION WITH CIRCULAR POLARIZATION YAW ERROR - UPPER 20 DEGREE SYSTEM

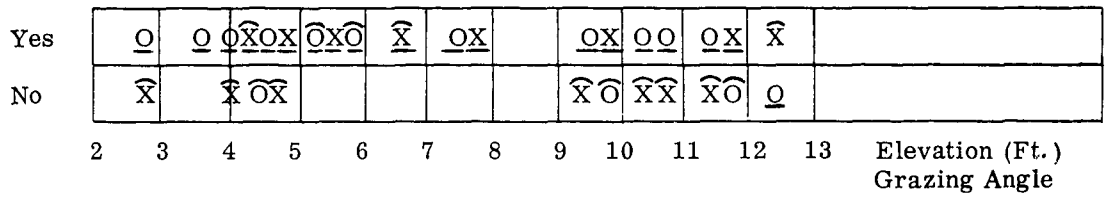

OBSERVATIONS:

1. Vertical polarization and circular polarization minimum-maximum position coincide.
2. Horizontal polarization data is too limited to predict trend (Figures 50, 51, 52).
3. Horizontal polarization has large excursions and zero median.
4. Circular polarization has a +8 milliradian offset.
5. Vertical polarization has a -. 6 milliradian offset with smallest excursions.

Horizontal Polarization - ⌒
Vertical Polarization - _
Maximum - X
Minimum - O

BORESIGHT ERROR - MINIMUM AND MAXIMUM COINCIDENCE OF VERTICAL POLARIZATION AND HORIZONTAL POLARIZATION WITH CIRCULAR POLARIZATION YAW ERROR - UPPER 4 DEGREE SYSTEM

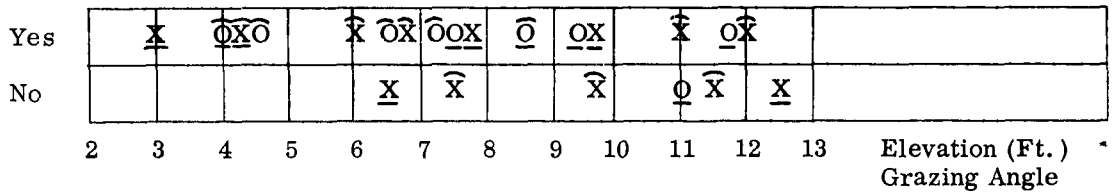

OBSERVATIONS:

1. Random characteristics between vertical polarization, horizontal polarization, and circular polarization maximum and minimum.
2. Position of maximum and minimum generally same. (Figures 53, 54, 55).
3. Circular polarization has negative offset of 1.3 milliradian above six feet - largest excursions.
4. Horizontal polarization has zero median.
5. Vertical polarization has -1/2 milliradian median below six feet.

Horizontal Polarization - ⌒
Vertical Polarization - —
Maximum - X
Minimum - O

BORESIGHT ERROR - MAXIMUM AND MINIMUM COINCIDENCE OF HORIZONTAL POLARIZATION AND VERTICAL POLARIZATION WITH CIRCULAR POLARIZATION PITCH ERROR - UPPER 4 DEGREE SYSTEM

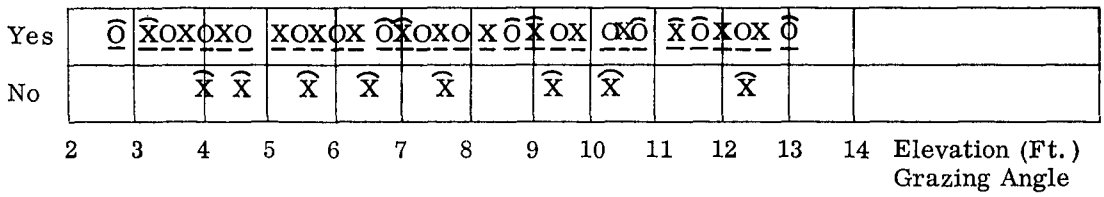

OBSERVATIONS:

1. Vertical polarization and circular polarization minimum and maximum coincide very well.

2. Horizontal polarization cyclically coincide with vertical polarization and circular polarization.

Horizontal Polarization - ⌒
Vertical Polarization - _
Peak - X
Minimum - O

BORESIGHT ERROR - MINIMUM AND MAXIMUM COINCIDENCE OF HORIZONTAL POLARIZATION AND VERTICAL POLARIZATION WITH CIRCULAR POLARIZATION PITCH ERROR - UPPER 20 DEGREE SYSTEM

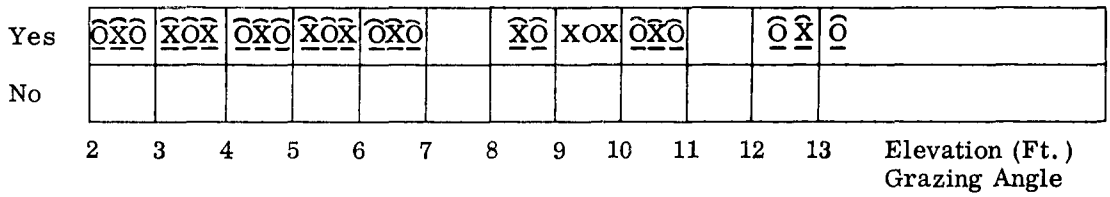

OBSERVATION:

1. Vertical polarization, horizontal polarization, and circular polarization maximum and minimum coincide very well.

It is recognized that circular polarization has one distinct system advantage. Cross polarization of linear antennas would occur without roll stabilization. The ensuing nulls in the direct transmission would present further guidance difficulties. It is conceivable that an improved system may be realized by the use of a hybrid (vertical polarization-circular polarization) antenna link; accepting a 3 db transmission loss. It is expected that a greater reduction in the reflected vertical polarization would occur under operating field conditions. A further reduction in error magnitude could be obtained from the enhanced scattering characteristic at higher frequencies. Error reduction may also be improved by applying beam shape discrimination techniques to the design of the missile antenna.

5.1 THE NATURE OF THE BORESIGHT DEVIATIONS

The periodic positive and negative boresight errors characterized by the vertical, horizontal, and circular polarization indicate interference between direct and ground reflected waves. The 20 degree system indicates a concurrence of maximum and minimum position as a function of grazing angle for the three polarizations. It is concluded from this data (equal geometry) that the reflected phase properties of the ground must be identical for both vertical and horizontal polarization.

Assuming the magnitude of the reflection coefficients also to be equal to unity, a direct substitution in the expressions for the linear components of circular polarization indicates that no sense reversal occurs. The above assumption is justified both experimentally and theoretically.

The rejection of circular polarization for normal incidence is compared to the transmission by reflection at angles less than Brewster's angle in Figure 70. Note the same boundary conditions are defined.

It is seen that direction of observation of circular polarization reflection determines its acceptance or rejection. It is understood that a right hand circular polarization antenna both receives and radiates right hand circular polarization.

A physical system that illustrates this same effect is shown in Figure 71.

In view of the above illustrations, it is difficult to analyze the 4 degree system. It appears that vertical polarization and horizontal polarization are not in phase with each other, except in a cyclical manner as a function of grazing angle. The substantial reduction in error magnitude is noted from Figure 47, 48, and 49. This observation only occurs at the upper test site. As this could be interpreted as a circular polarization rejection characteristic, a further analysis is necessary.

Similarly, yaw and pitch offsets have not been analyzed at this time.

5.2 APPLICATION ANALYSIS

Application considerations require that the dynamics of the error contributing function be examined as they might occur in a typical missile trajectory. The boresight errors measured during the test show a frequency variation as a function of the grazing angle. Since the grazing angle itself is a time varying function during missile flight (Figure 72), the boresight error will also be a time function. Figures 73 and 74 show the time variation of the grazing angles for several selected trajectories.

Further analysis of these trajectories, combined with a consideration of the zero crossings experienced in the test, will permit the establishment of a basic frequency range of the pitch-plane boresight error. It is to be anticipated that this frequency is also time variant and will be lowest at the impact end of the trajectory. Since the boresight error does not have a purely sinusoidal variation with grazing angle, the amplitude spectrum of this error would contain components over a range of frequencies with a maximum of components occurring at some average frequency which could be employed as an analytical tool.

The applicability of the information to a practical guidance problem involves, therefore, two successive steps. First, the range of frequency involved in the pitch-plane boresight error for the trajectory in question must be determined. Secondly, assuming that these frequencies do not extend into the region where missile control is involved, the residual bias with suitable signal processing should be determined.

The guidance loop for the Derringer system (Figure 75) without an autopilot contains two integrations, two sets of quadratic poles, and guidance loop shaping. The system response will be underdamped and slow, with quantitative values depending on whether an autopilot is used, missile velocity, nature of the guidance loop filter, etc. The guidance system will be virtually insensitive to 20 cps error inputs with a peak to peak value of four milliradians, providing no bias exists.

The variation in boresight error amplitude as a function of grazing angle is due to the lobing pattern of the field strength at the receiving antenna.[1] The width of the lobes in this pattern is a direct function of wavelength, and an inverse function of the height of the receiving antenna. An increase in the frequency of the transmitted wave will result in a corresponding increase in the frequency of the boresight error for a given trajectory. An increase in the frequency of the transmitted wave by a factor of three or more should enable the proposed Derringer guidance system to substantially overcome the effect of boresight error variations down to a grazing angle of 1.5 degrees at a launch range of 6,600 feet corresponding to a minimum average frequency of 21 cps, provided that the boresight error behaves as the test data indicates. The actual guidance error due to the boresight error will be a function of the bandwidth of the guidance system and of the amplitude-frequency distribution of the boresight error.

1. Multipath Effects for Rough Terrain

The normal operating environment for the Derringer on air-to-ground missions will rarely include terrain of the type over which the boresight error tests were conducted. Instead, the usual terrain is apt to be basically irregular, and to contain grass, trees, brush, etc.

The amplitude of the field strength of the reflected wave depends on ground contour, surface composition, frequency, polarization, and grazing angle. Unfortunately, no quantitative means of analytically assessing the effect of these factors is available, even for carefully selected terrain, except when a smooth, plane surface is present.

One of the widely used qualitative measures of the efficiency of specular reflection from irregular surfaces is that postulated by Lord Rayleigh.

The quantity of interest in this criterion is:

$$K = \frac{4\pi h}{\lambda} \sin \theta$$

h = difference between adjacent terrain levels

θ = grazing angle

K = phase difference between rays reflected from the two levels

If K is large, the effect of the roughness is pronounced, scattering occurs, and the effect of the reflected energy on the resultant field is substantially decreased. A grazing angle of 1.5 degrees (0.026 radian) requires that h/λ be approximately 5 in order that K be of a reasonably high value ($\pi/2$). For a λ of 2.25 cm, h would then be approximately 11.25 cm. A reduction of wave length to 0.75 cm would lower the requirement in level difference to 3.75 cm, or about 1.5 inches. It must be emphasized that no way to quantitatively compute the effect of this "roughness" is available. Furthermore, this concept excludes the diffraction that occurs due to the surface elements having dimensions comparable to the wave length.

Experiments[2] have indicated that if K is about 2.5, the magnitude of the reflection coefficient will be about half its smooth surface value; while a K of about 6.3 results in a reflection coefficient of magnitude about one-tenth the smooth surface value. Other experiments[3] indicate that for a K ranging between 0.7 and 4, the magnitude of the reflection coefficient is less than 1/5 the smooth surface value for vertical polarization at grazing angles of approximately 3-4 degrees.

In addition to the effects due to irregular terrain, values of the reflection coefficient can differ from test results due to time variations in the surface and to missile motion.

Time variations of the surface can be due to wind blowing over leaves, grass, and weeds, and to ripples or waves in the surface of water. Missile motion will be both transverse and parallel to the line of sight between launch aircraft and target.

These time variations will result in time variations of the magnitude and phase of the reflected wave. The net effect will probably be similar to increasing the irregularity of the surface.

One would expect the magnitude of the reflection coefficient (under most operating conditions) to take on statistical characteristics, possibly possessing a Gaussian probability density function with mean and variance depending on the general nature of the terrain and the instantaneous grazing angle.

For most applications, therefore, the boresight error due to reflection will appear to the guidance system as a source of noise, with its power (for a given interval in grazing angle) having perhaps a normal distribution with frequency, centered at the "average frequencies" measured during the Bendix field tests. Most of this noise should not seriously effect the guidance accuracy for the proposed system, particularly if the frequency of the transmitted wave is increased by a factor of three or more. However, the quantitative effects will not be known until thorough system analyses and/or flight tests are conducted.

The preceding discussion relates to trajectories over fairly open terrain, and does not consider the guidance problem when the target is in close proximity to buildings, canyon walls, etc.

Section 6

SYSTEM IMPROVEMENTS

The following changes appear desirable as a result of the Bendix field tests:

1. The receiving antenna beamwidth should be as narrow as system considerations allow. Such considerations include the capture problem and equipment design, construction, and packaging.
2. The operating frequency should be increased to the highest feasible value. Such a change should result in increasing the frequency of boresight error variations, and should also result in less specular reflections, thereby decreasing the boresight error due to reflected energy present at the missile antenna.
3. A vertically polarized transmitted wave should be used for the directed beam.

Section 7

CONCLUSIONS

1. The benefits from using circularly polarized r. f. energy are not realized when operating at very low grazing angles (below the Brewster angle).
2. Boresight deviations due to specular reflection are sinusoidal in nature with nominal value coinciding with, or closely approximating the propagation axis.
3. Inconsistancies in this sinusoidal boresight deviation result from terrain irregularities (roughness) and the geometry of the test range itself when making static simulations.
4. Application of the results of these investigations to the solution of the Army aircraft armament problem is feasible provided sufficient multipath discrimination and interference lobe smoothing is achieved.

REFERENCES

1. "Propagation of Short Radio Waves" by D. E. Kerr (book), McGraw-H 11, 1951

2. "Microwave Propagation Over Rough Surfaces" by M. P. Bachynski, RCA Review - June, 1959

3. "Reflection Coefficients of Irregular Terrain at 10 cm" by E. M. Sherwood and E. L. Gintson, Proceedings of the IRE - July, 1955

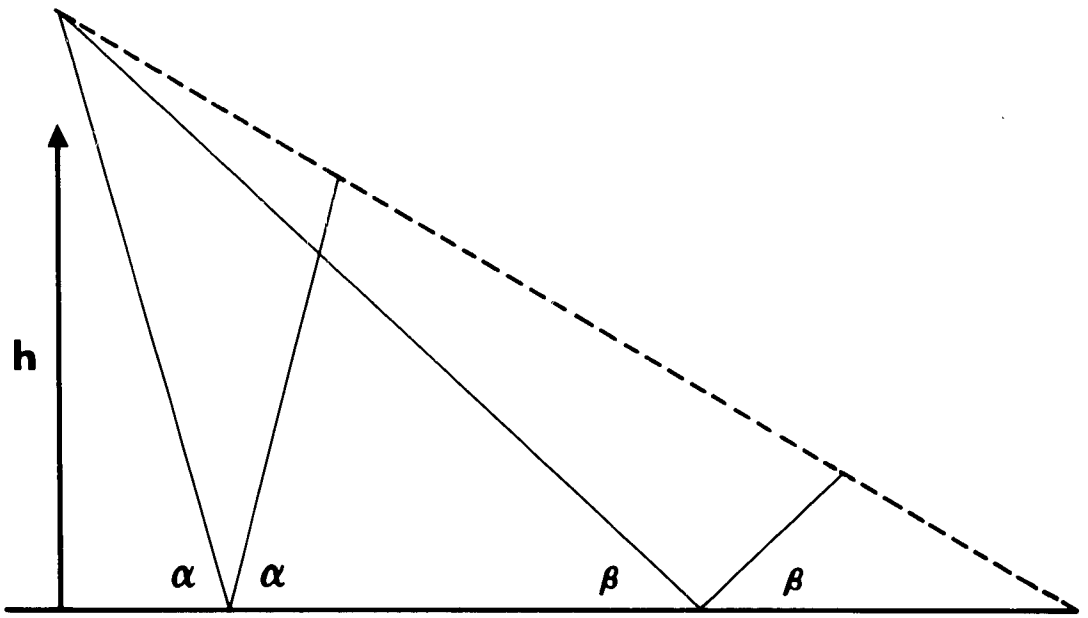

Figure 1. Multipath Considerations

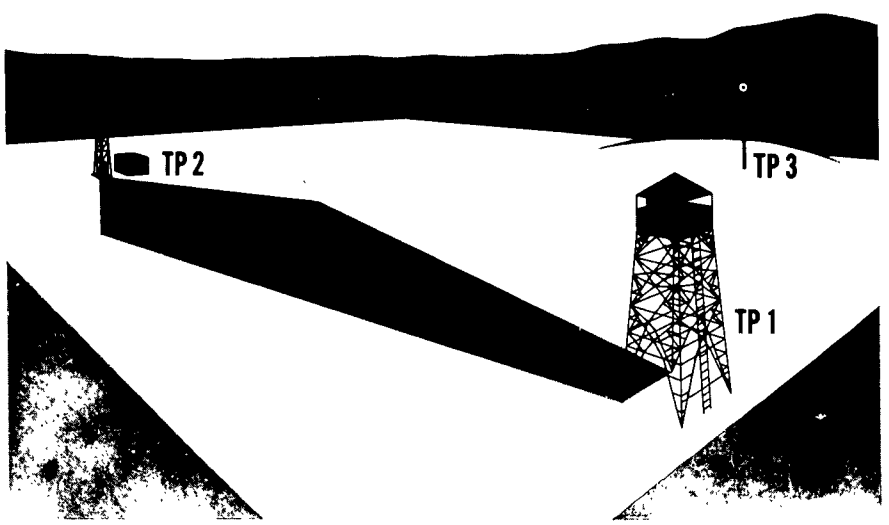

Figure 2. Derringer Test Site

Figure 3. The Beam Director System

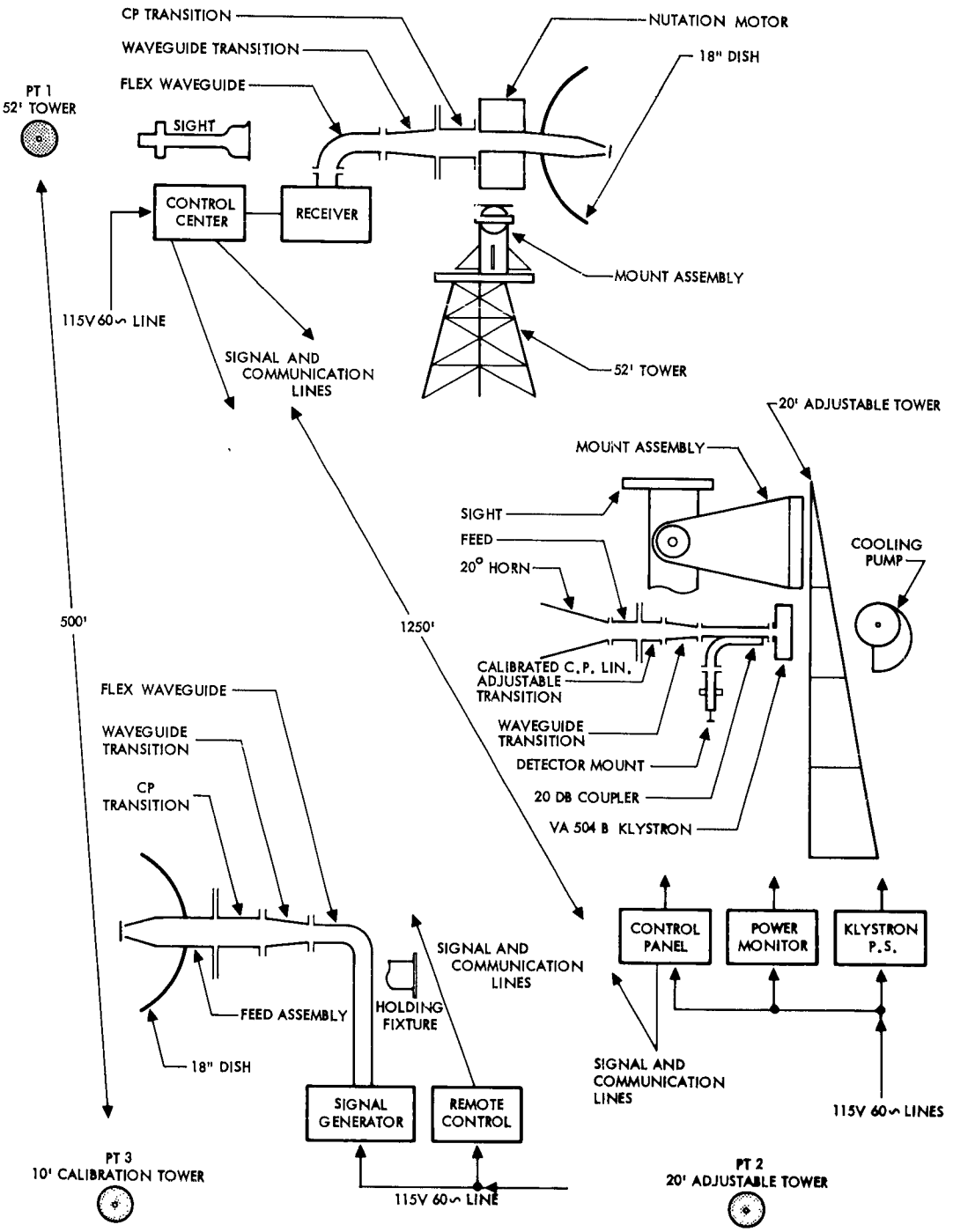

Figure 4. Antenna Pattern Measurement Test Installation Diagram

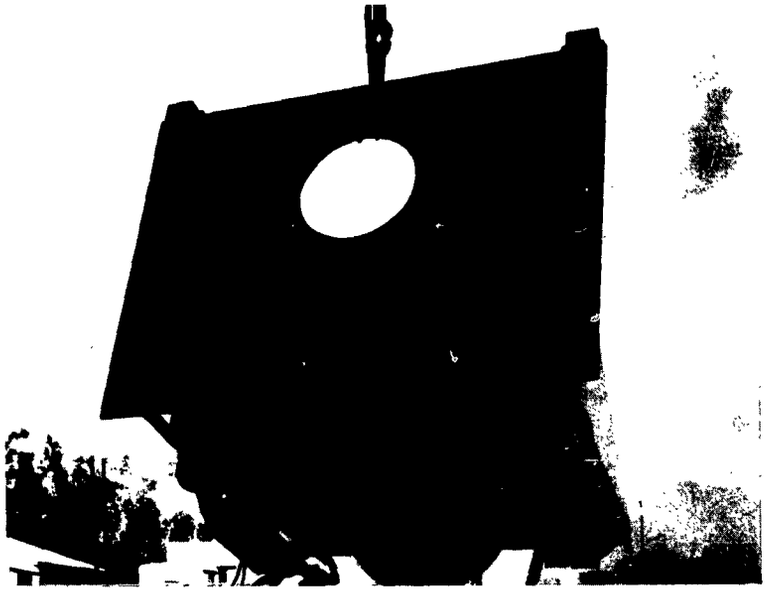

Figure 5. Test Point No. 2 Assembly (Front View)

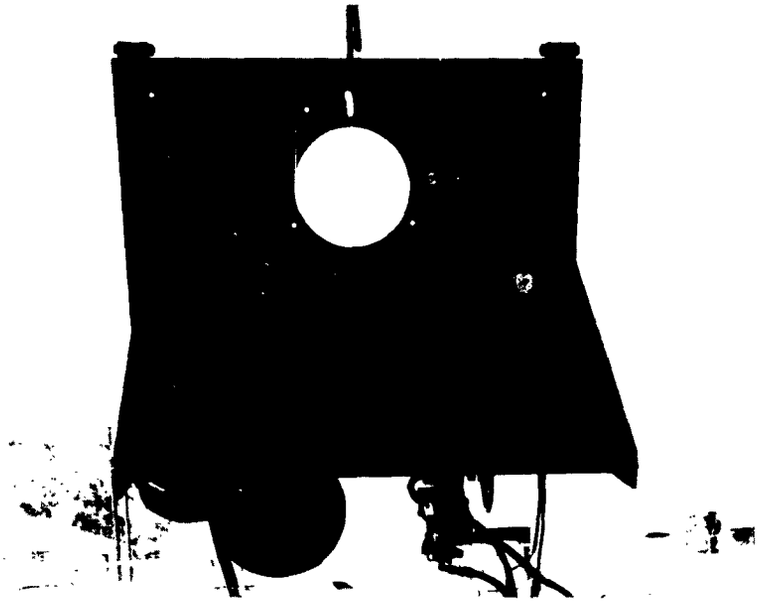

Figure 6. Test Point No. 2 Assembly (Rear View)

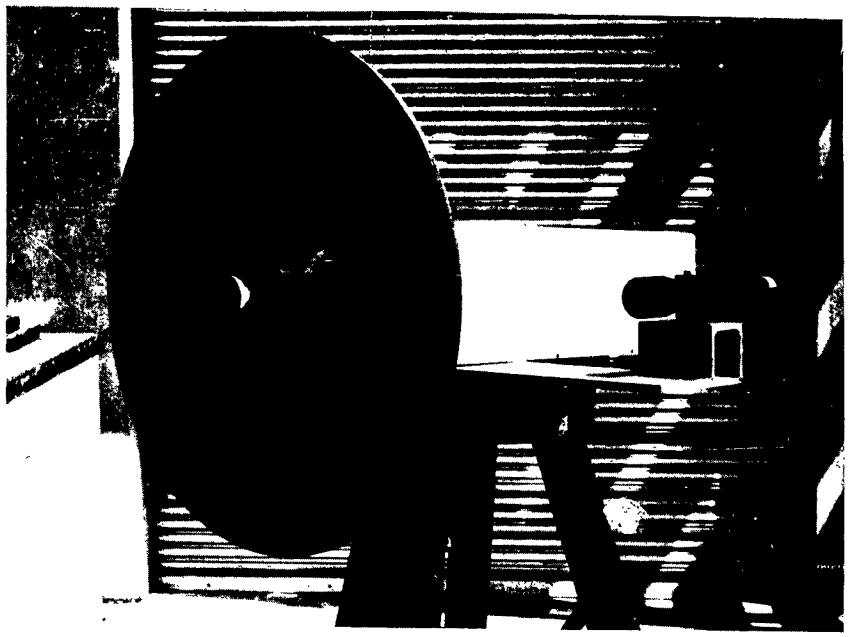

Figure 7. Test Point No. 3 Assembly

Figure 8. The Bendix-Pacific Engineering Test Range

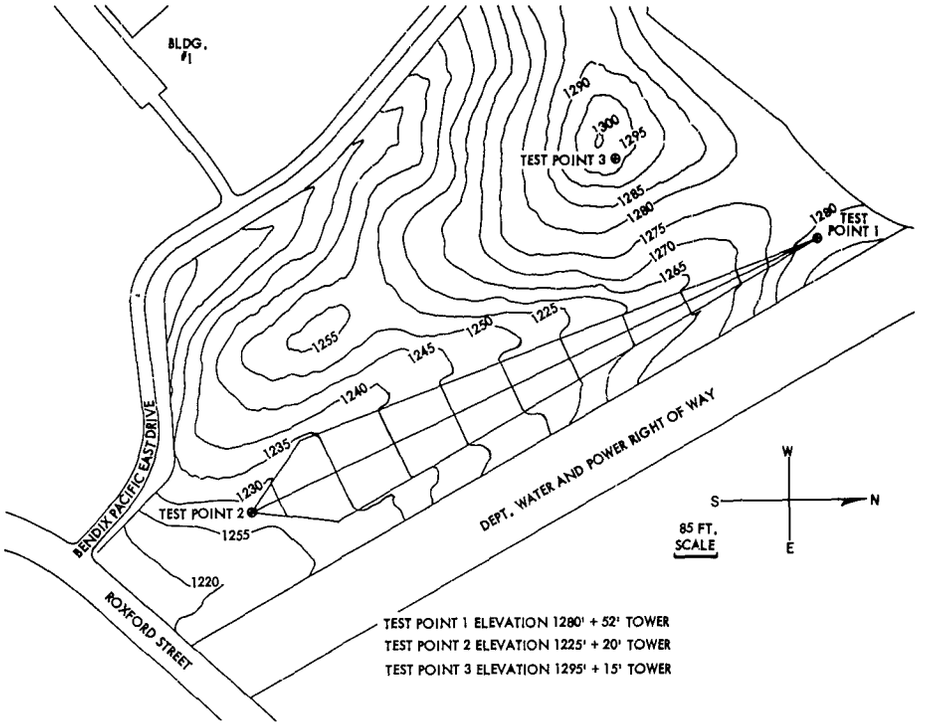

Figure 9. The Bendix Sylmar Range

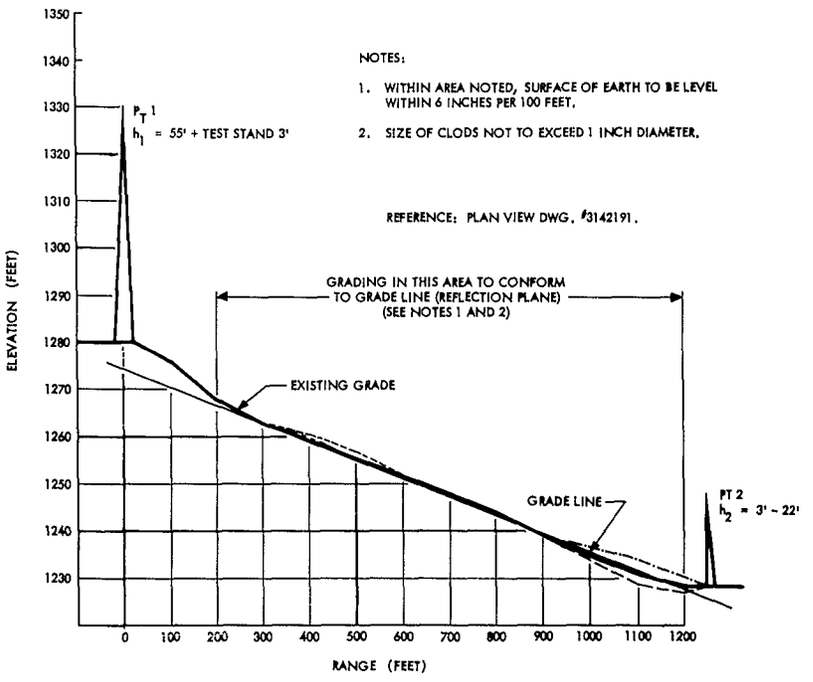

Figure 10. Derringer Test Site Elevation Profile

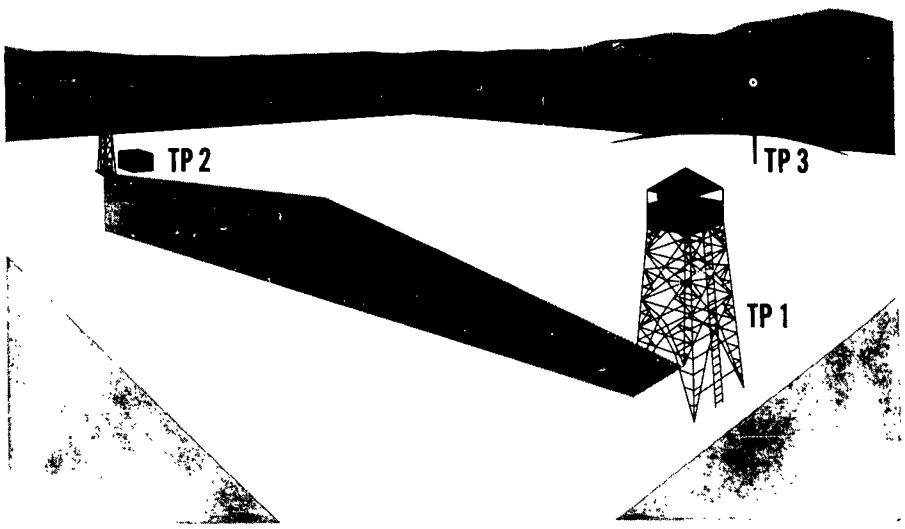

Figure 11. Derringer Test Site

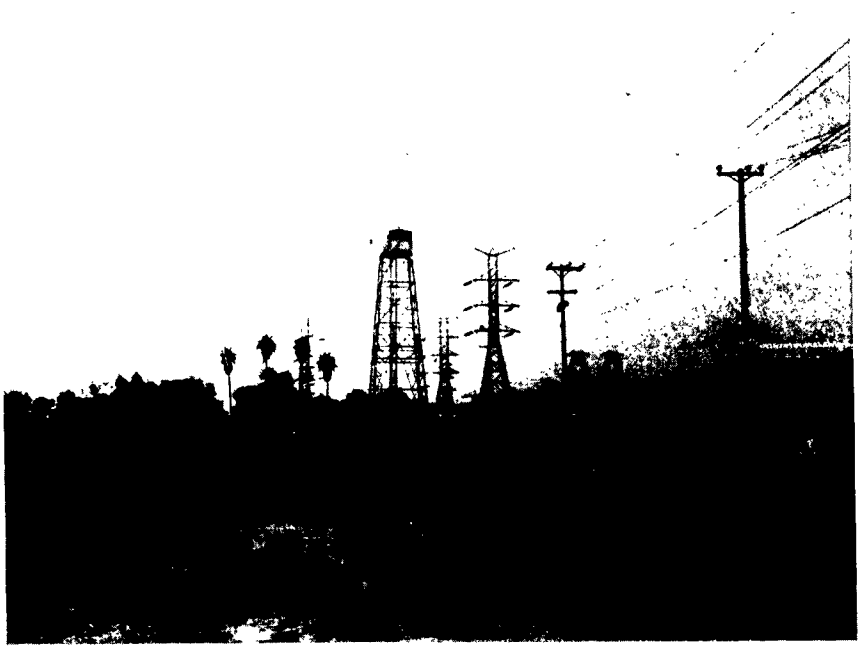

Figure 12. Tower at Test Point No. 1

Figure 13. Tower at Test Point No. 2

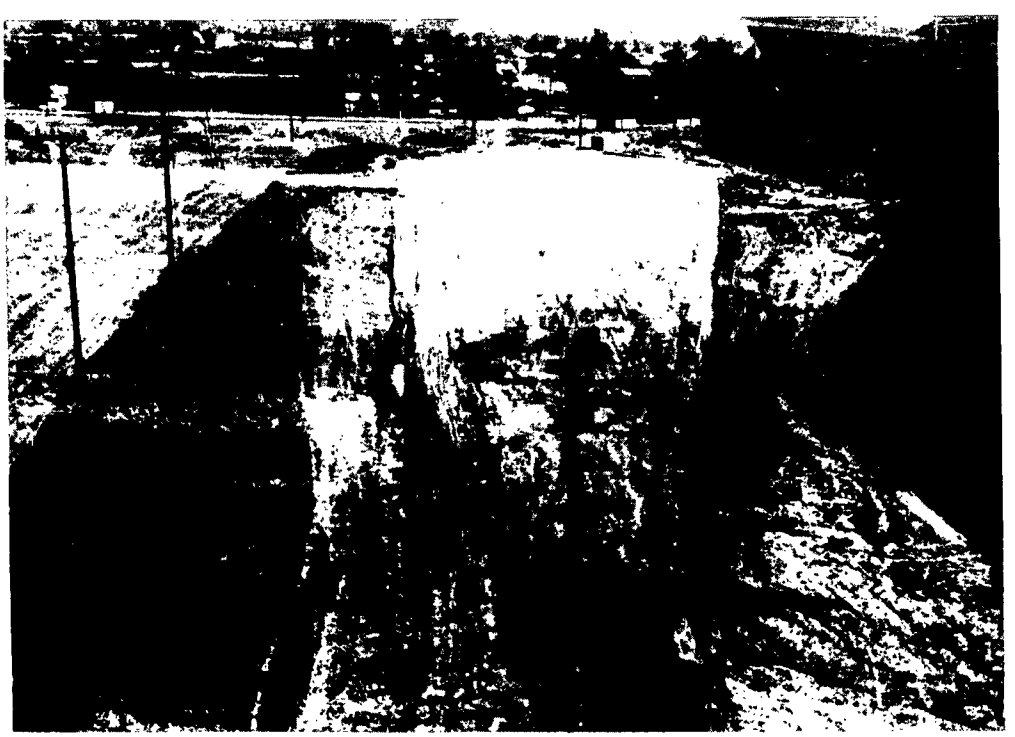

Figure 14. The Reflection Plane

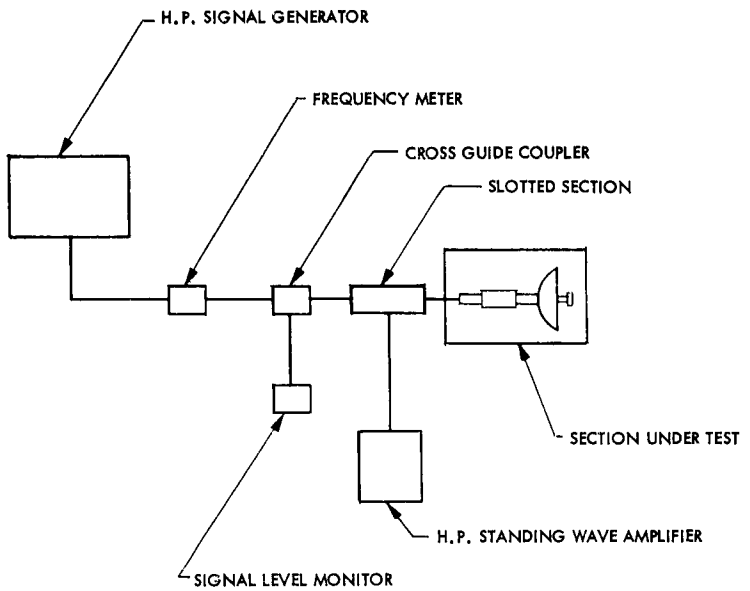

Figure 15. V. S. W. R. Test Layout

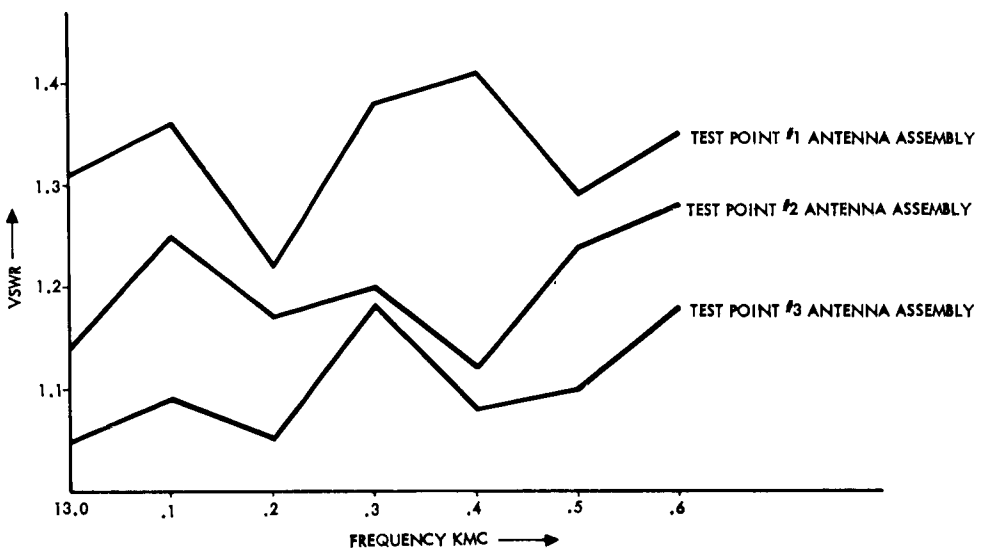

Figure 16. V. S. W. R. Test Results

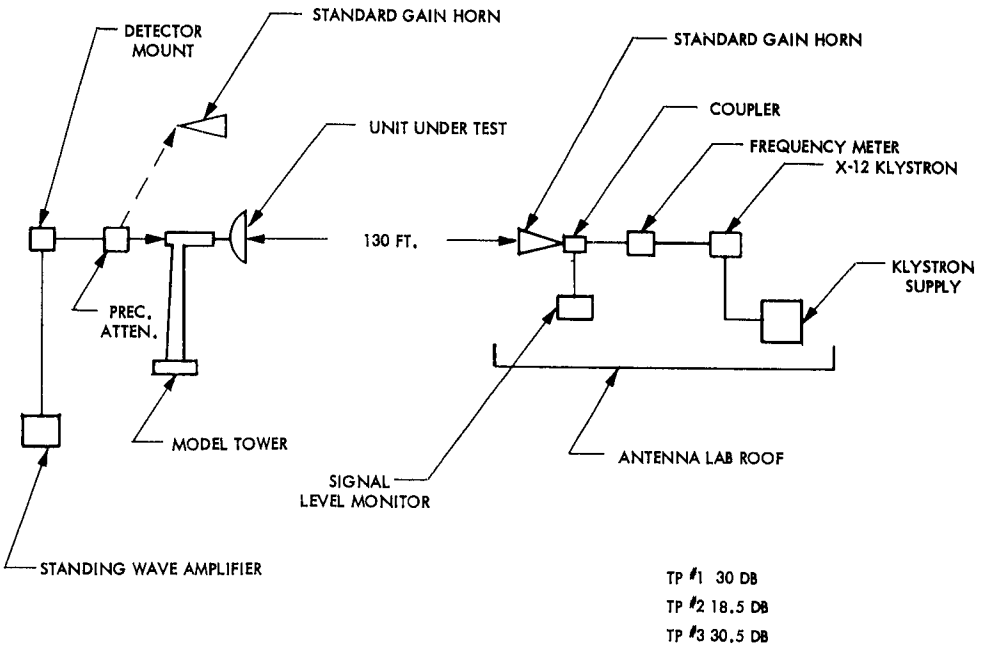

Figure 17. Gain Measurements

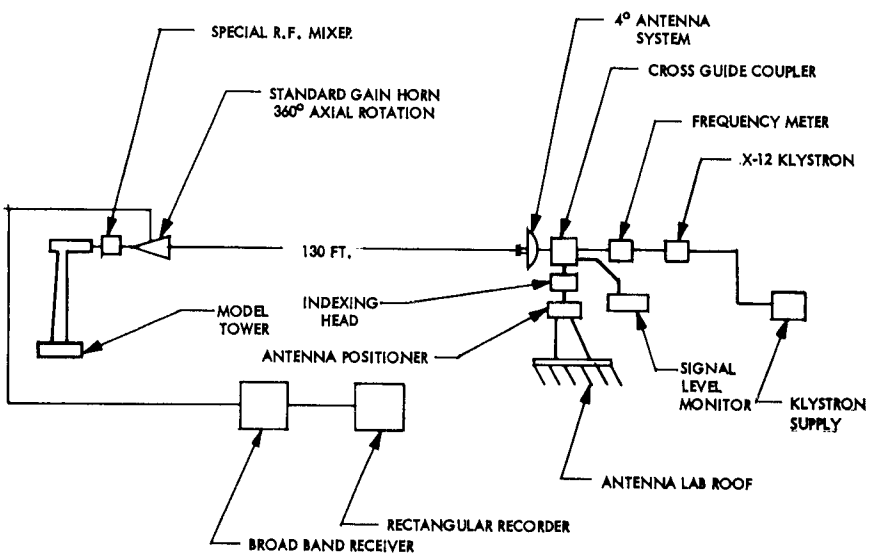

Figure 18. Pattern Calibration Test Point No. 3 Assembly

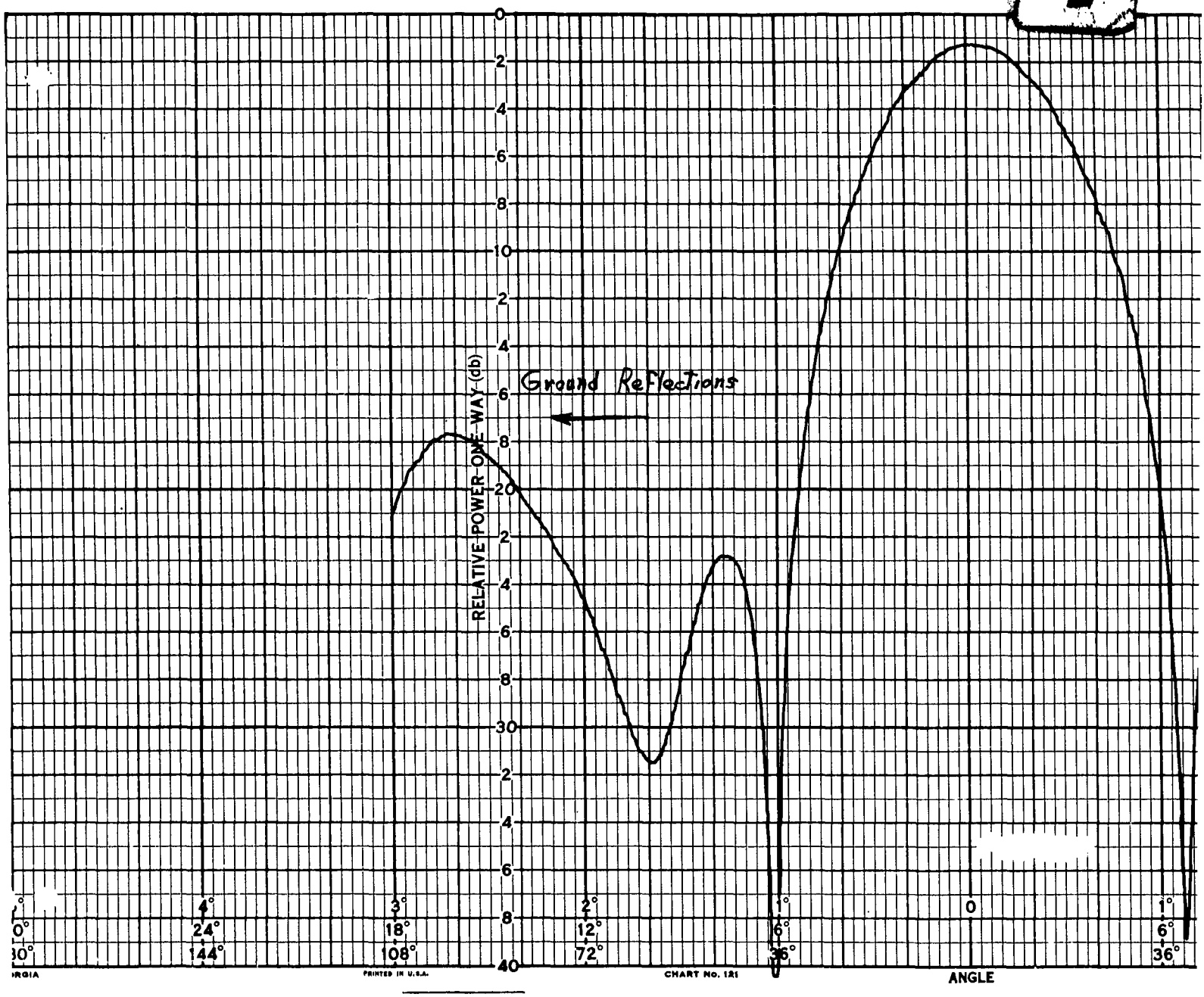
Ground Reflections
RELATIVE POWER-ONE WAY (db)
0
2
4
6
8
10
2
4
6
8
20
2
4
6
8
30
2
4
6
8
40
4°
24°
144°
3°
18°
108°
2°
12°
72°
1°
6°
36°
0
1°
6°
36°
ANGLE
PRINTED IN U.S.A.
CHART No. 121

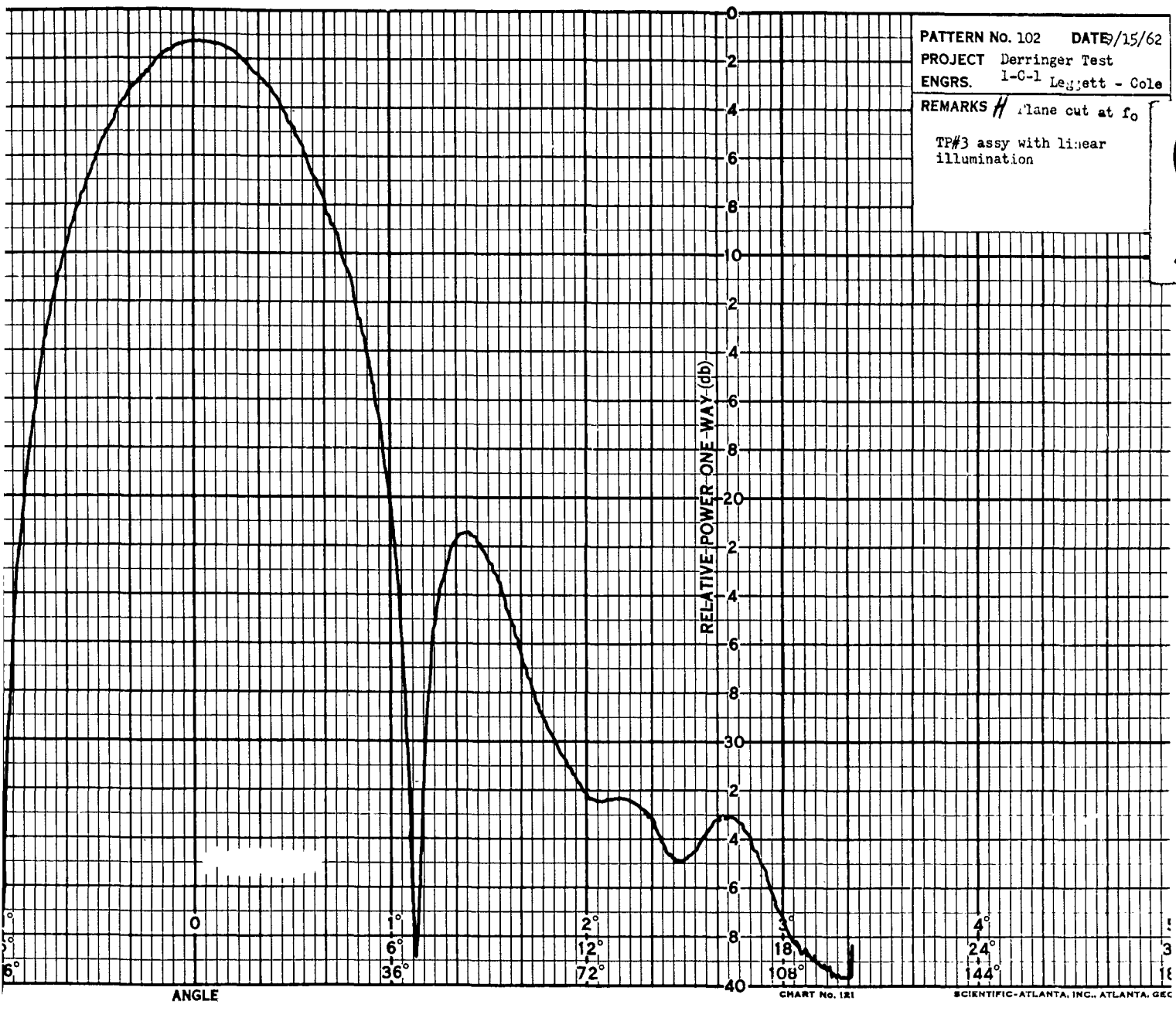

Figure 19. H Plane Pattern Test Point No. 3 Assembly

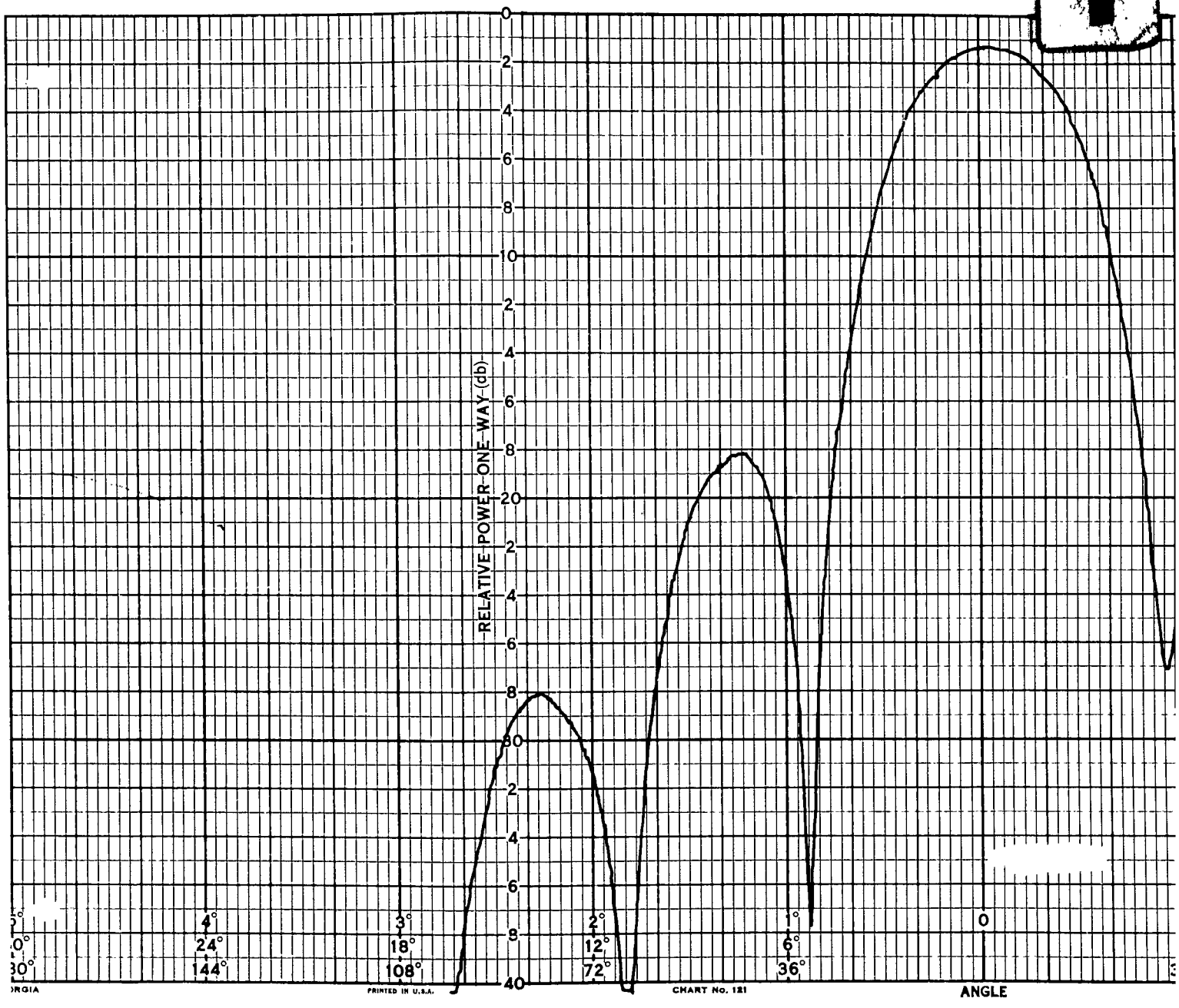
RELATIVE POWER ONE WAY (db)
0
2
4
6
8
10
2
4
6
8
20
2
4
6
8
30
2
4
6
8
40
4°
24°
144°
3°
18°
108°
2°
12°
72°
1°
6°
36°
0
ANGLE
PRINTED IN U.S.A.
CHART No. 121

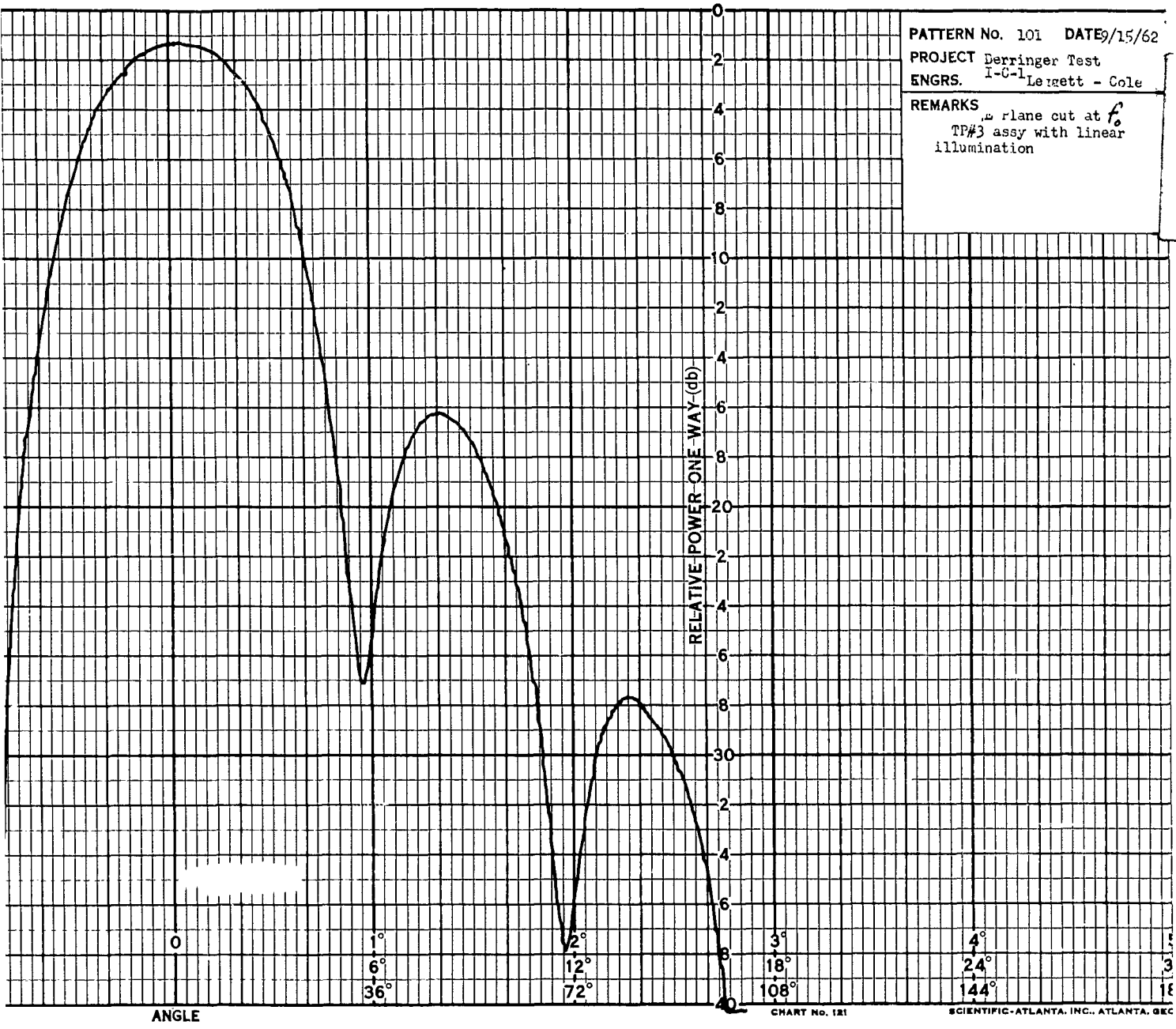

Figure 20. E Plane Pattern Test Point No. 3 Assembly

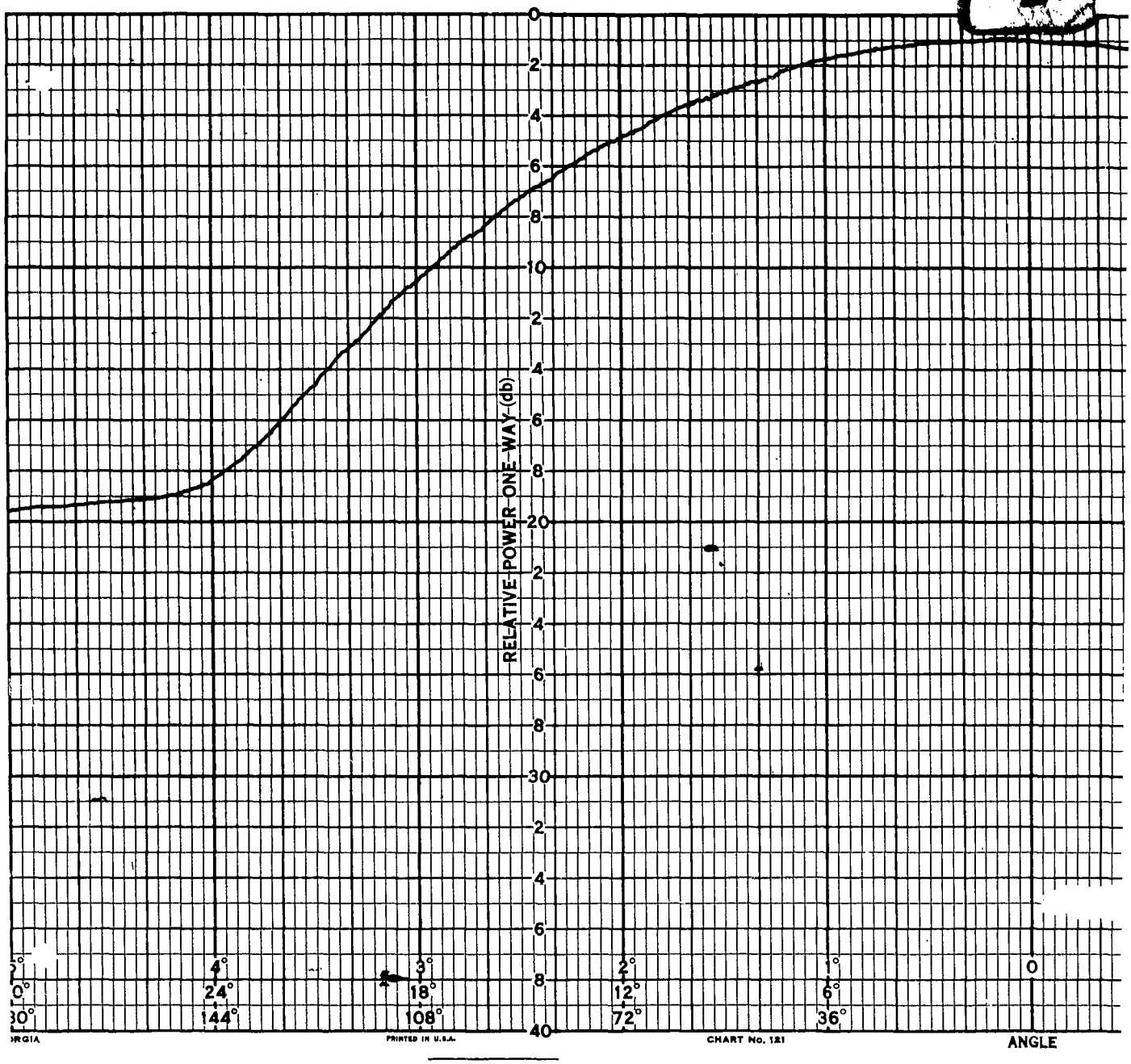
RELATIVE-POWER-ONE-WAY-(db)
0
2
4
6
8
10
2
4
6
8
20
2
4
6
8
30
2
4
6
8
40
4°
24°
144°
3°
18°
108°
2°
12°
72°
1°
6°
36°
0
ANGLE
PRINTED IN U.S.A.
CHART No. 121

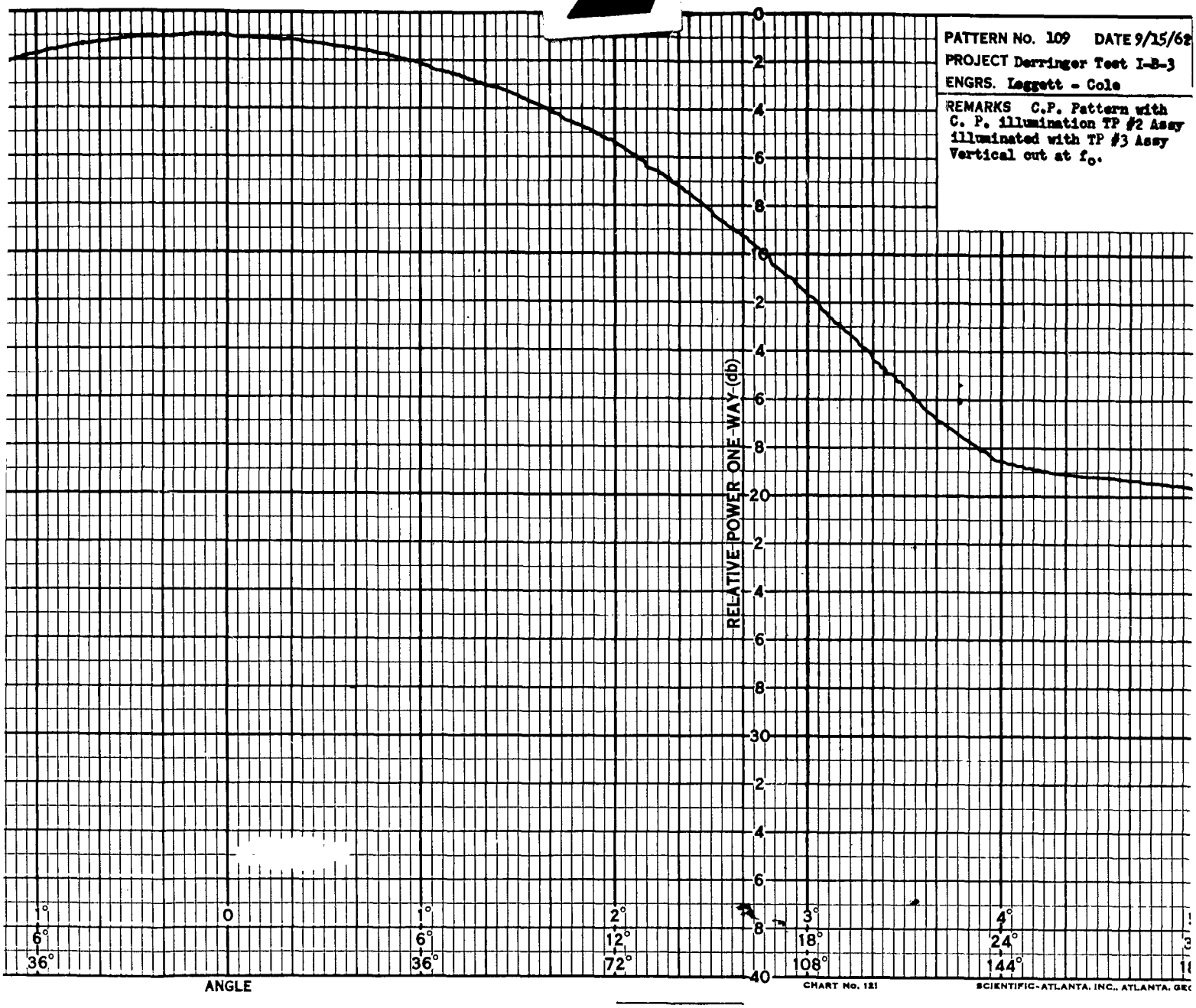

Figure 21. Vertical Cut Test Point No. 2 Assembly

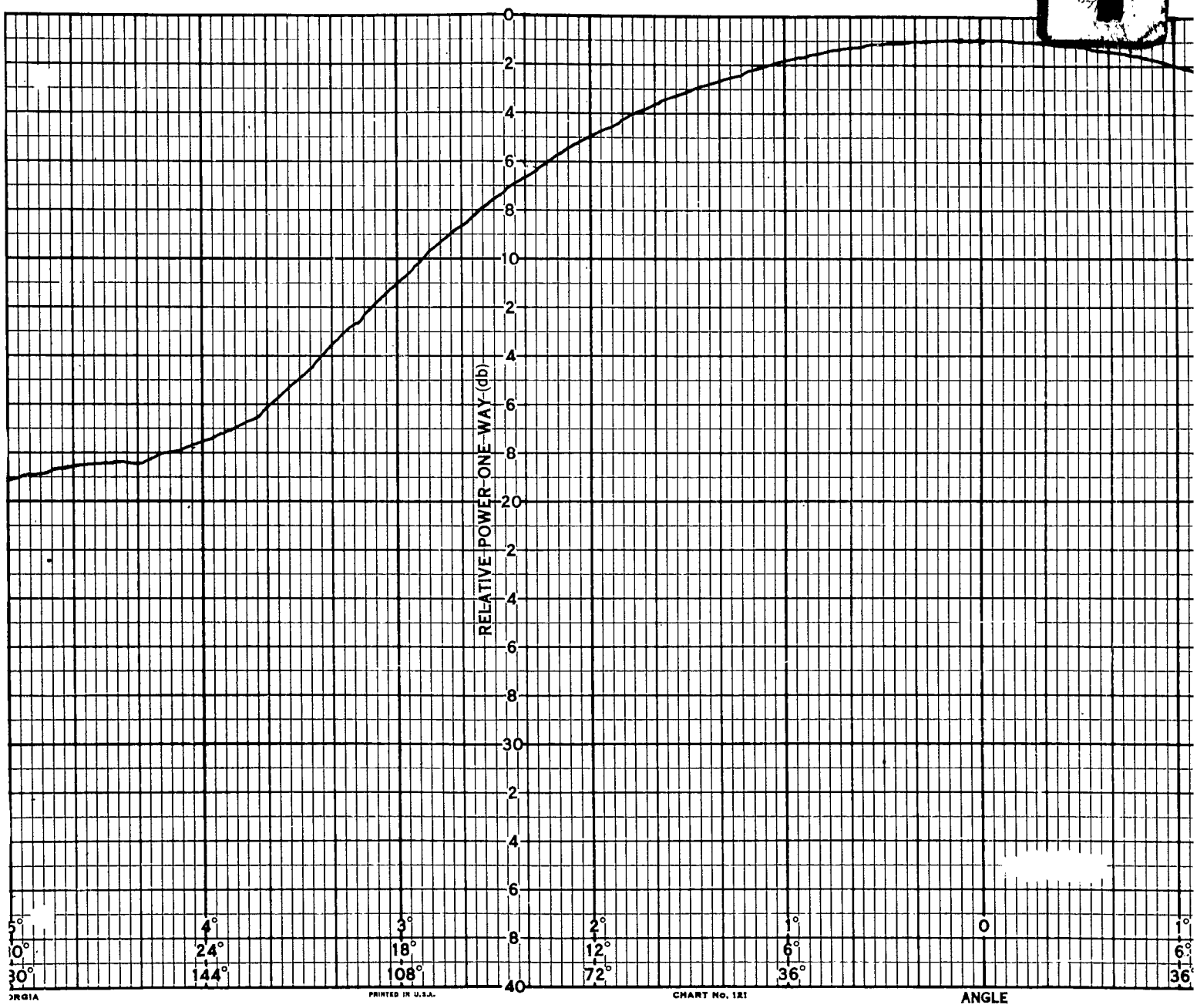
RELATIVE POWER-ONE-WAY-(db)
0
2
4
6
8
10
2
4
6
8
20
2
4
6
8
30
2
4
6
8
40
5°
4°
3°
2°
1°
0
1°
30°
24°
18°
12°
6°
6°
30°
144°
108°
72°
36°
36°
ANGLE

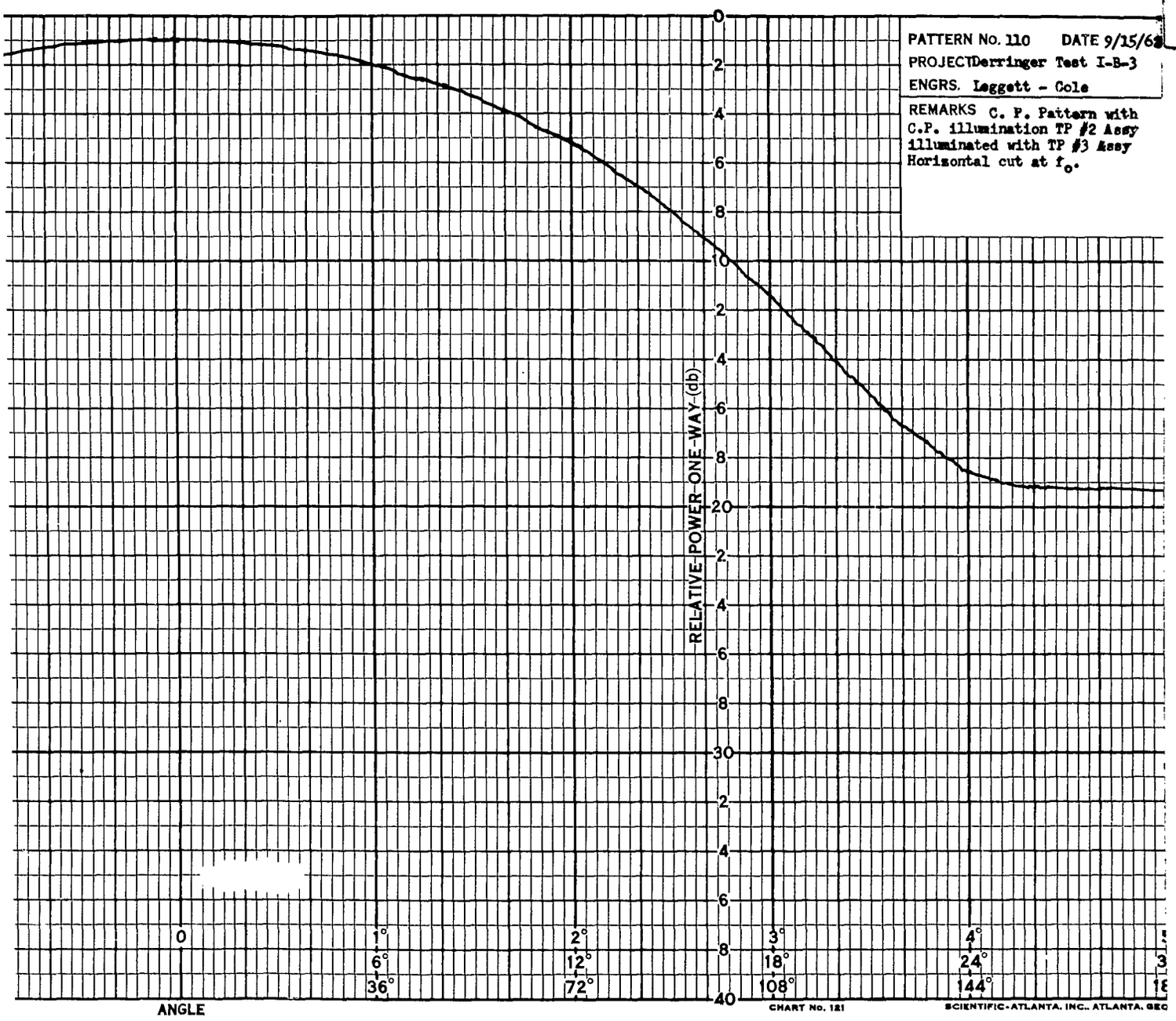

Figure 22. Horizontal Cut Test Point No. 2 Assembly

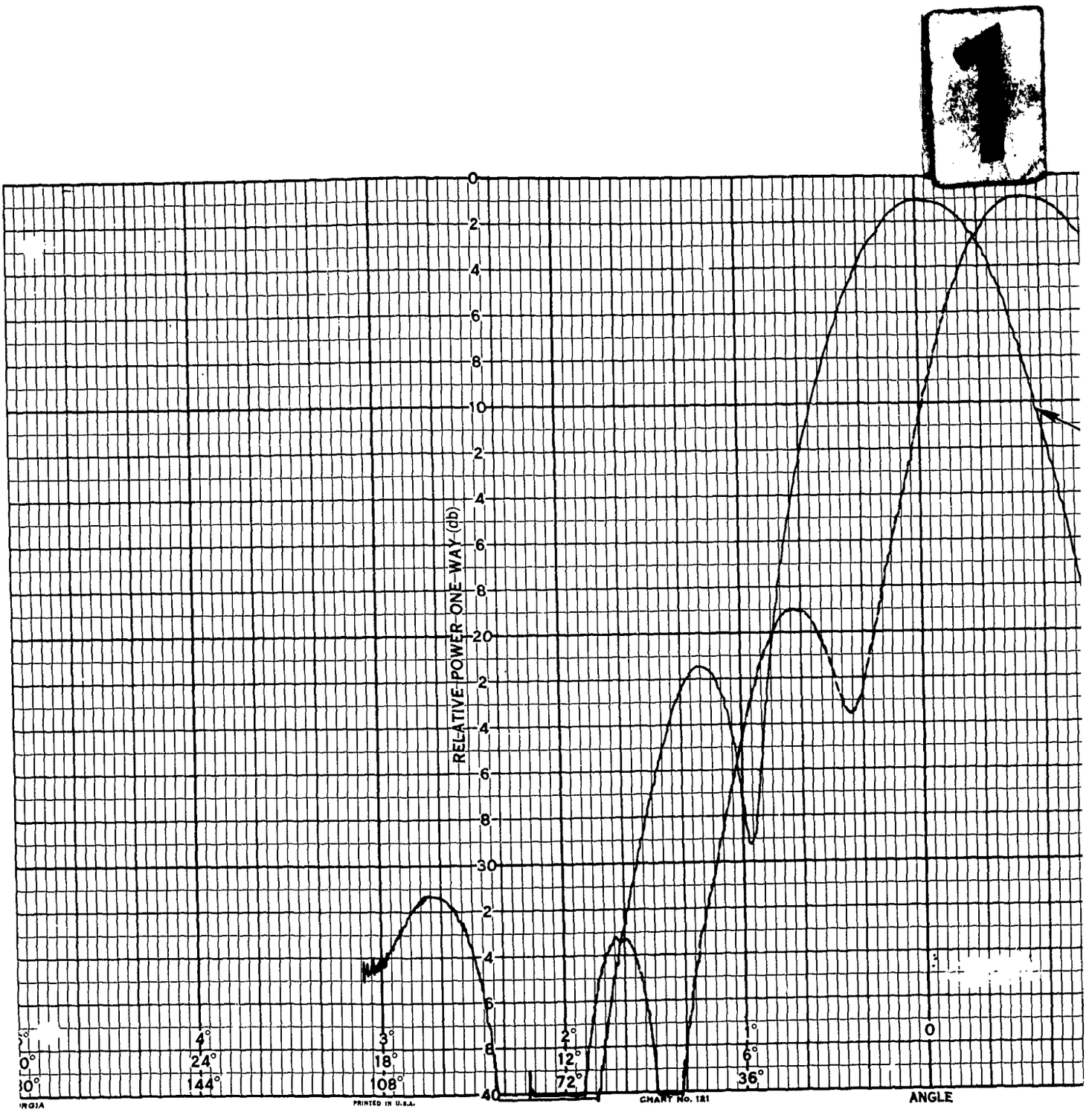
RELATIVE POWER ONE WAY (db)
0
2
4
6
8
10
2
4
6
8
20
2
4
6
8
30
2
4
6
8
40
4°
24°
144°
3°
18°
108°
2°
12°
72°
1°
6°
36°
0
ANGLE
CHART No. 121
PRINTED IN U.S.A.

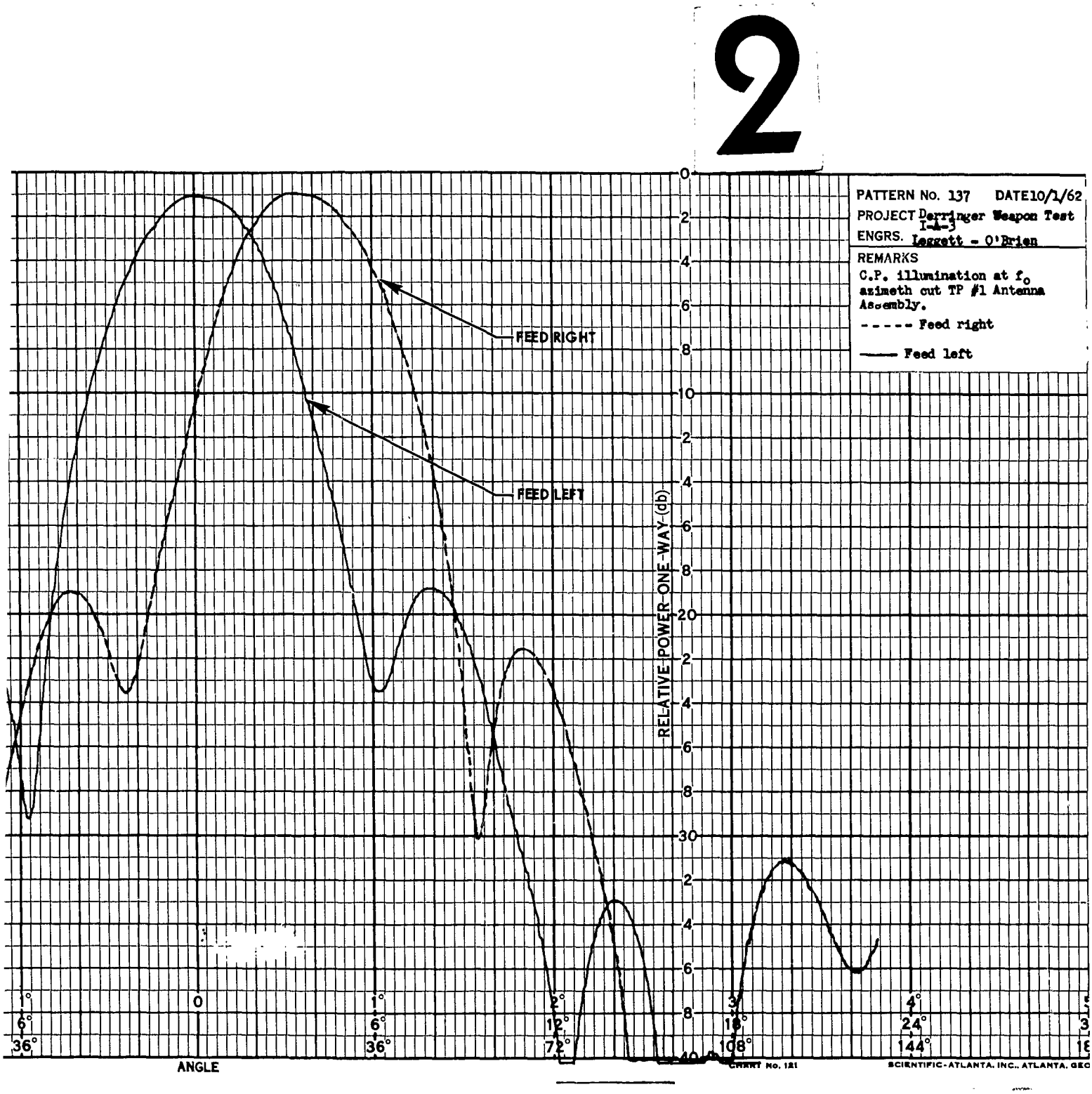

Figure 24. Symmetry Patterns Test Point No. 1 Assembly

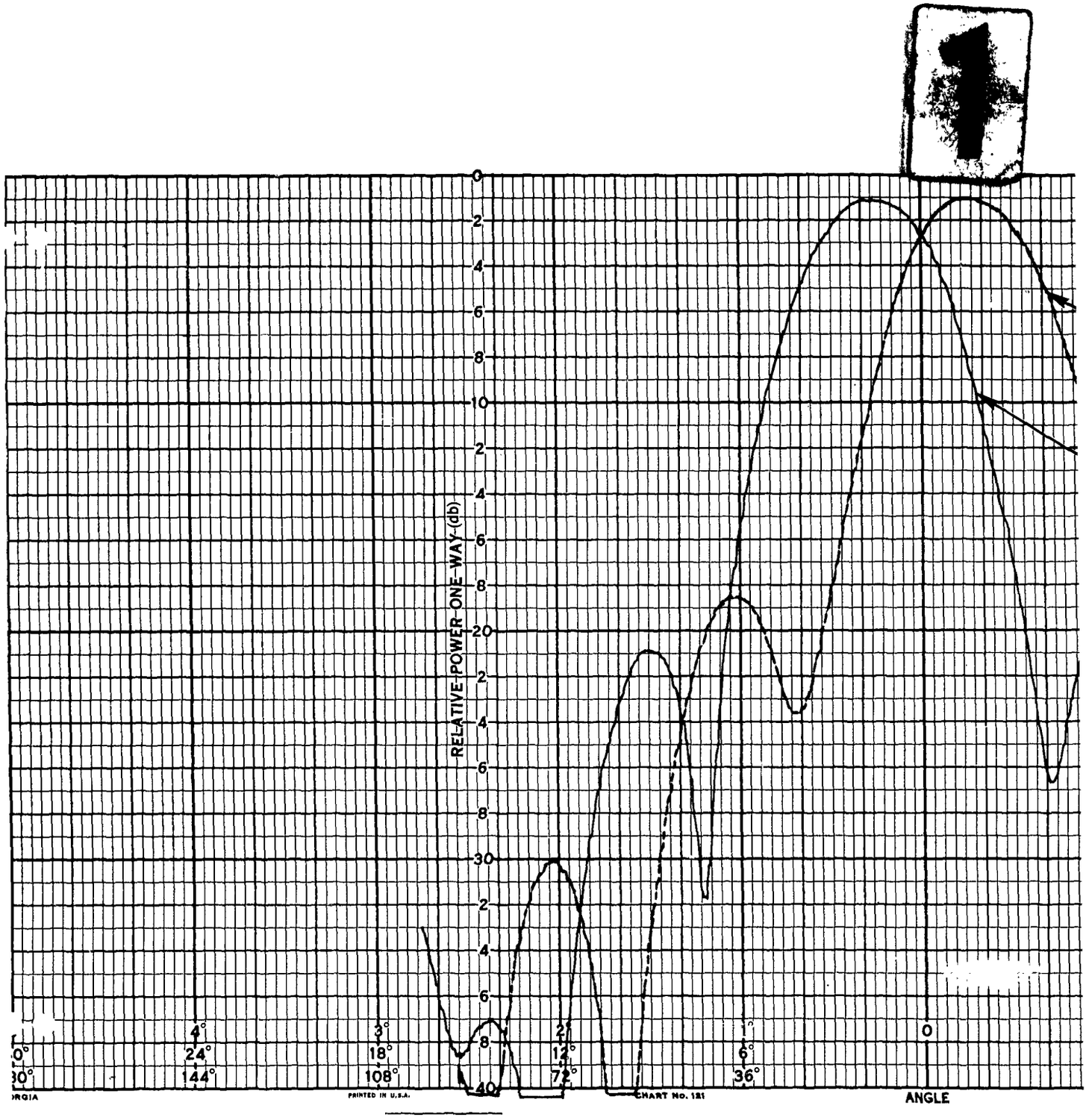
RELATIVE-POWER-ONE-WAY-(db)
0
2
4
6
8
10
2
4
6
8
20
2
4
6
8
30
2
4
6
8
40
4°
24°
144°
3°
18°
108°
2°
12°
72°
1°
6°
36°
0
ANGLE
PRINTED IN U.S.A.
CHART NO. 121

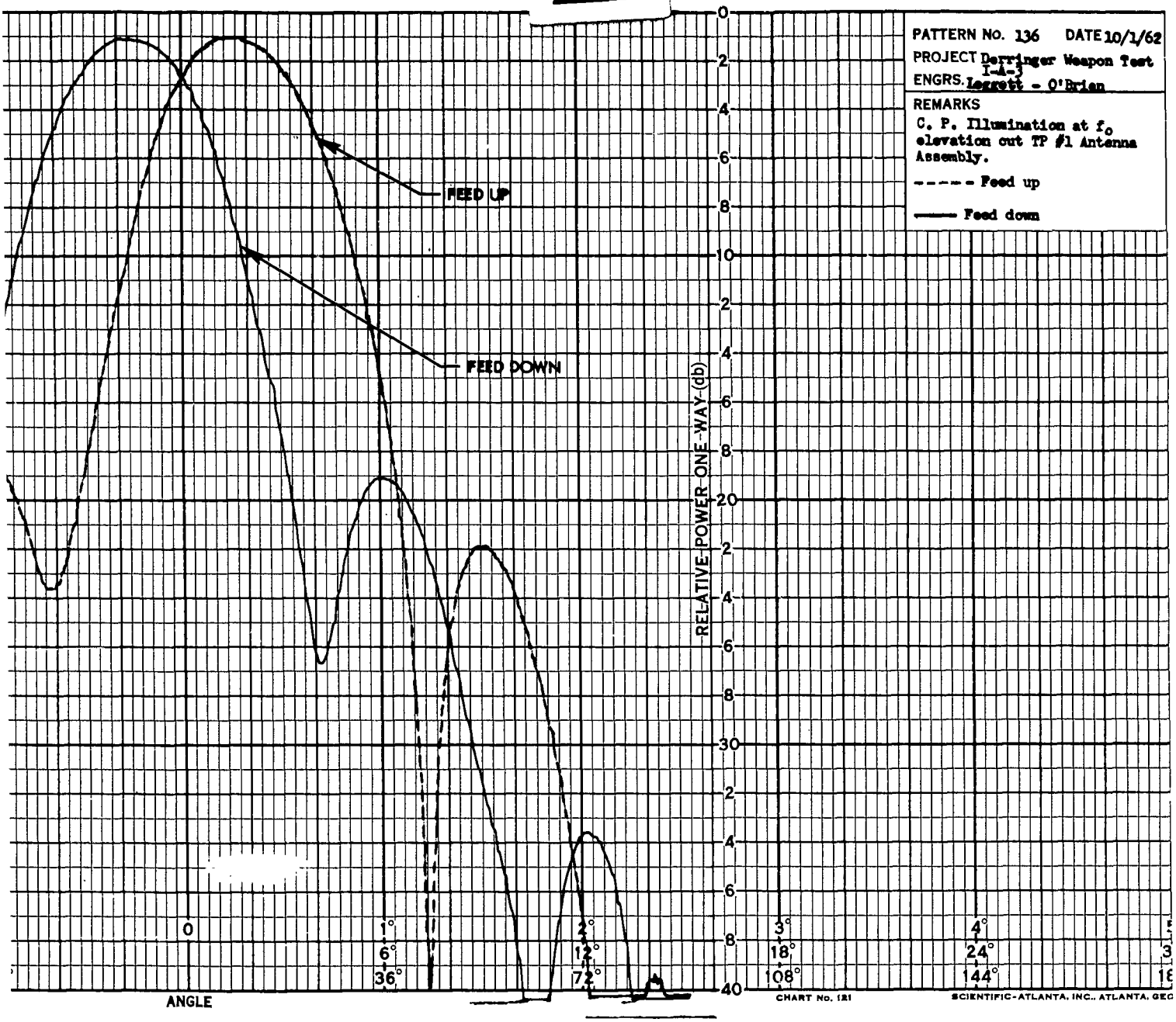

Figure 23. Symmetry Patterns Test Point No. 1 Assembly

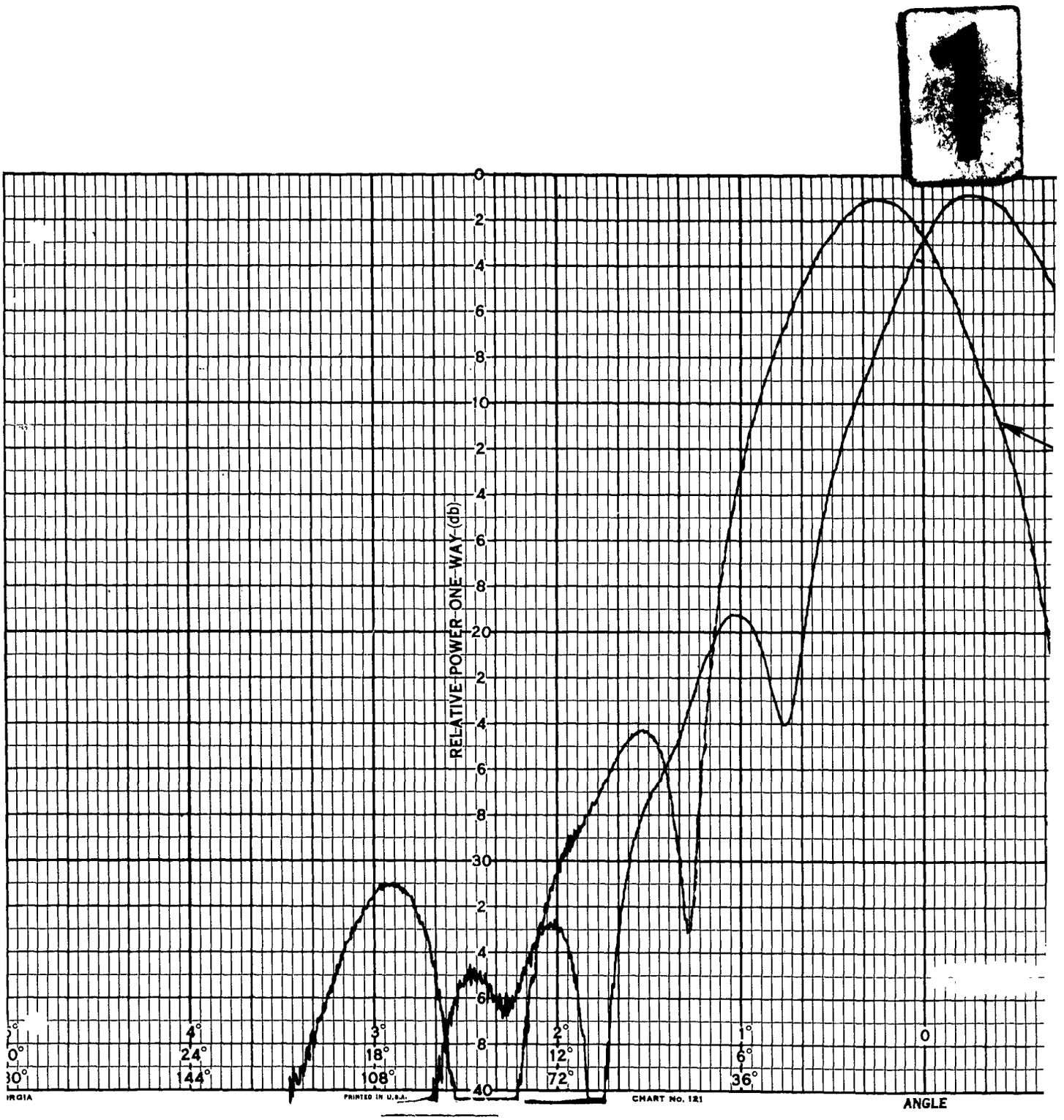
RELATIVE POWER-ONE-WAY (db)
0
2
4
6
8
10
2
4
6
8
20
2
4
6
8
30
2
4
6
8
40
4°
24°
144°
3°
18°
108°
2°
12°
72°
1°
6°
36°
0
ANGLE
PRINTED IN U.S.A.
CHART No. 121

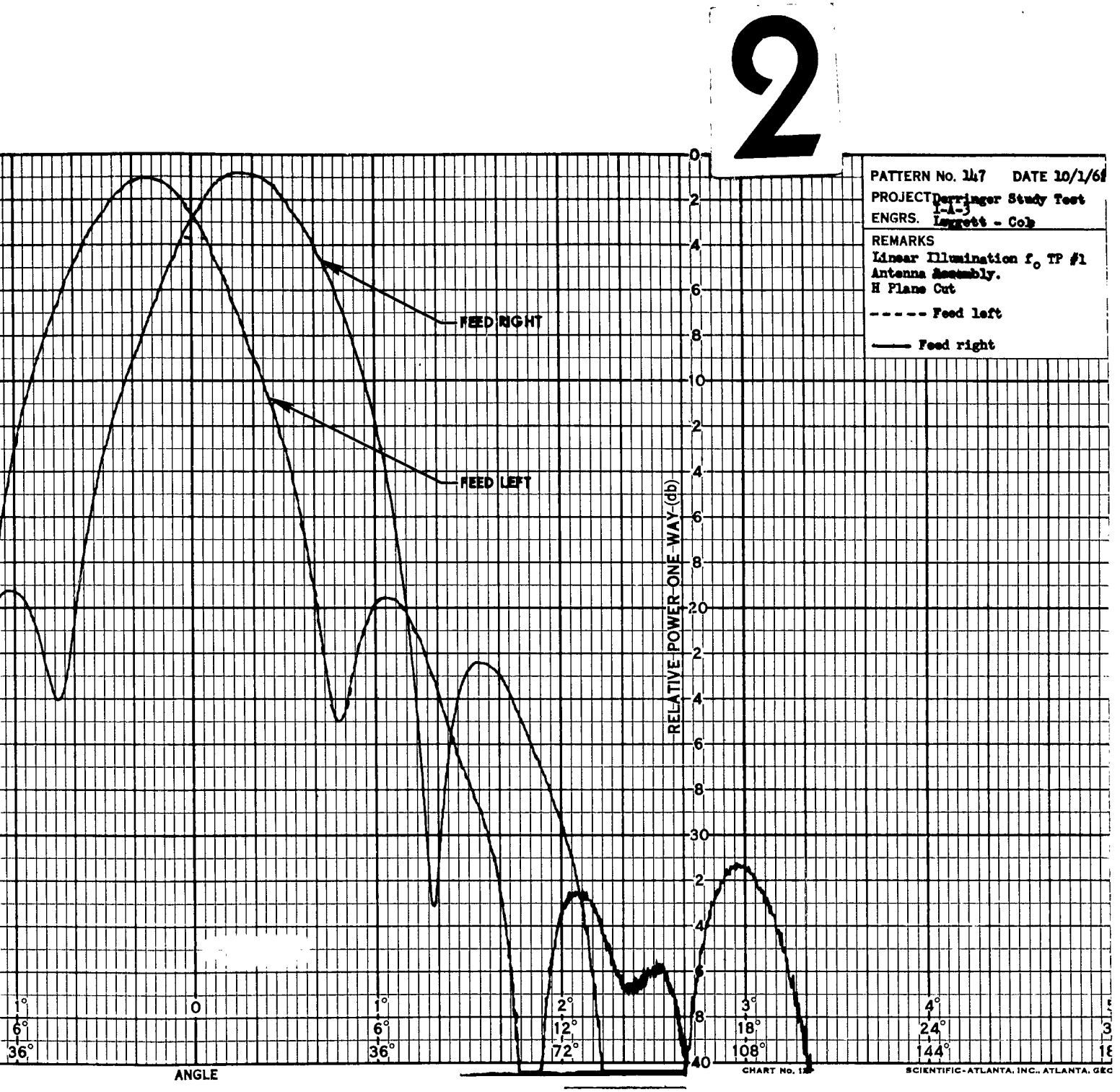

Figure 25. Symmetry Patterns Test Point No. 1 Assembly

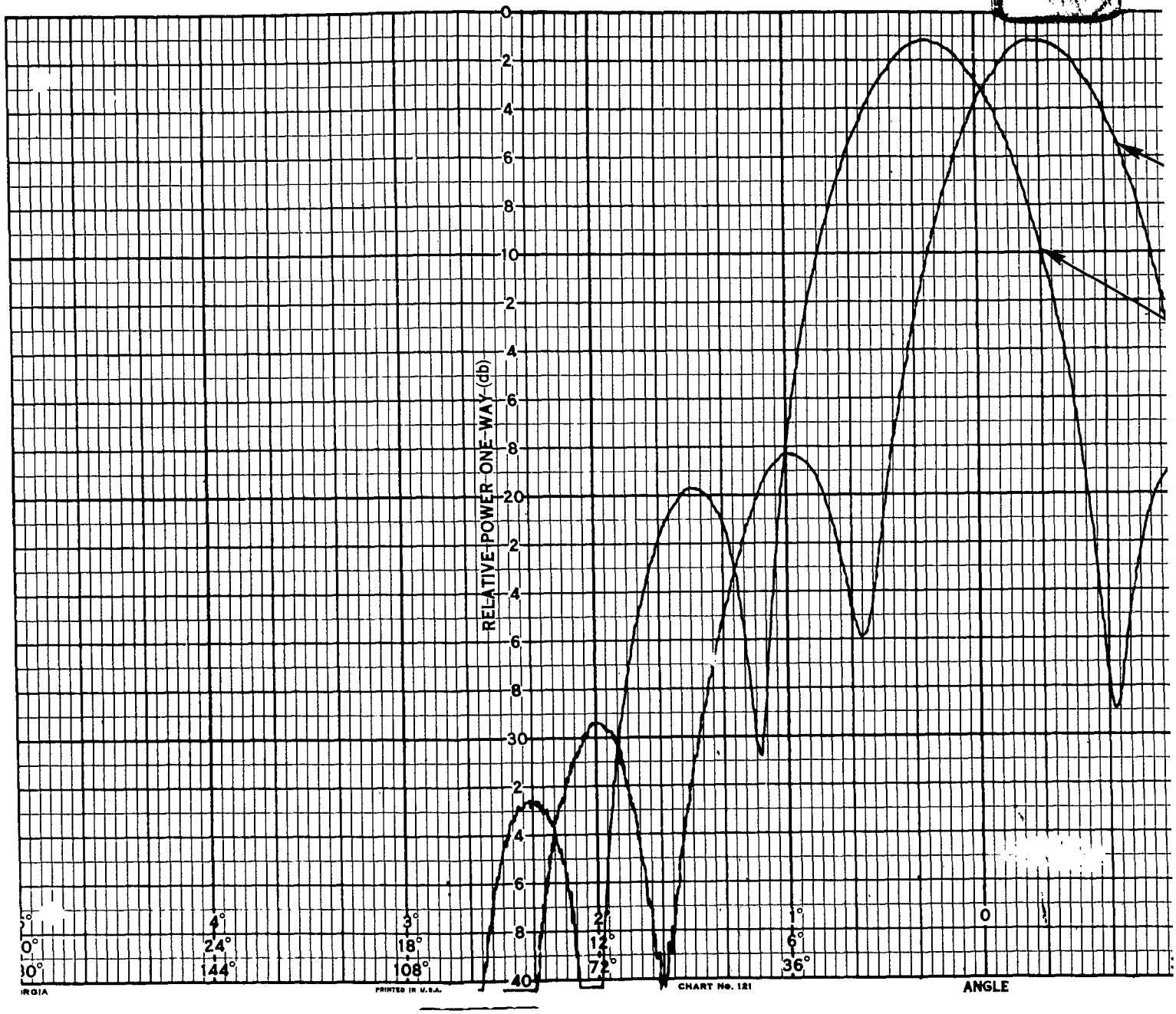
RELATIVE-POWER-ONE-WAY-(db)
0
2
4
6
8
10
2
4
6
8
20
2
4
6
8
30
2
4
6
8
40
4°
24°
144°
3°
18°
108°
2°
12°
72°
1°
6°
36°
0
ANGLE
PRINTED IN U.S.A.
CHART No. 121

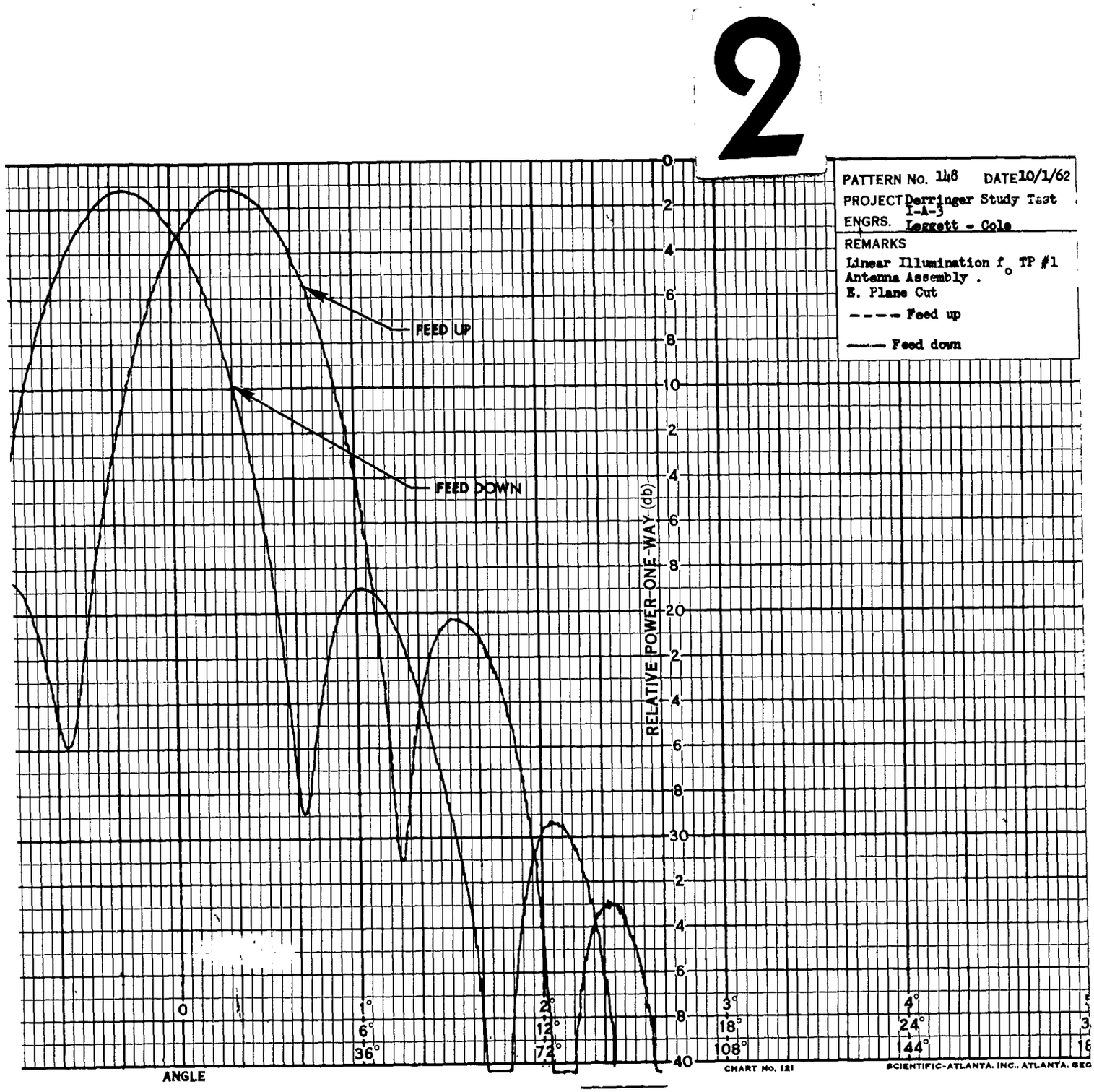

Figure 26. Symmetry Patterns Test Point No. 1 Assembly

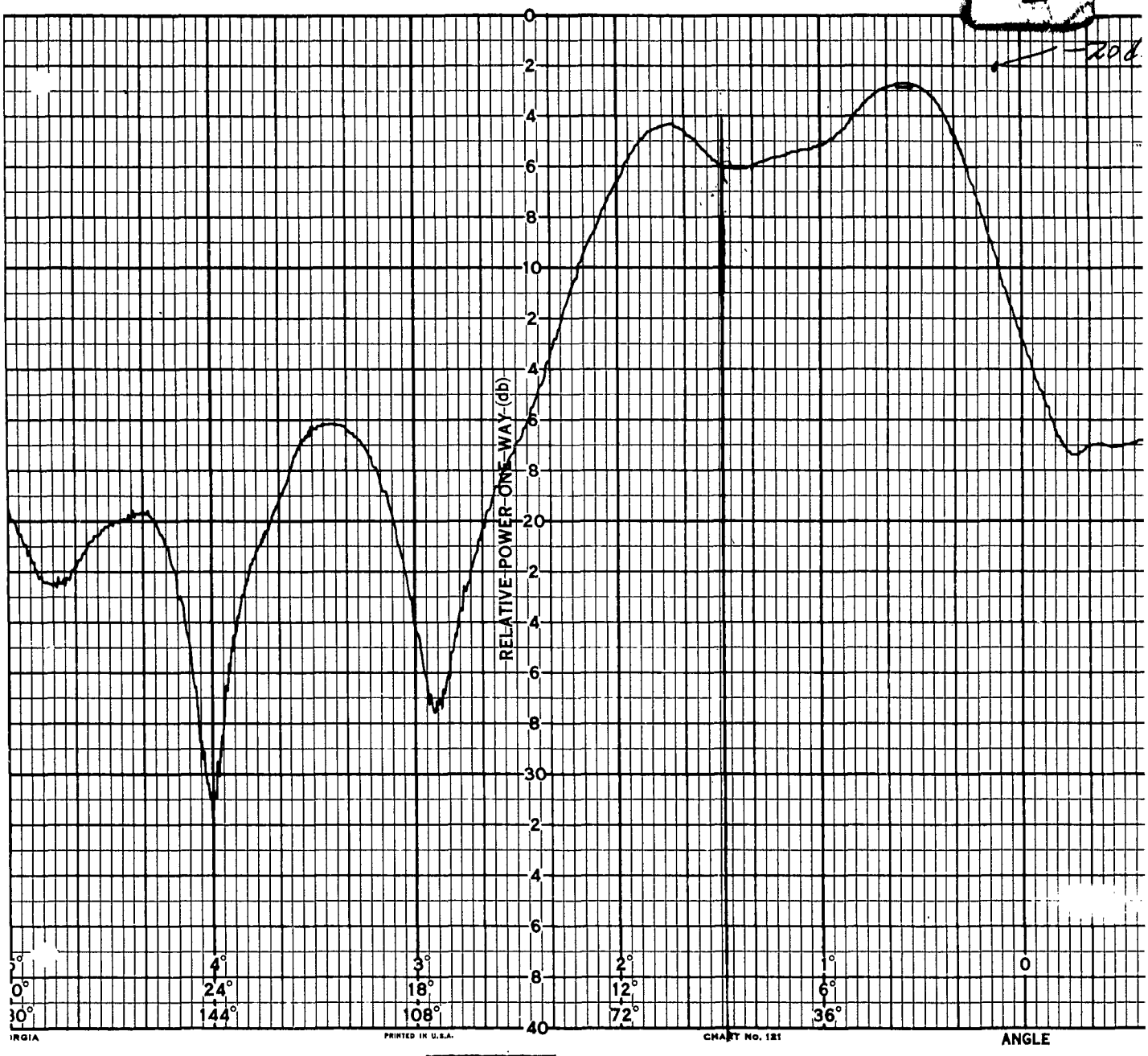
1
20d
RELATIVE POWER ONE WAY (db)
0
2
4
6
8
10
2
4
6
8
20
2
4
6
8
30
2
4
6
8
40
4°
24°
144°
3°
18°
108°
2°
12°
72°
1°
6°
36°
0
ANGLE
PRINTED IN U.S.A.
CHART No. 121

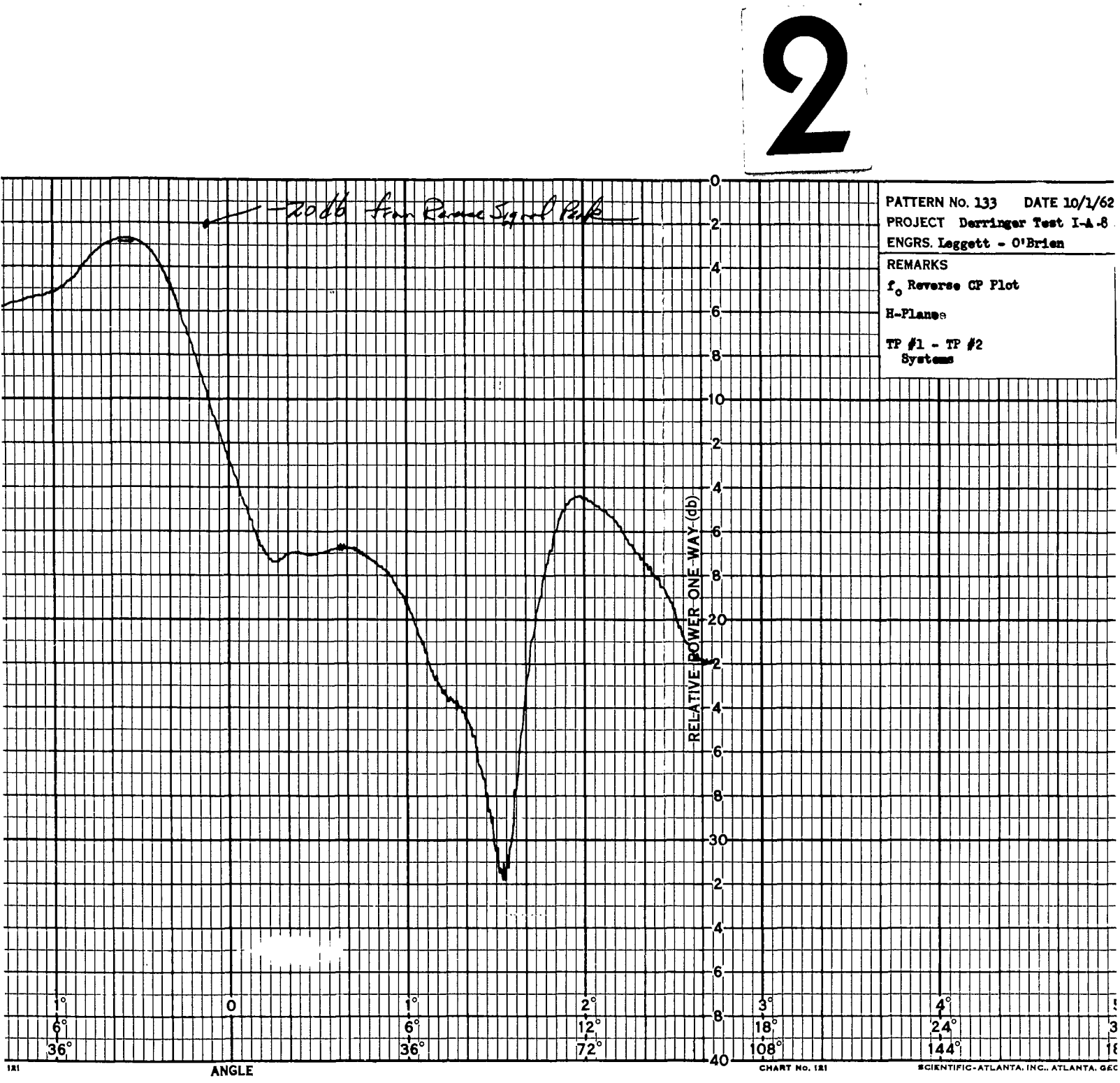

Figure 27. Reverse C. P. Plot

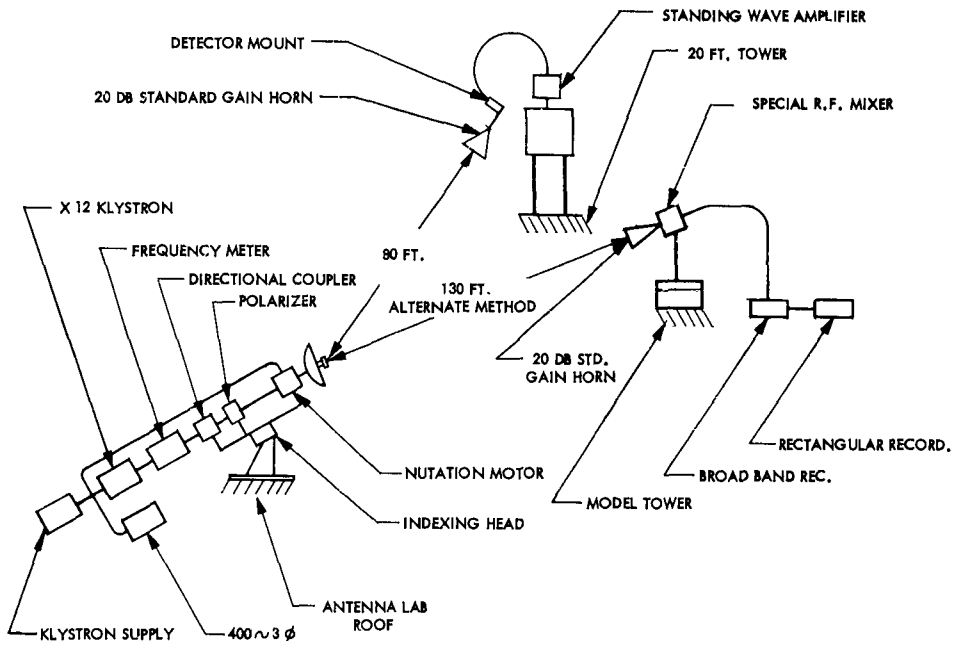

Figure 28. Elipticity Measurements Test Point No. 1 Assembly

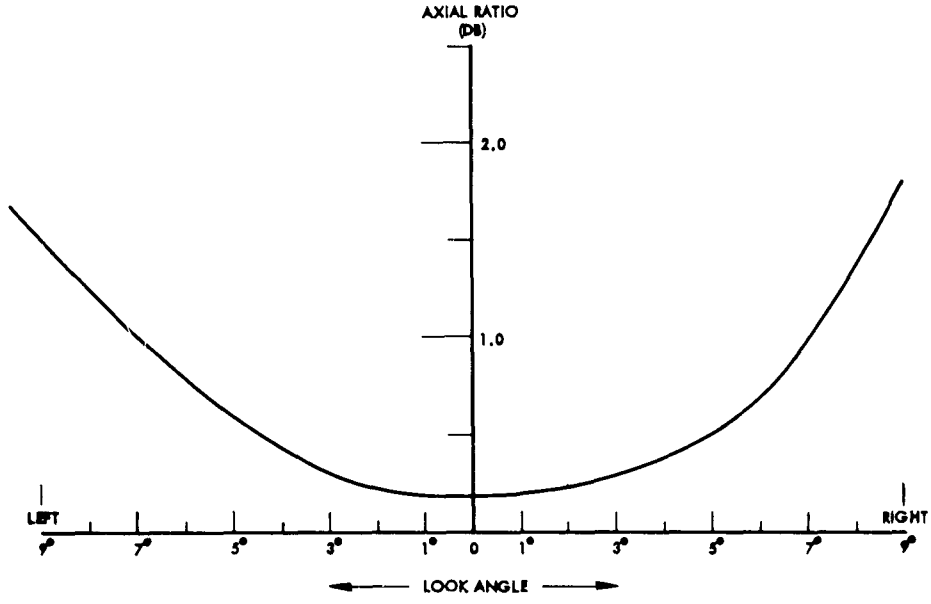

Figure 29. Axial Ratio vs. Look Angle Test Point No. 2 Assembly

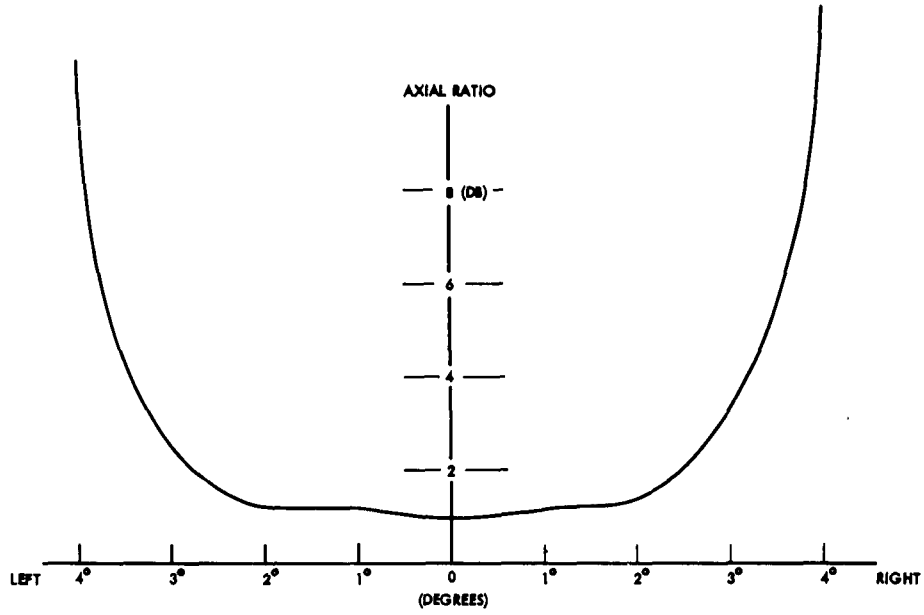

Figure 30. Axial Ratio vs. Look Angle Test Point No. 1 Assembly

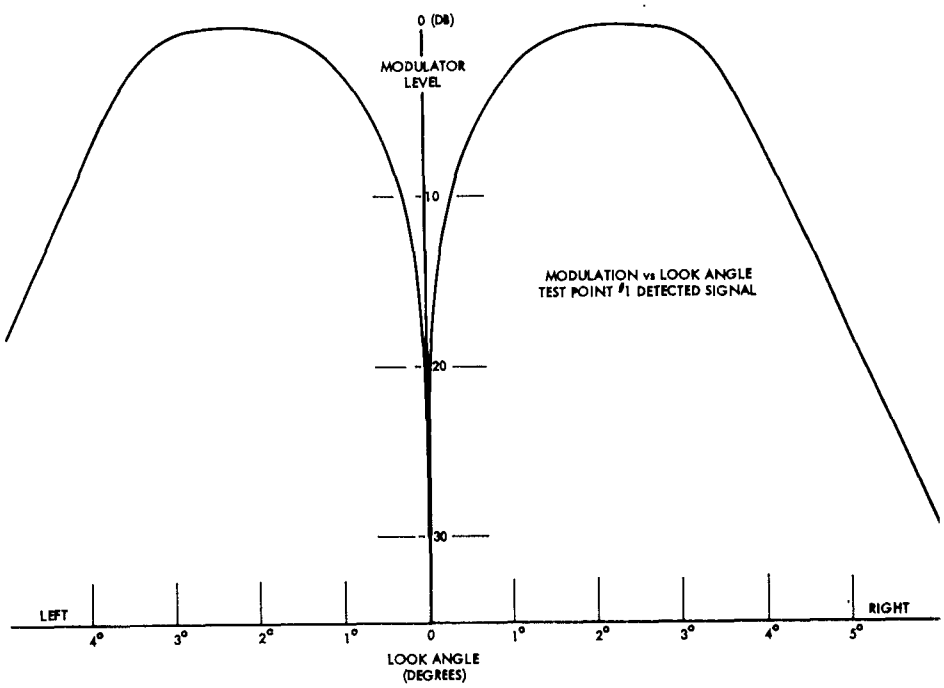

Figure 31. Modulation Envelope

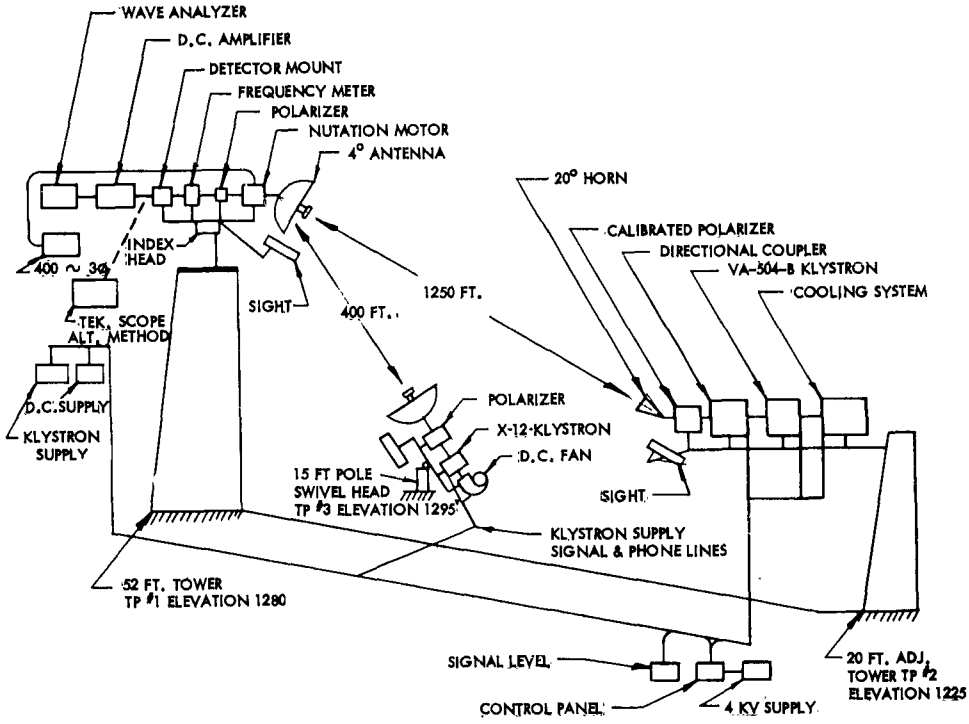

Figure 32. Basic Sylmar Test Range Equipments

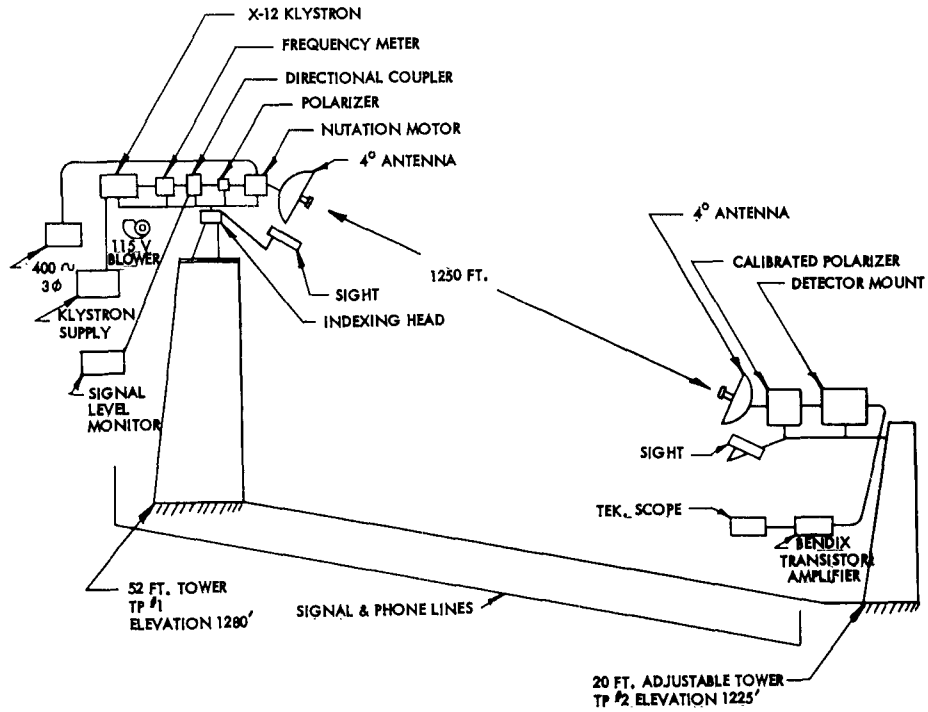

Figure 33. High Level Low Power Installation

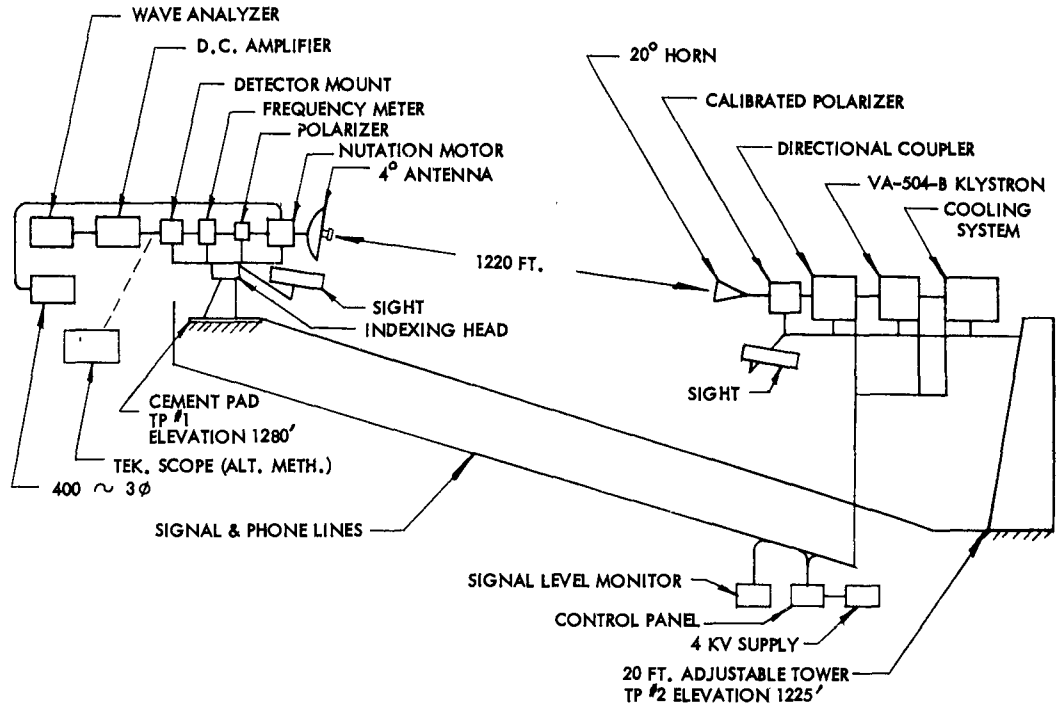

Figure 34. Low Level High Power Installation

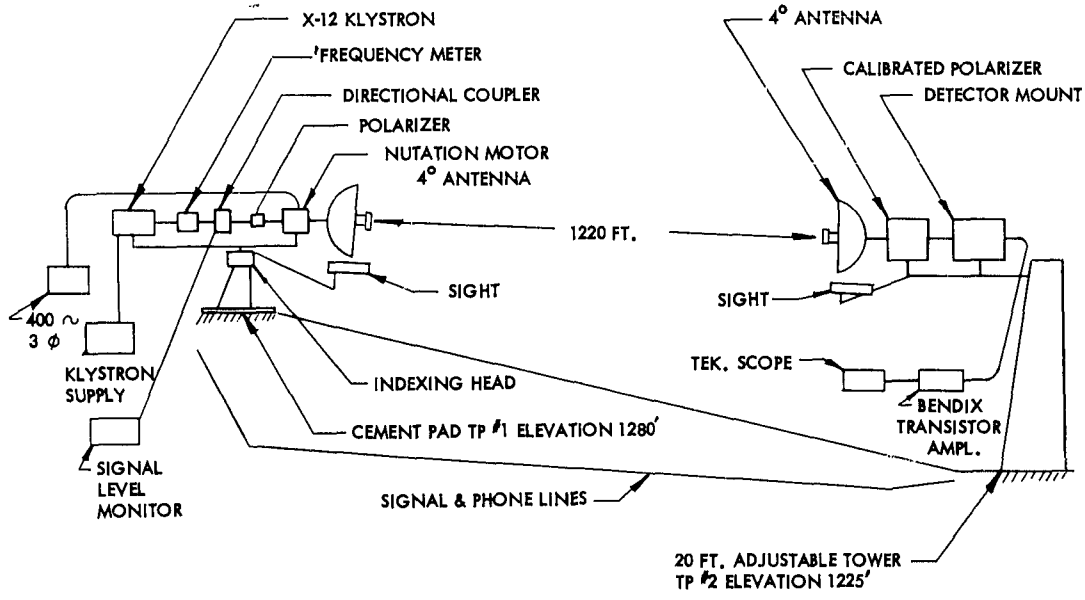

Figure 35. Low Level Low Power Installation

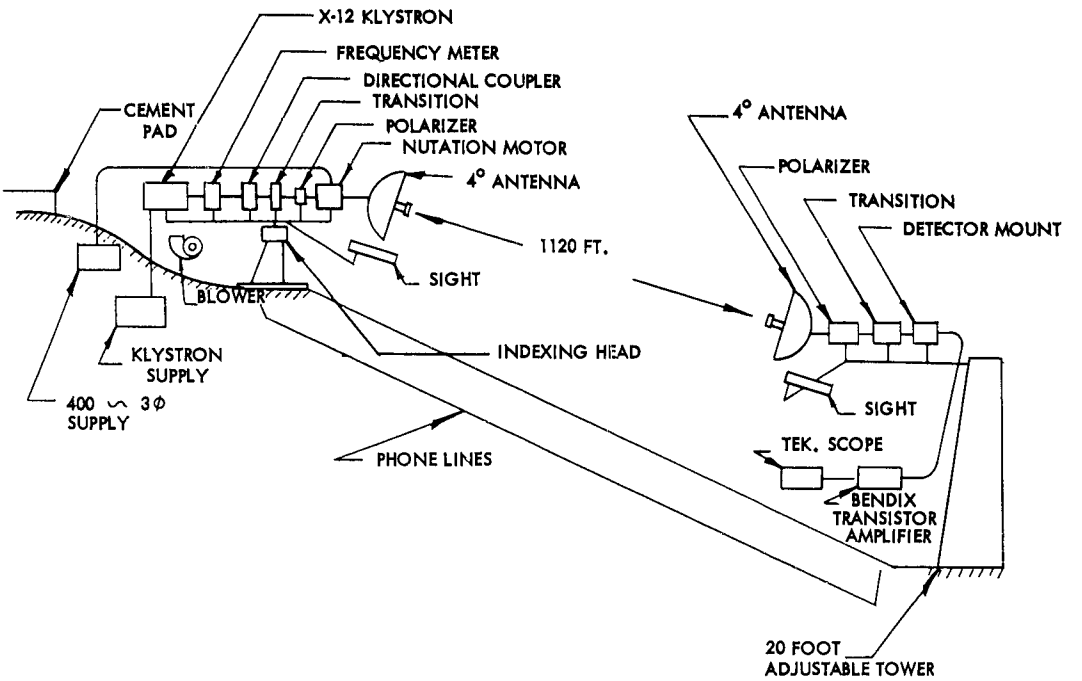

Figure 36. Low Level Displaced Installation

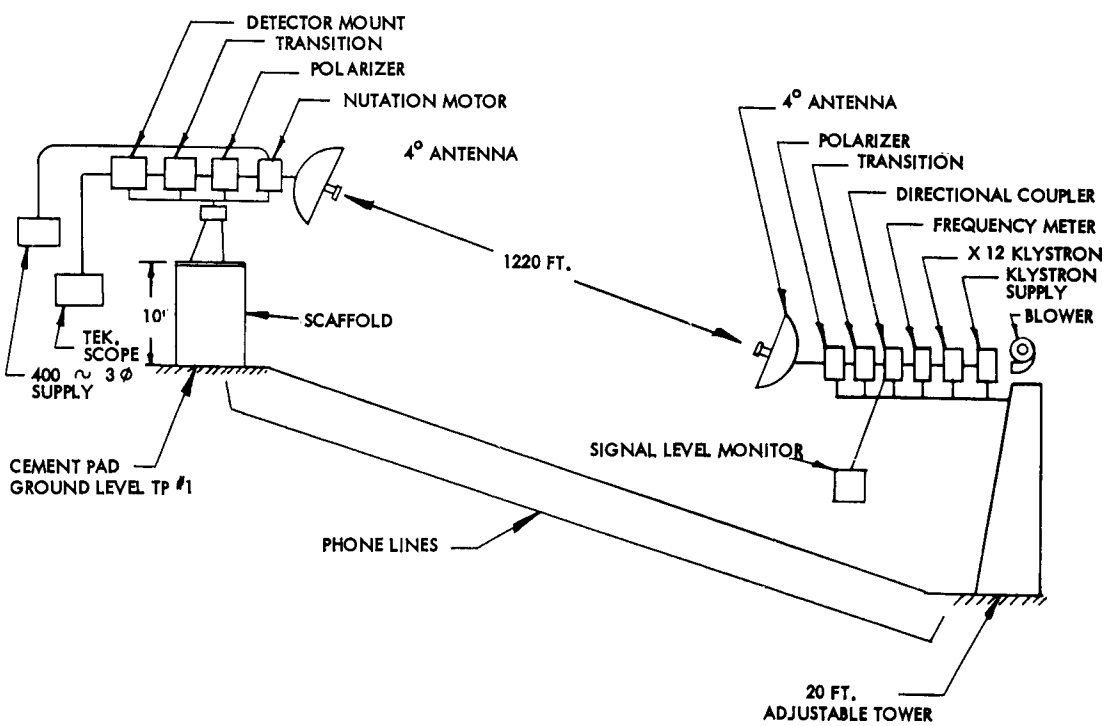

Figure 37. Intermediate Level Installation

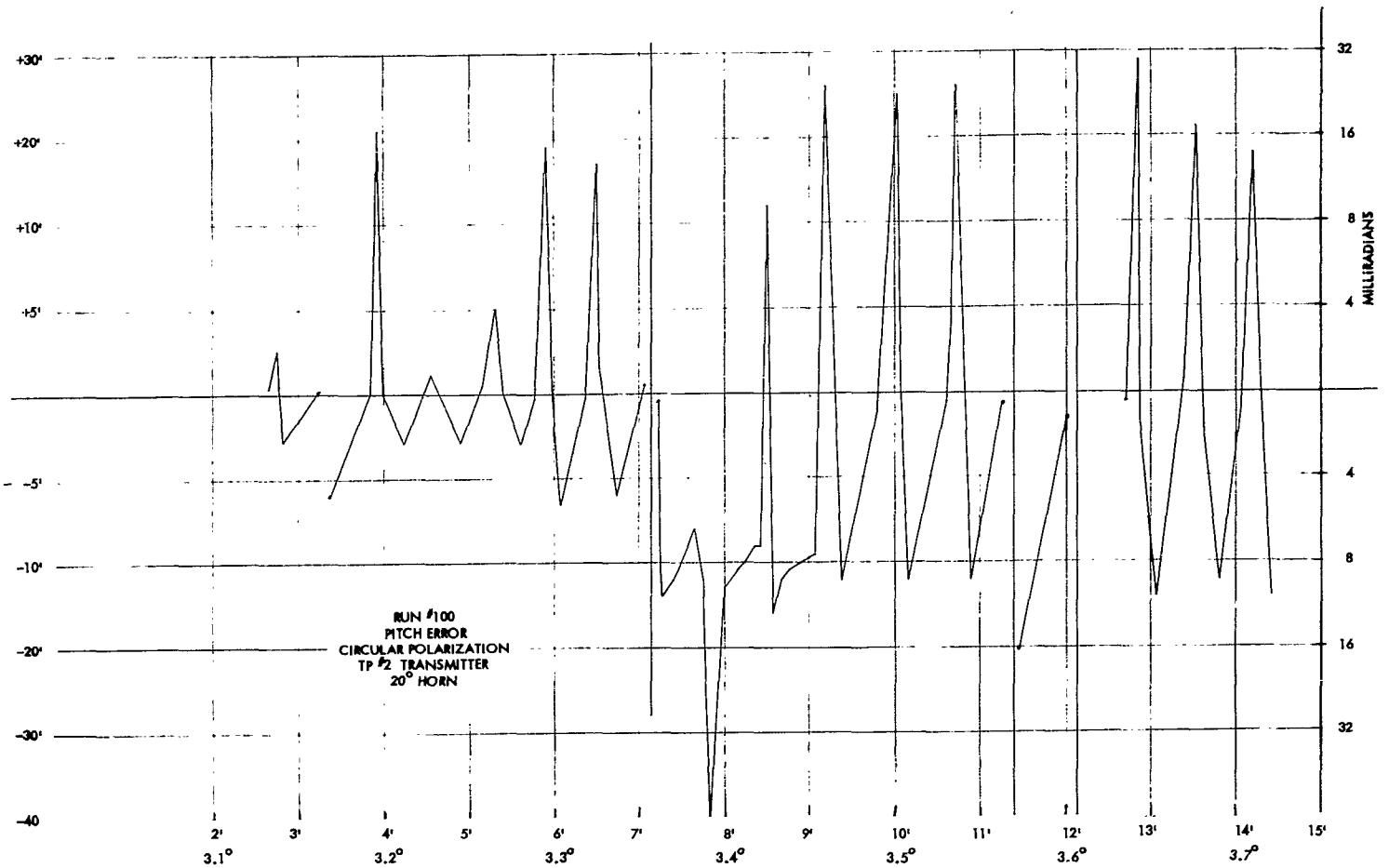

Figure 38. Boresight Error - Pitch - C. P. - 20° - Upper

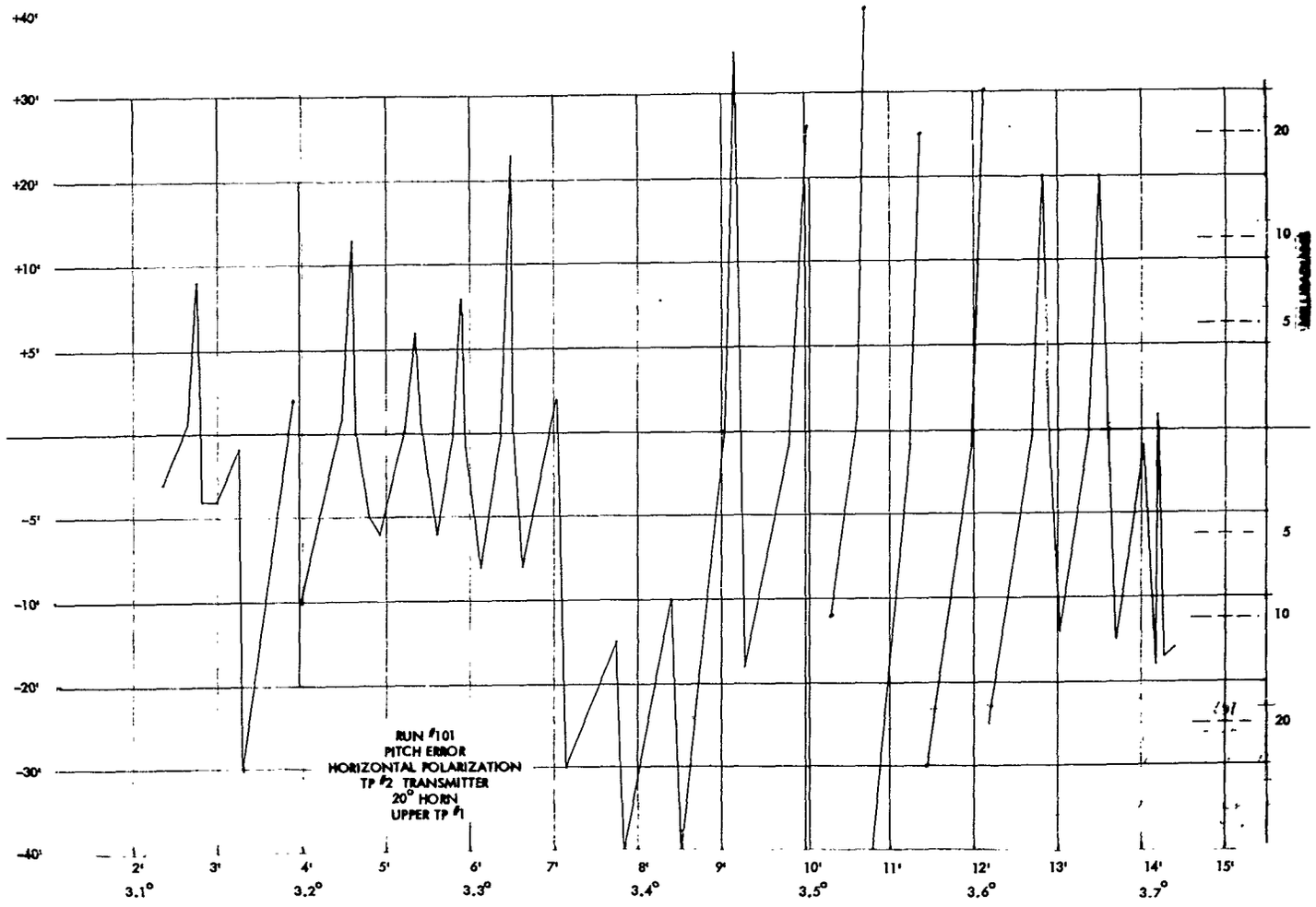

Figure 39. Boresight Error - Pitch - H. P. - 20° - Upper

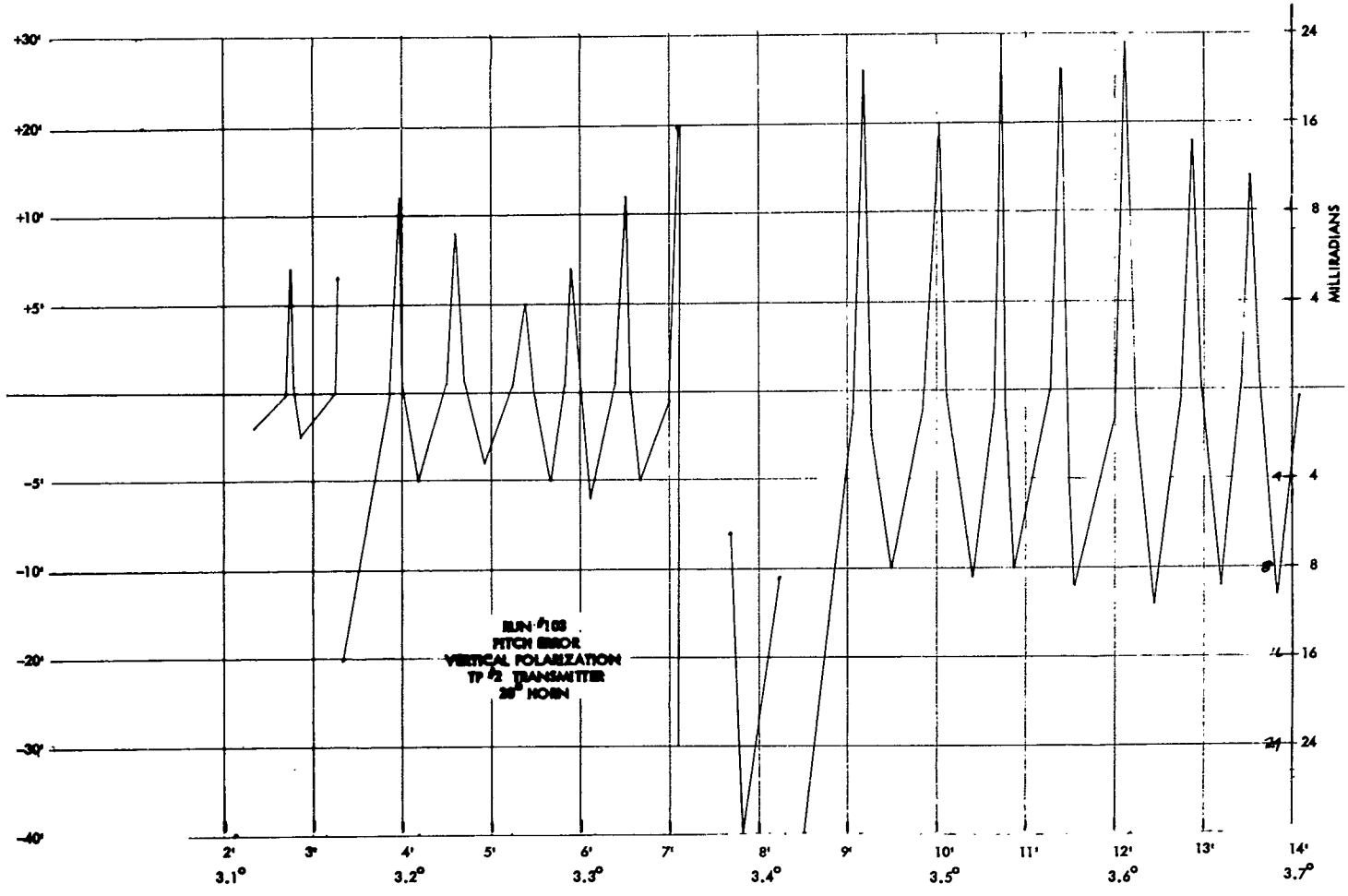

Figure 40. Boresight Error - Pitch - V. P. - 20° - Upper

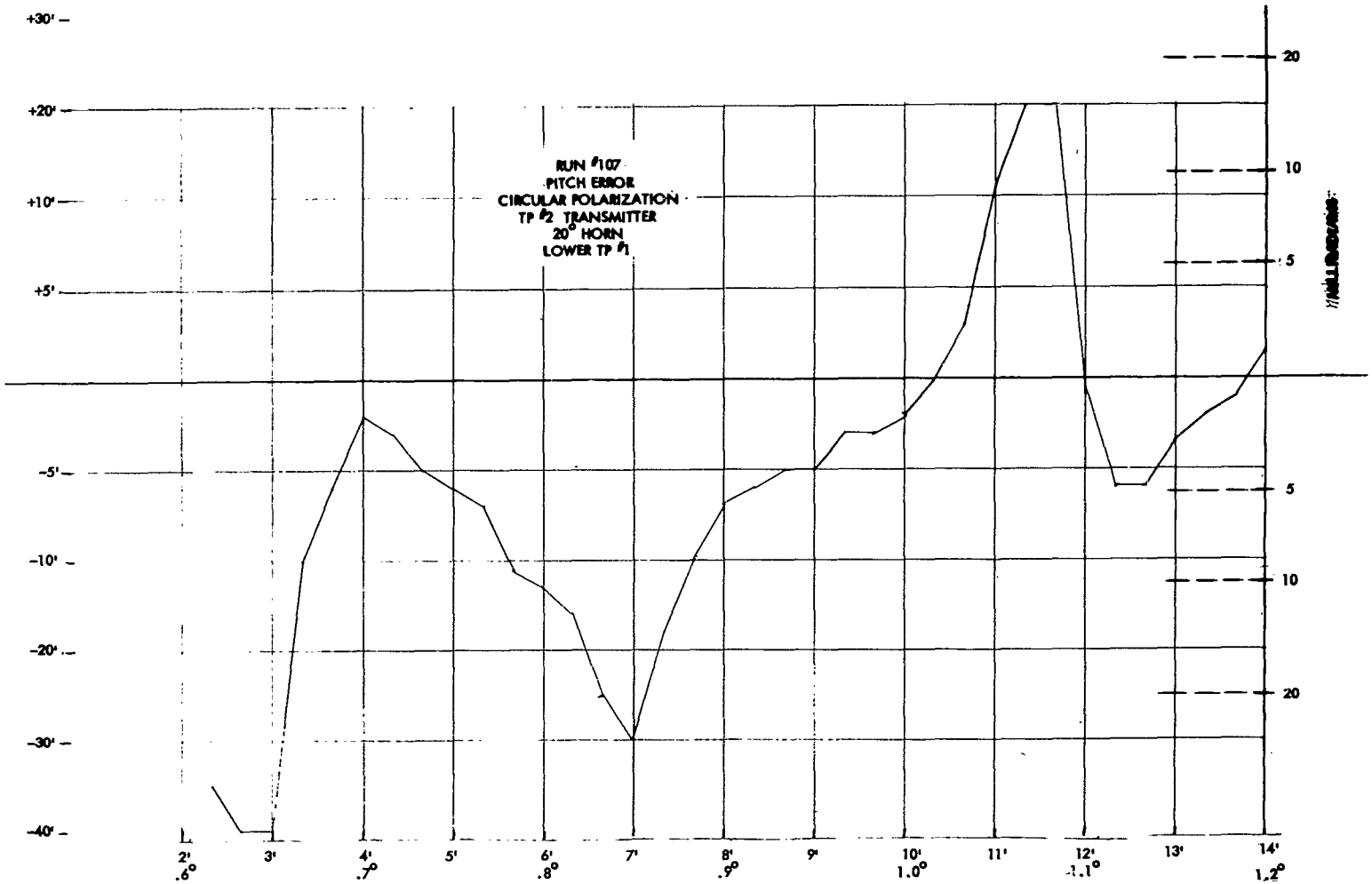

Figure 41. Boresight Error - Pitch - C. P. - 20° - Lower

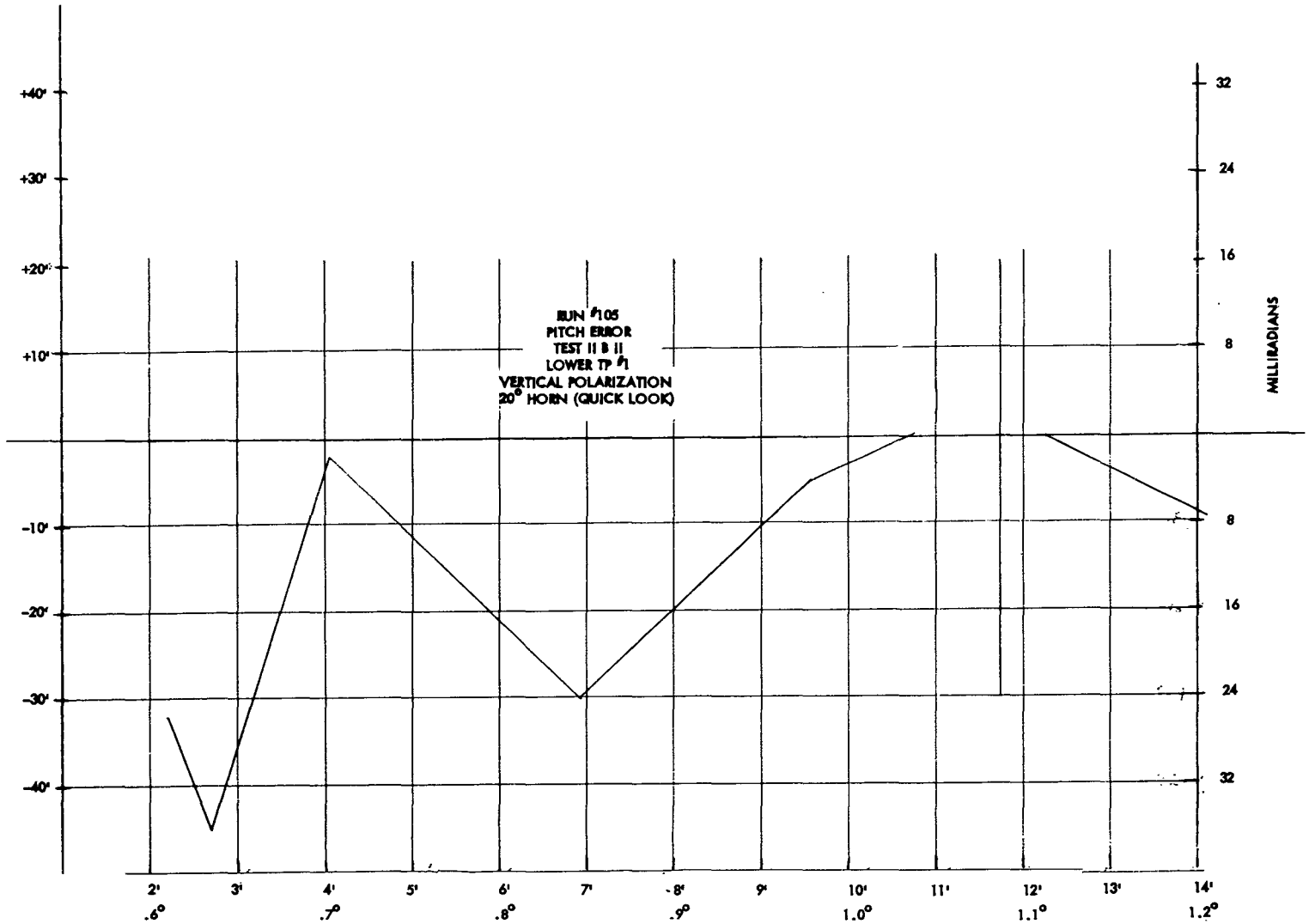

Figure 42. Boresight Error - Pitch - V. P. - 20° - Lower

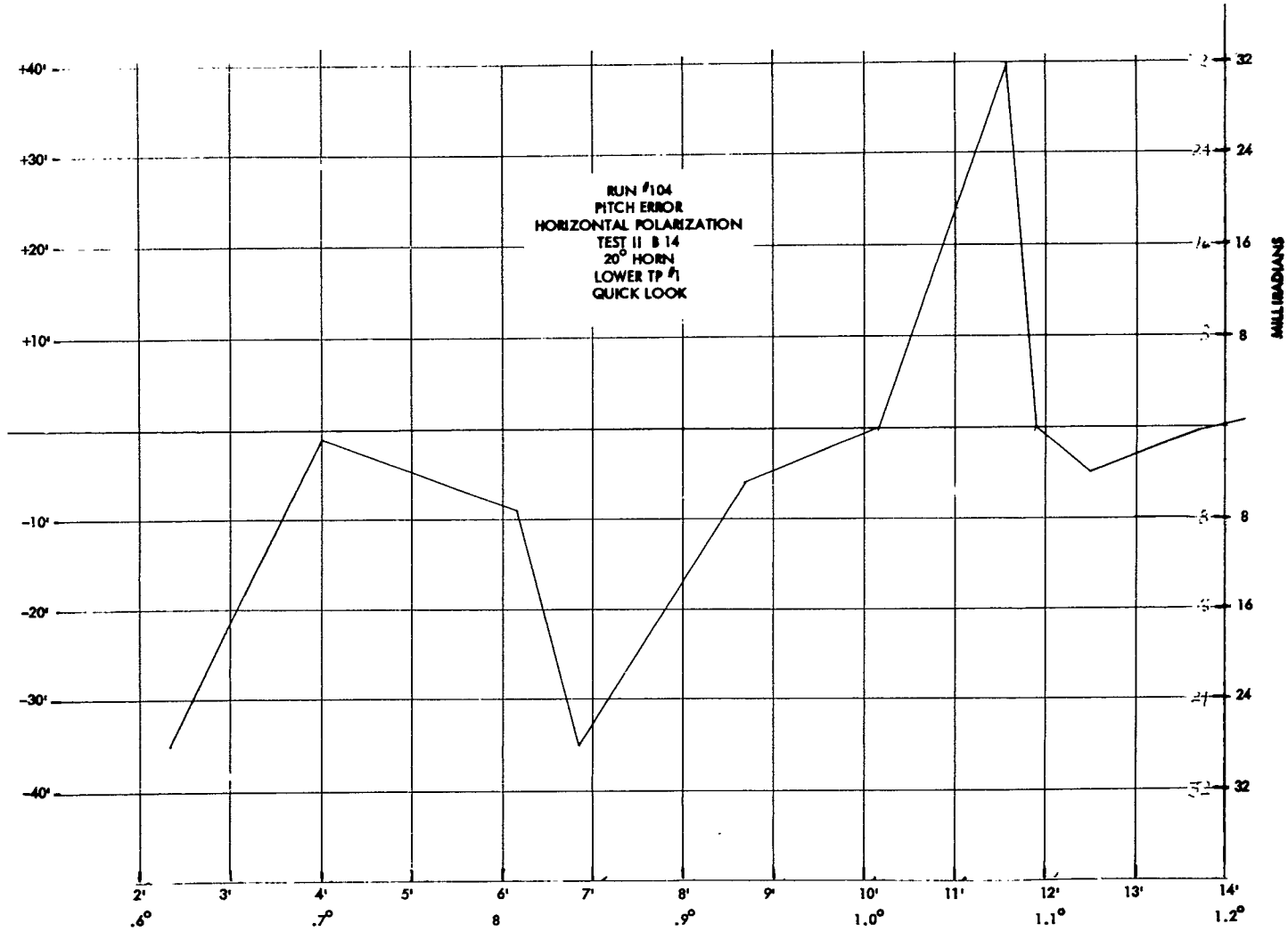

Figure 43. Boresight Error - Pitch - H. P. - 20° - Lower

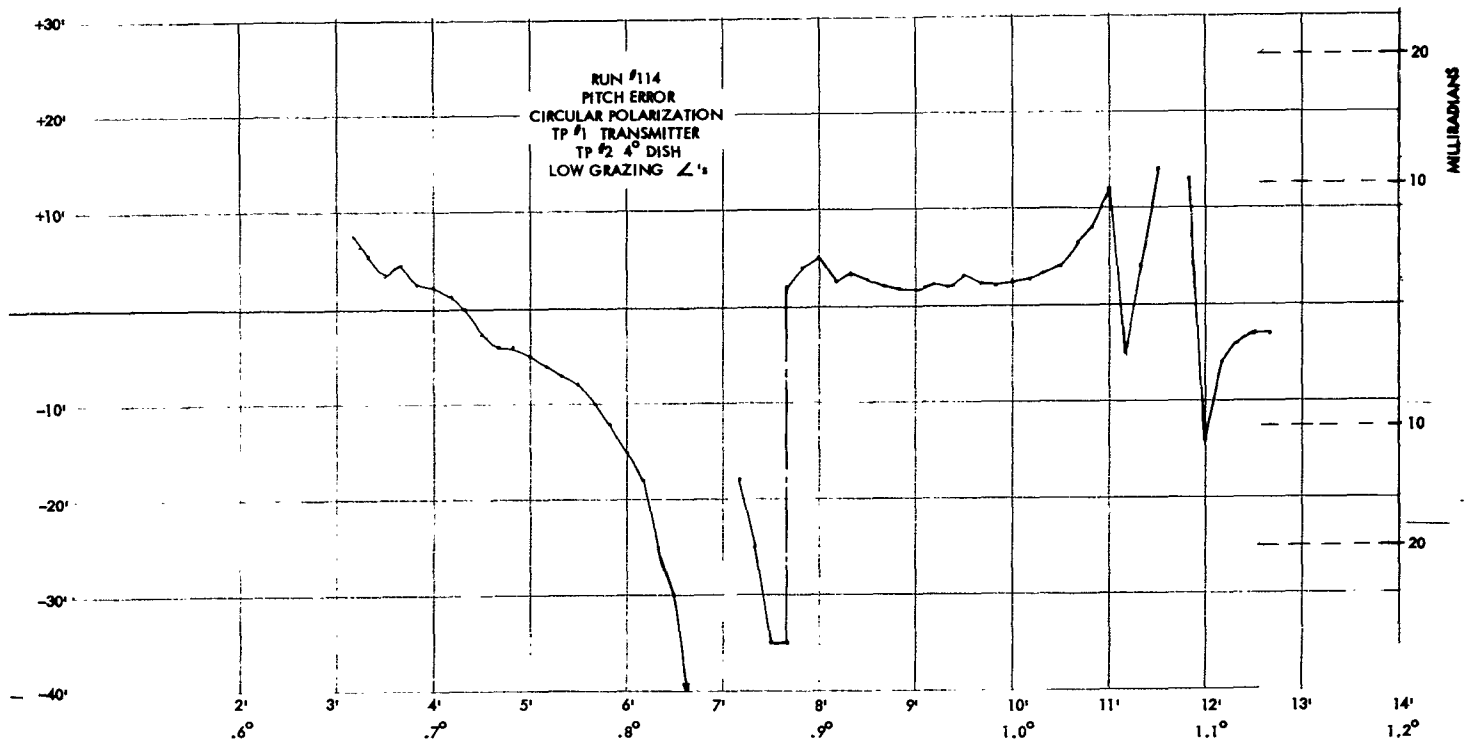

Figure 44. Boresight Error - Pitch - C. P. - 4° - Lower

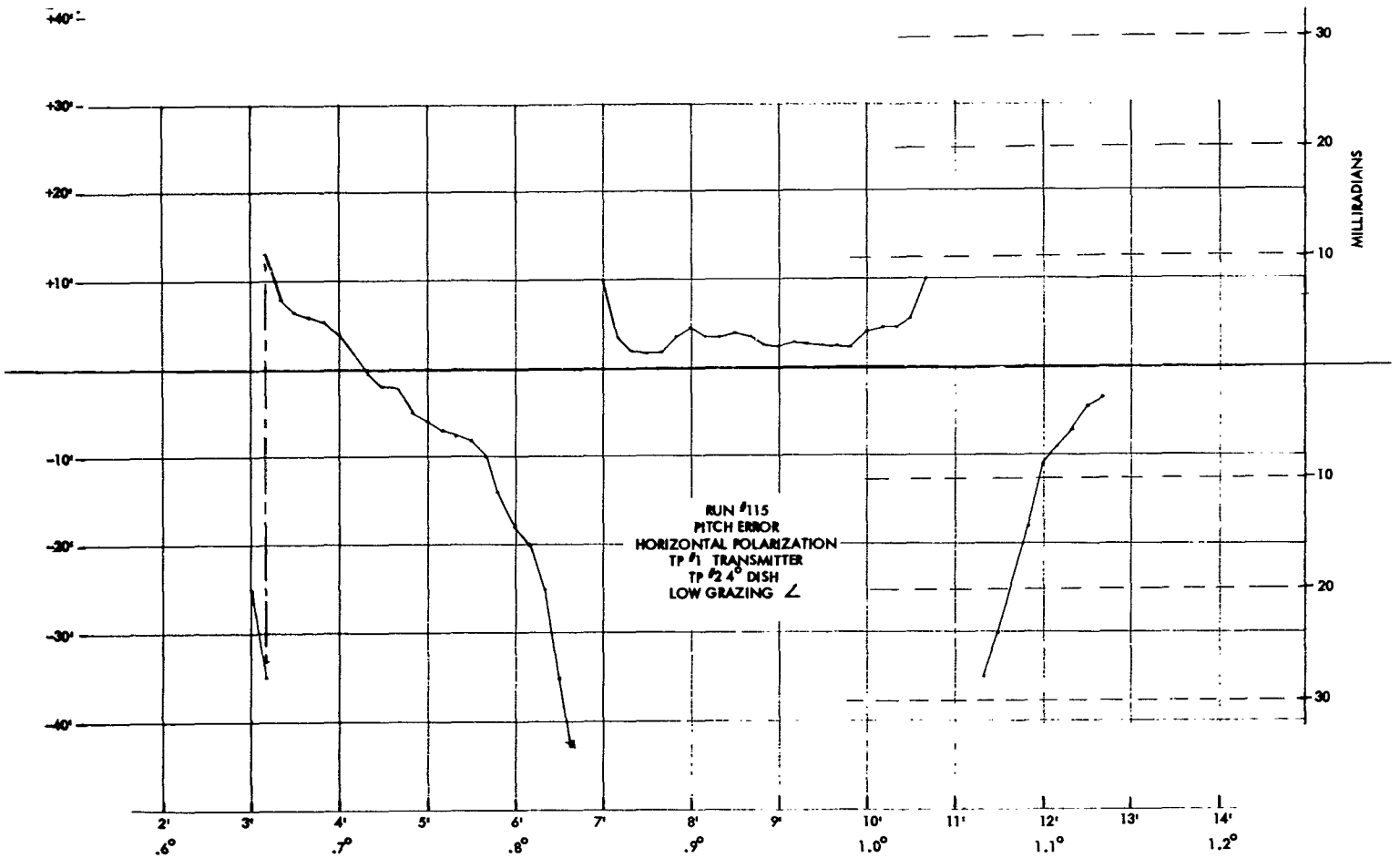

Figure 45. Boresight Error - Pitch - H. P. - 4° - Lower

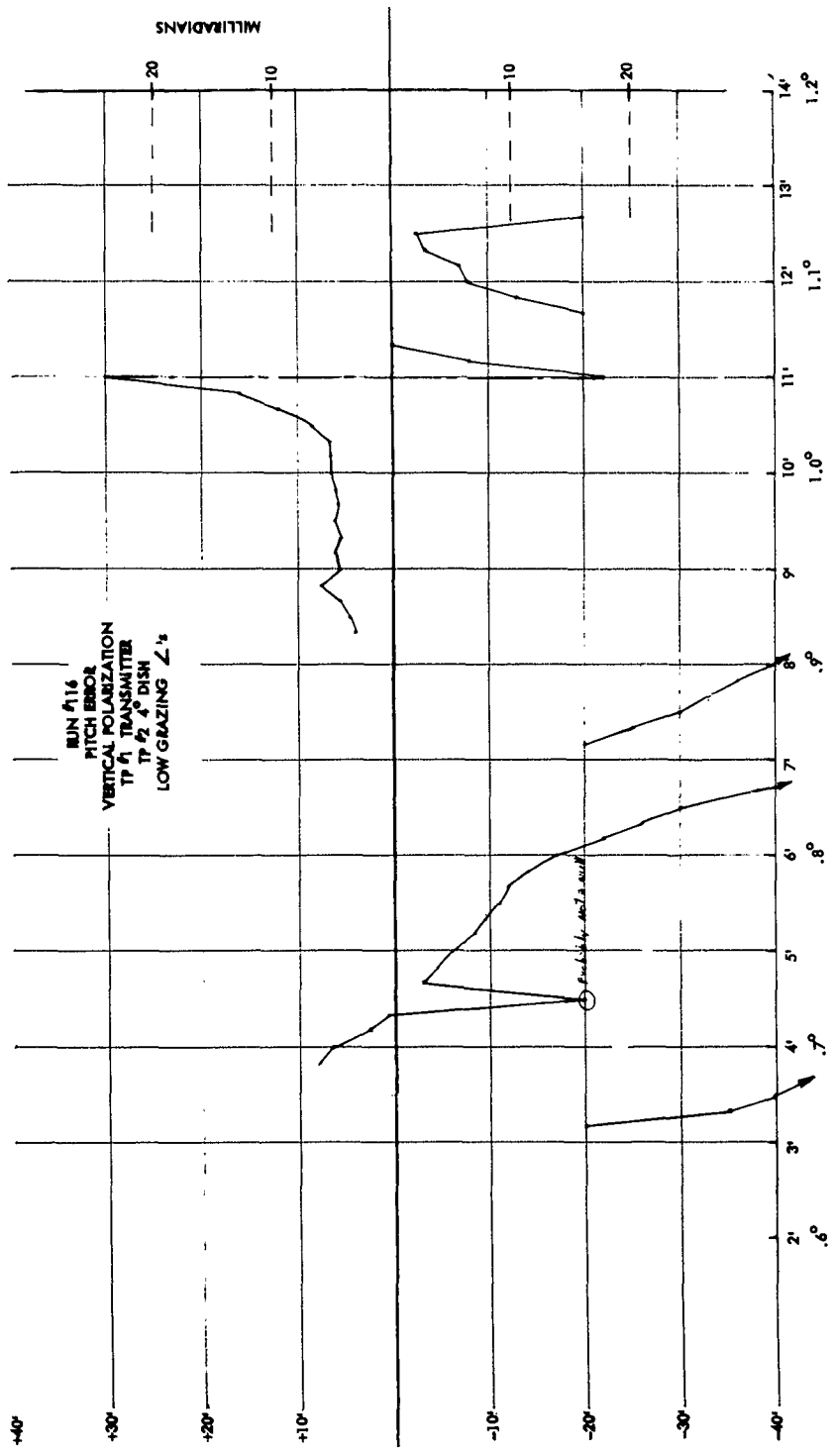

Figure 46. Boresight Error - Pitch - V. P. - 4° - Lower

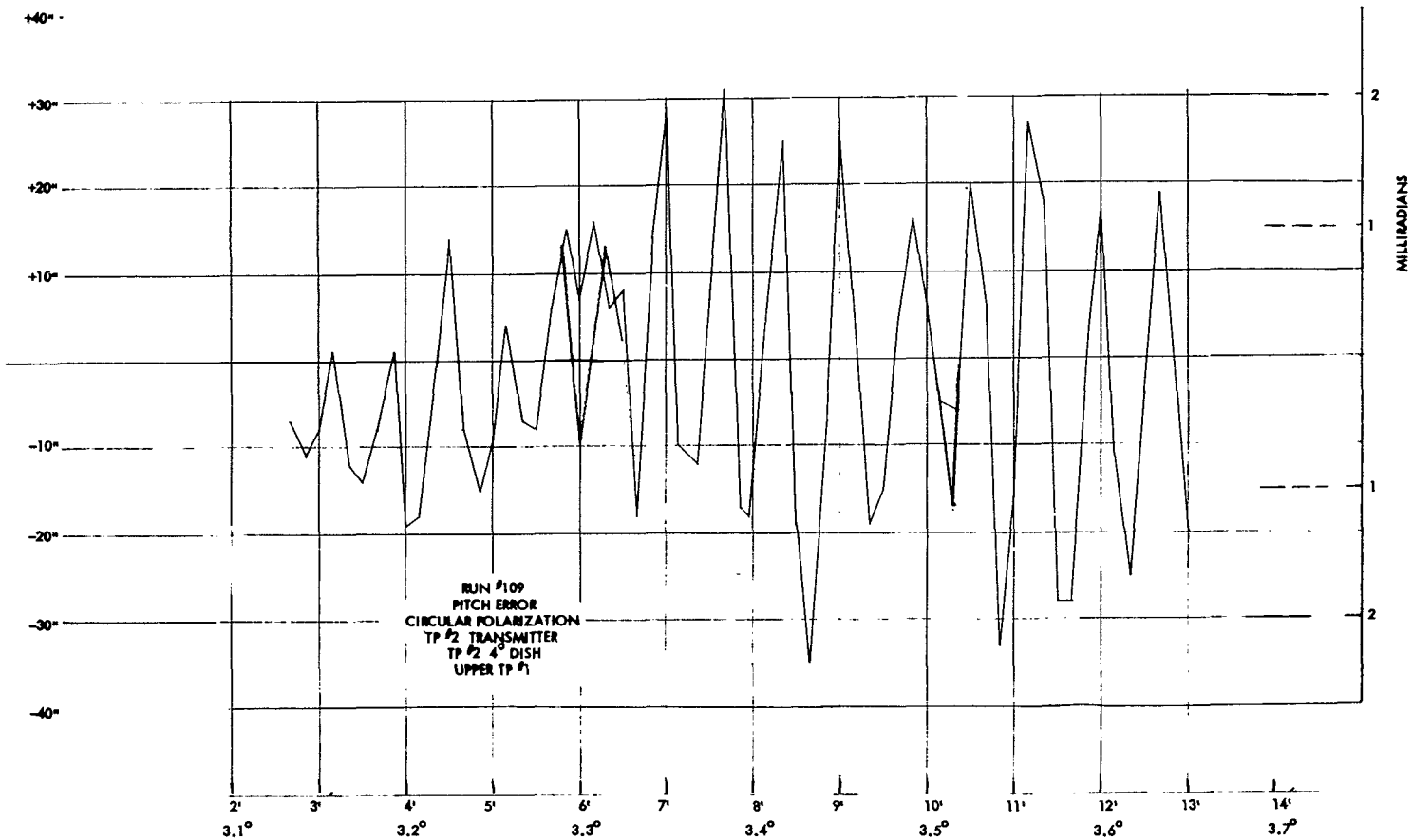

Figure 47. Boresight Error - Pitch - C. P. - 4° - Upper

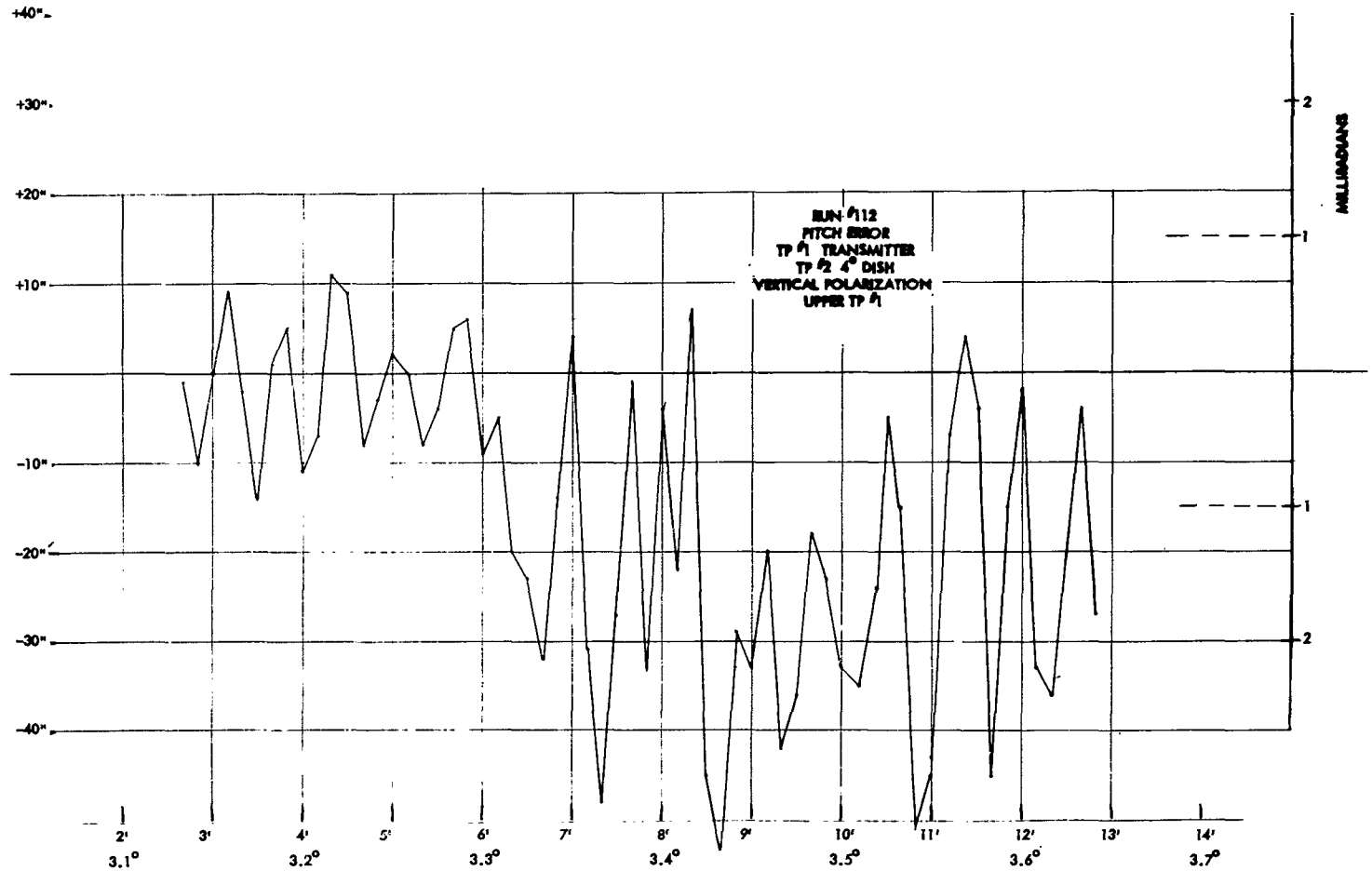

Figure 48. Boresight Error - Pitch - V. P. - 4° - Upper

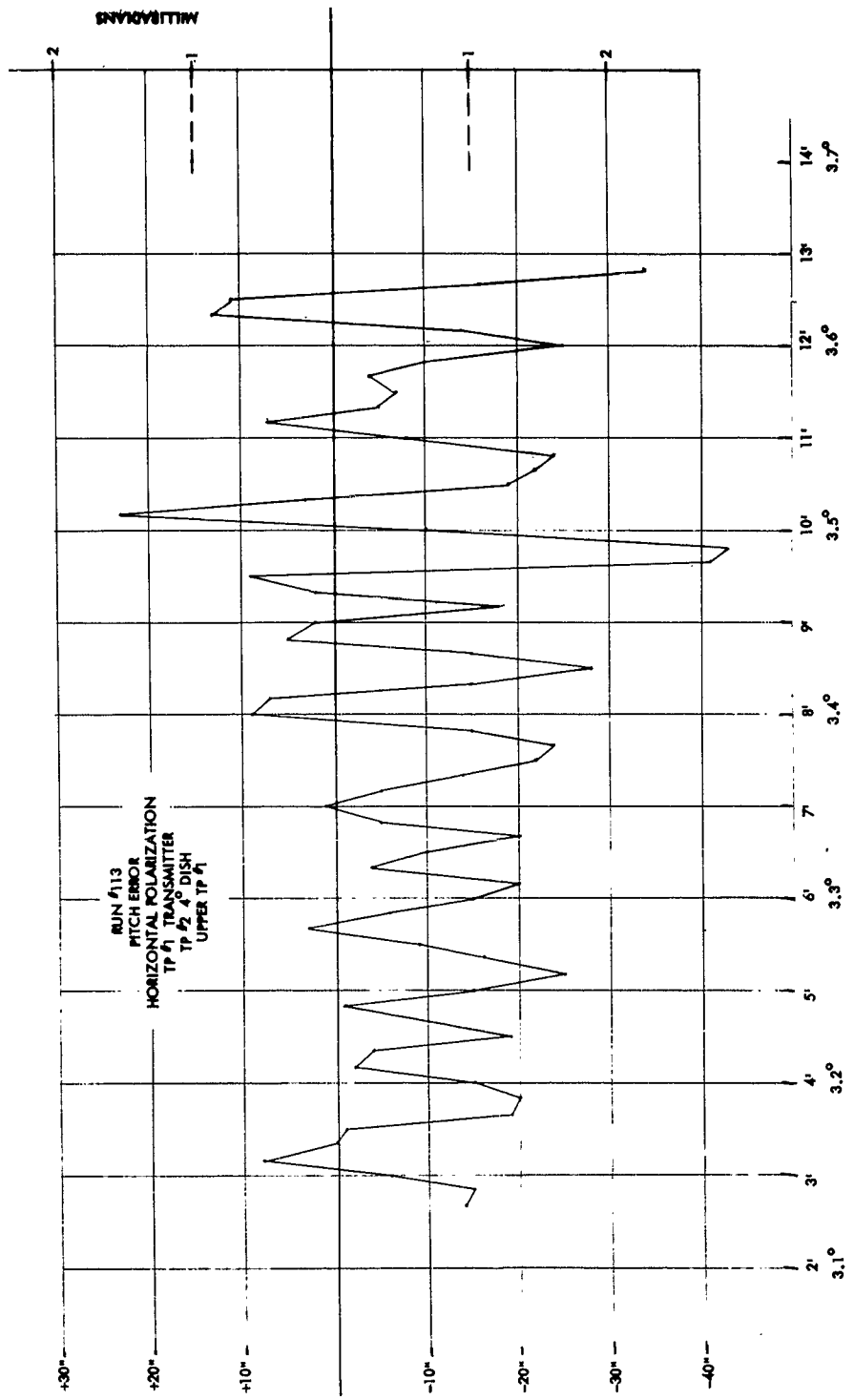

Figure 49. Boresight Error - Pitch - H. P. - 4° - Upper

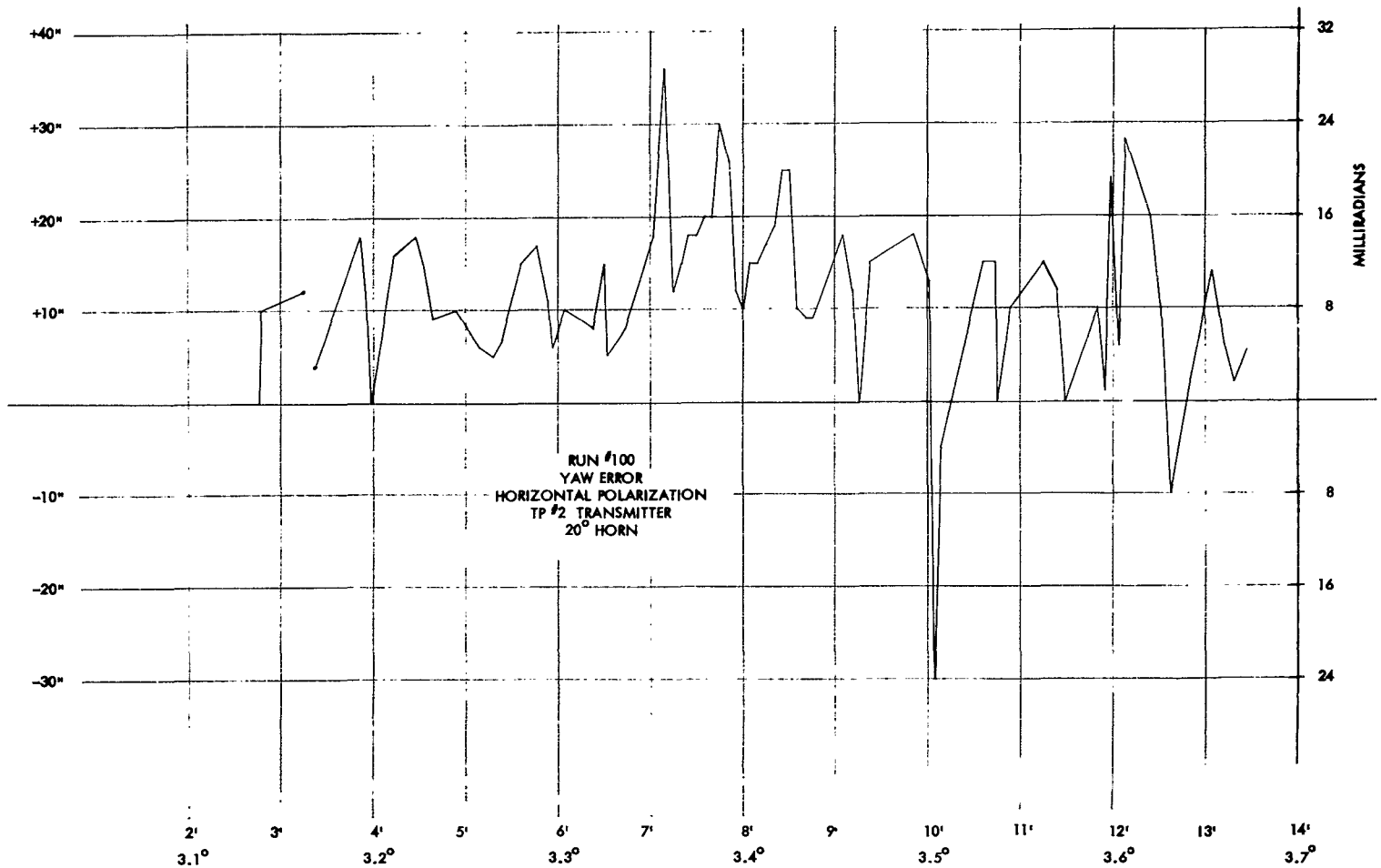

Figure 50. Boresight Error - Yaw - C. P. -20° - Upper

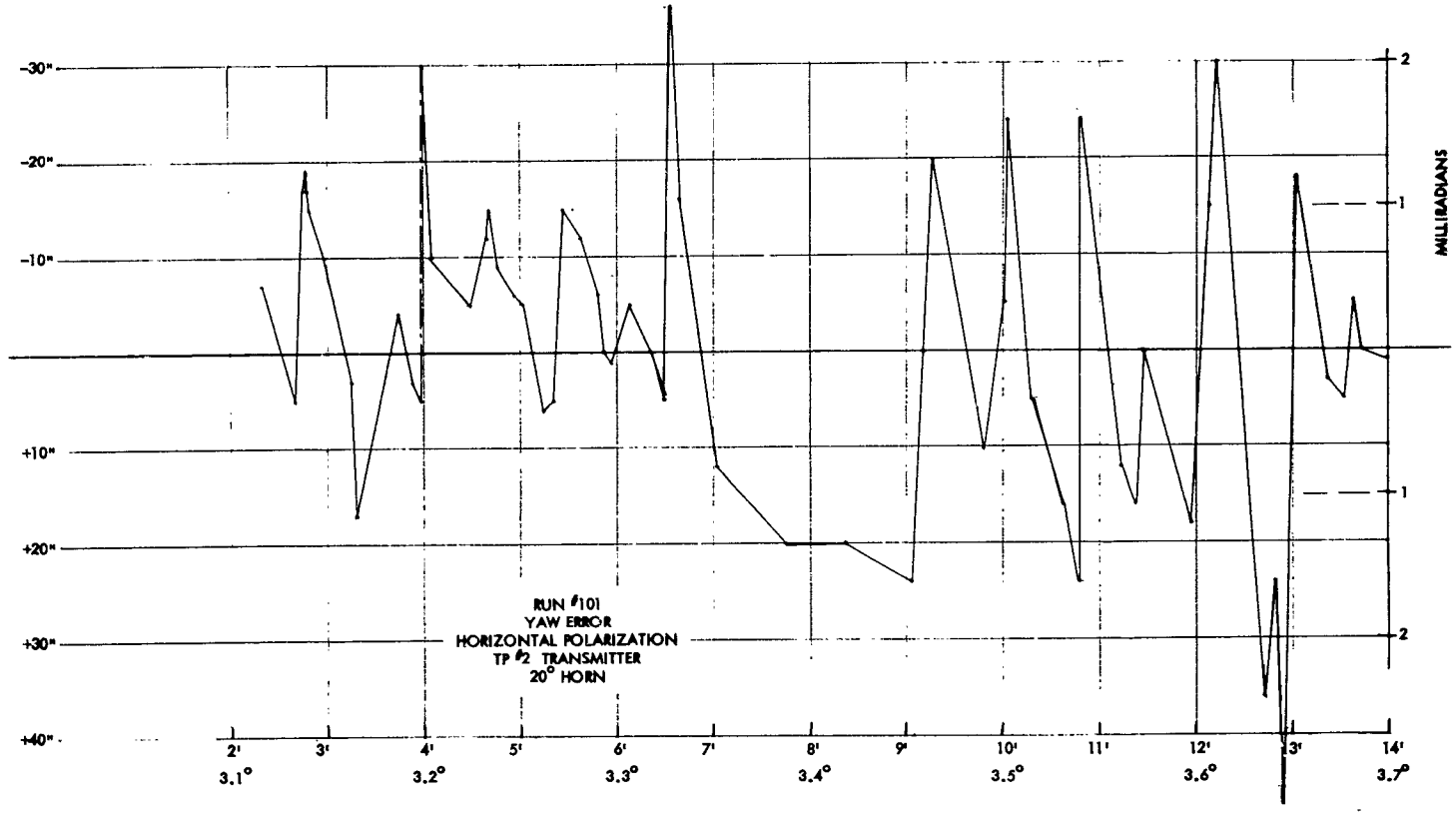

Figure 51. Boresight Error - Yaw - H. P. - 20° - Upper

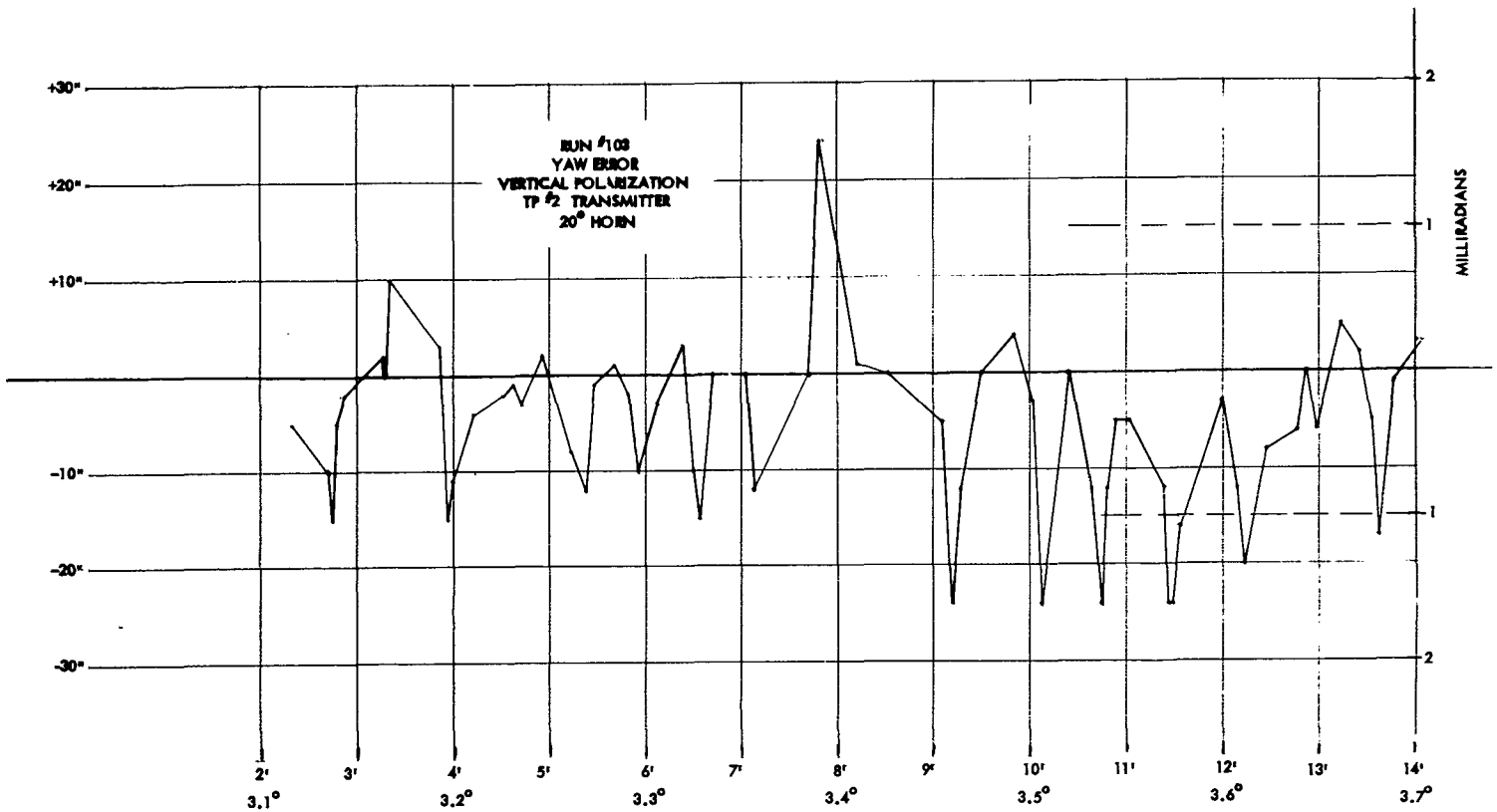

Figure 52. Boresight Error - Yaw - V. P. - 20° - Upper

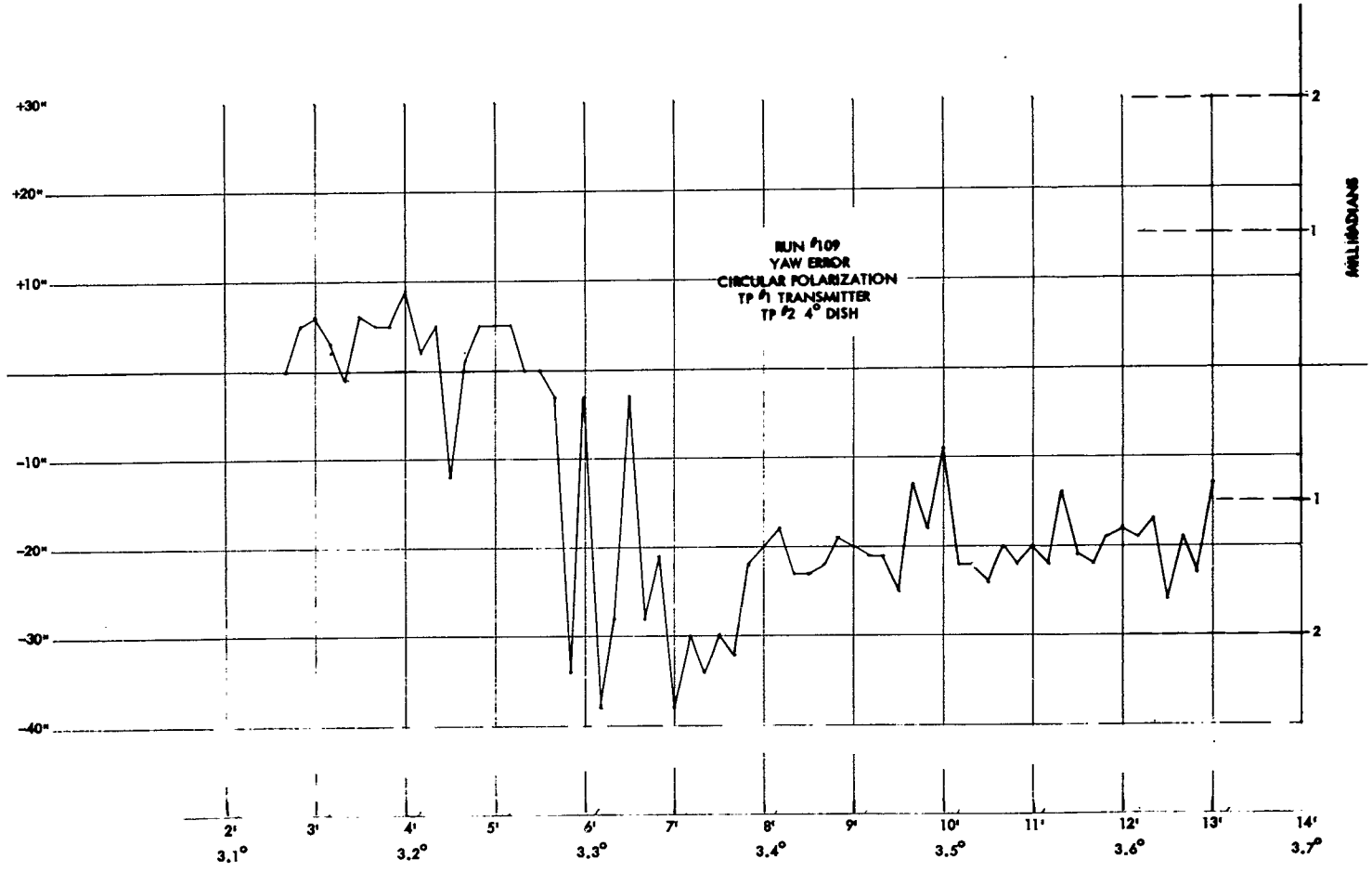

Figure 53. Boresight Error - Yaw - C. P. - 4° - Lower

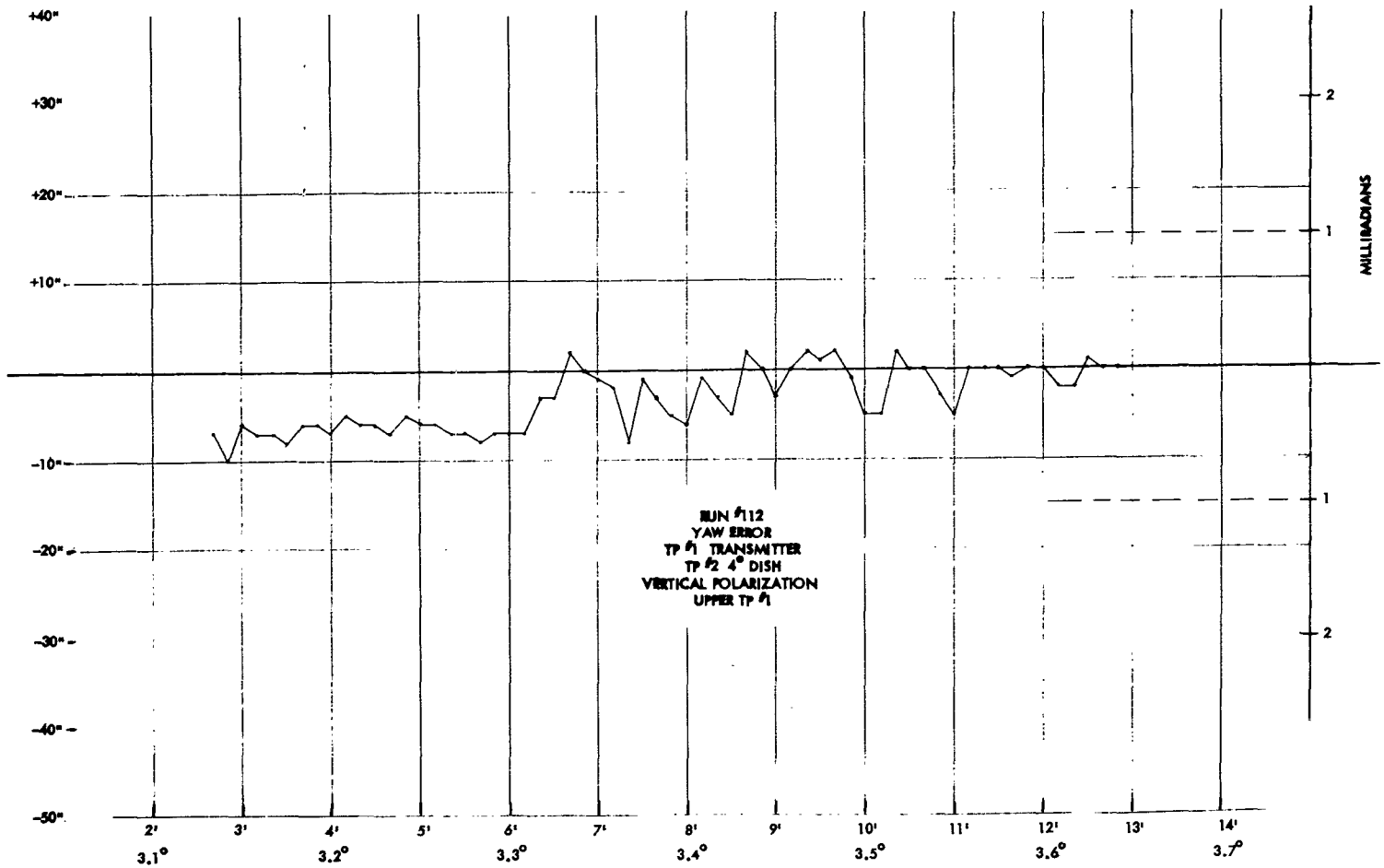

Figure 54. Boresight Error - Yaw - V. P. - 4° - Lower

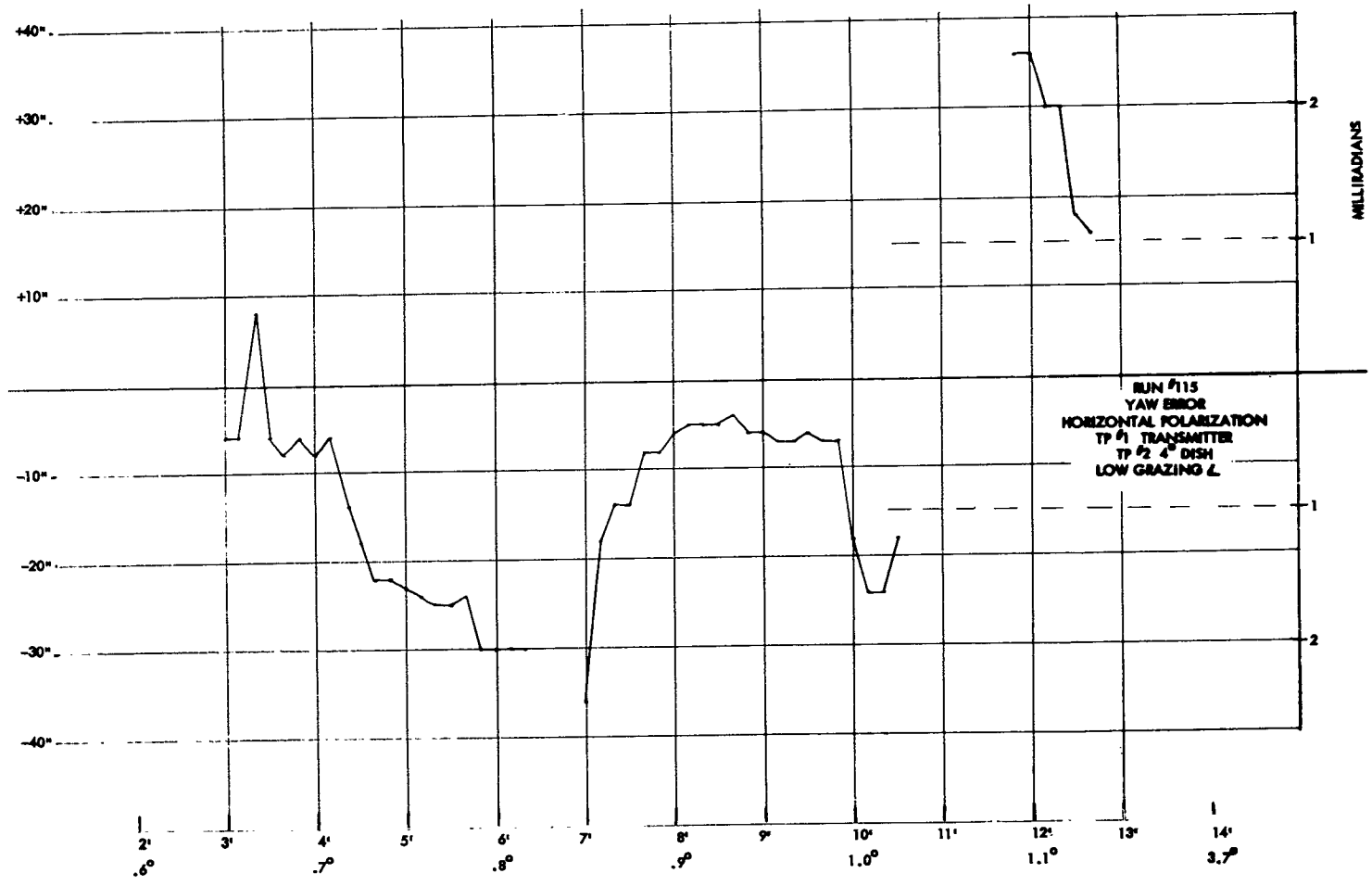

Figure 55. Boresight Error - Yaw - H. P. - 4° - Lower

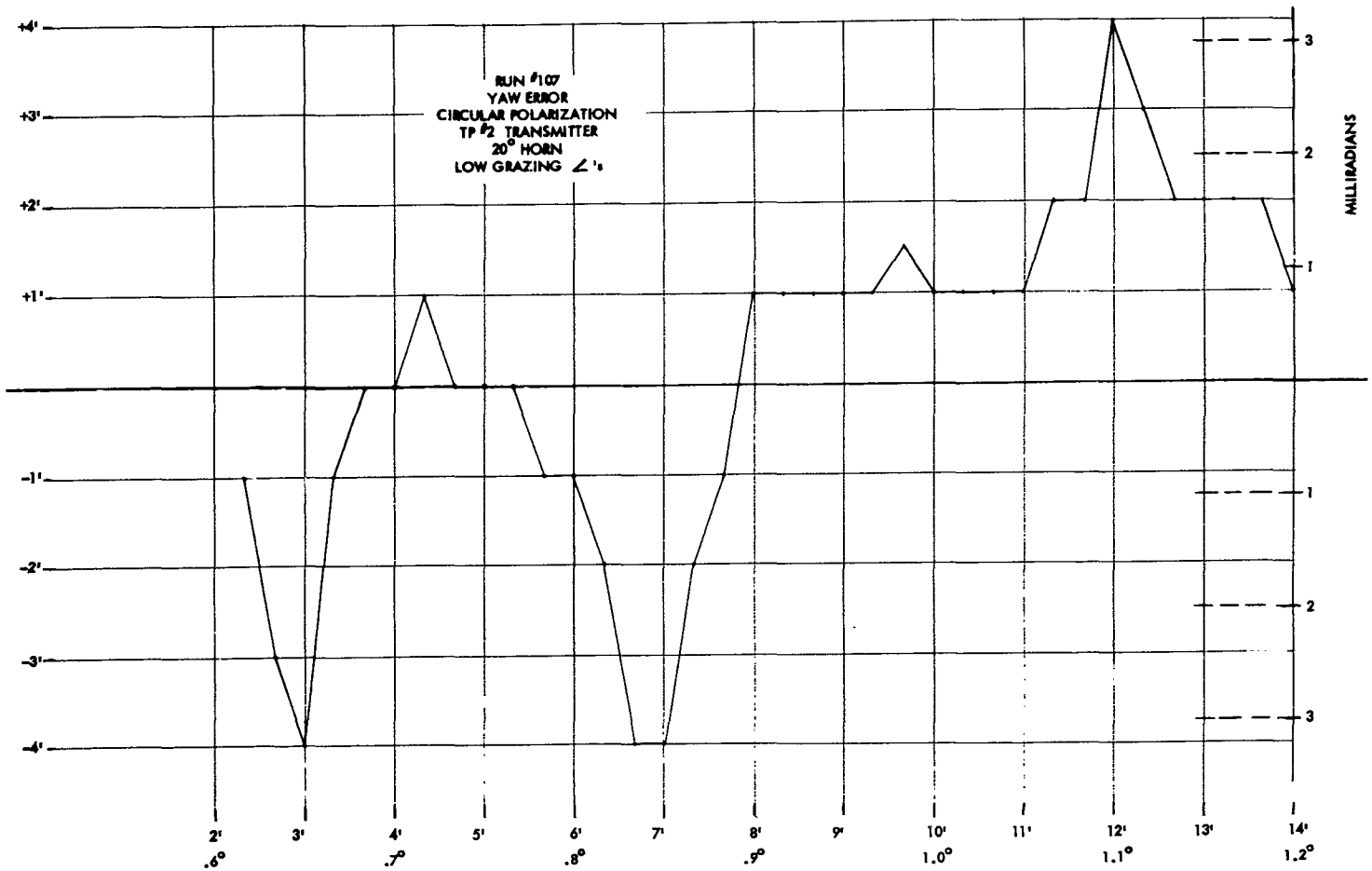

Figure 56. Boresight Error - Yaw - C. P. - 20° - Lower

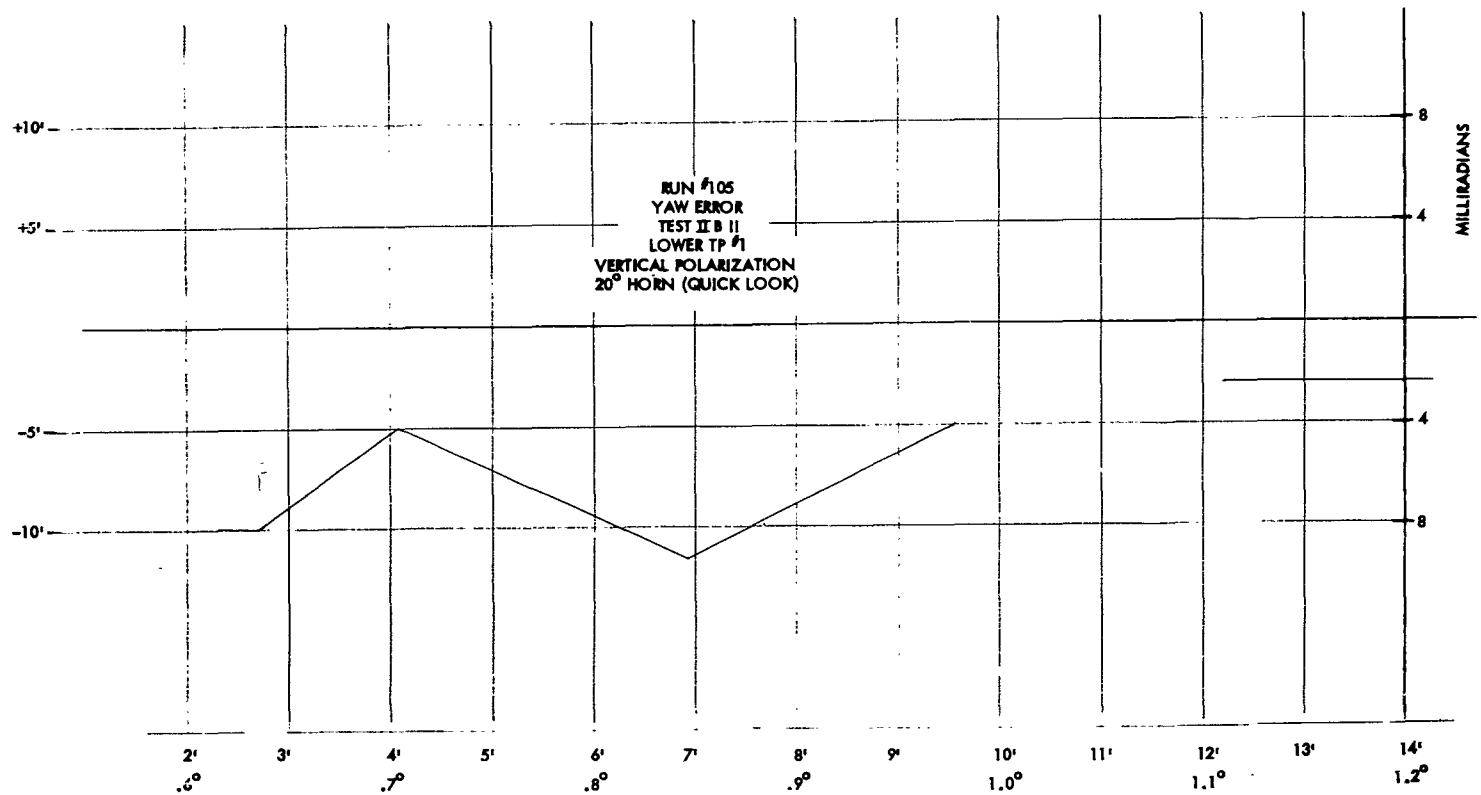

Figure 57. Boresight Error - Yaw - V. P. - 20° - Lower

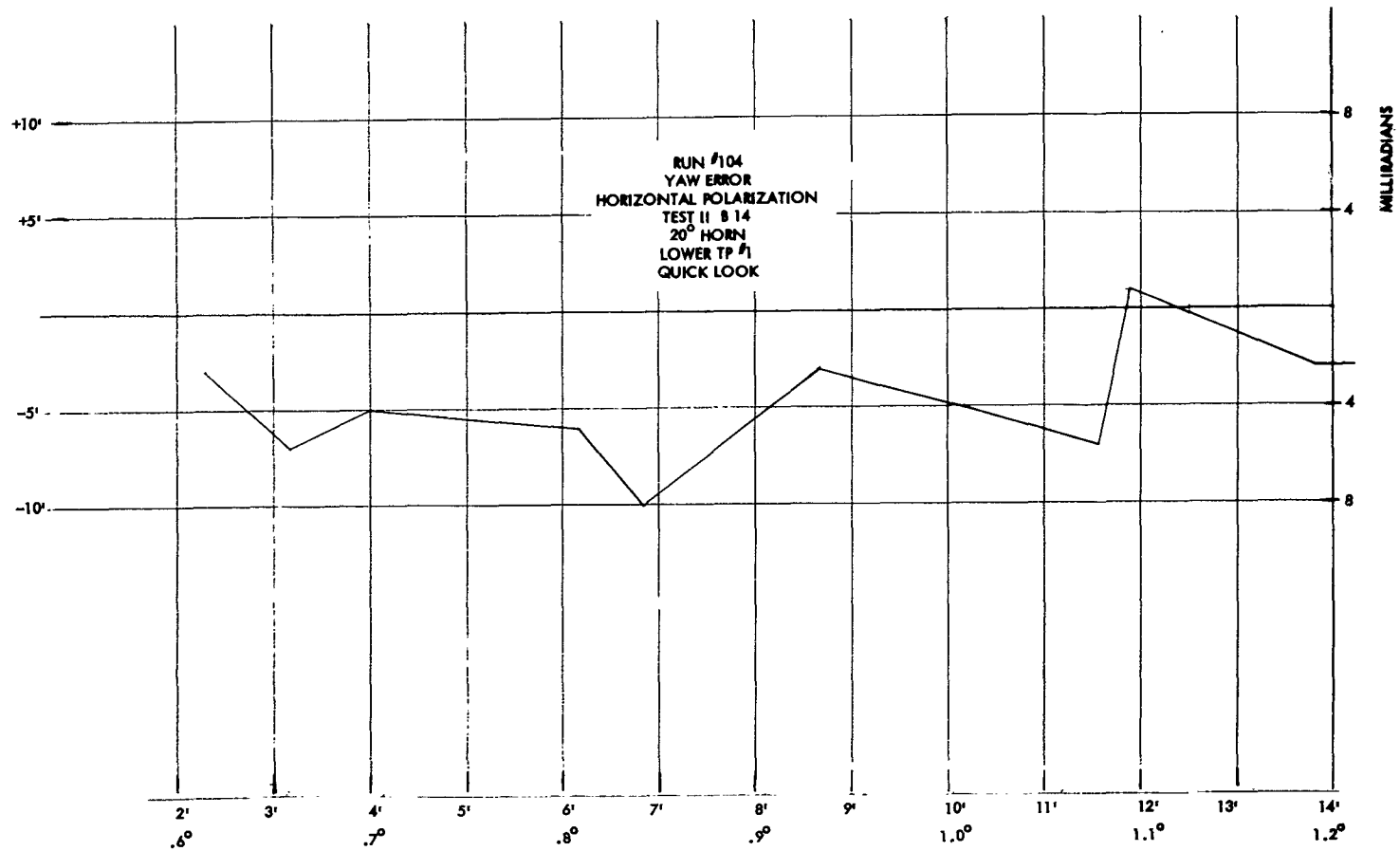

Figure 58. Boresight Error - Yaw - H. P. - 20° - Lower

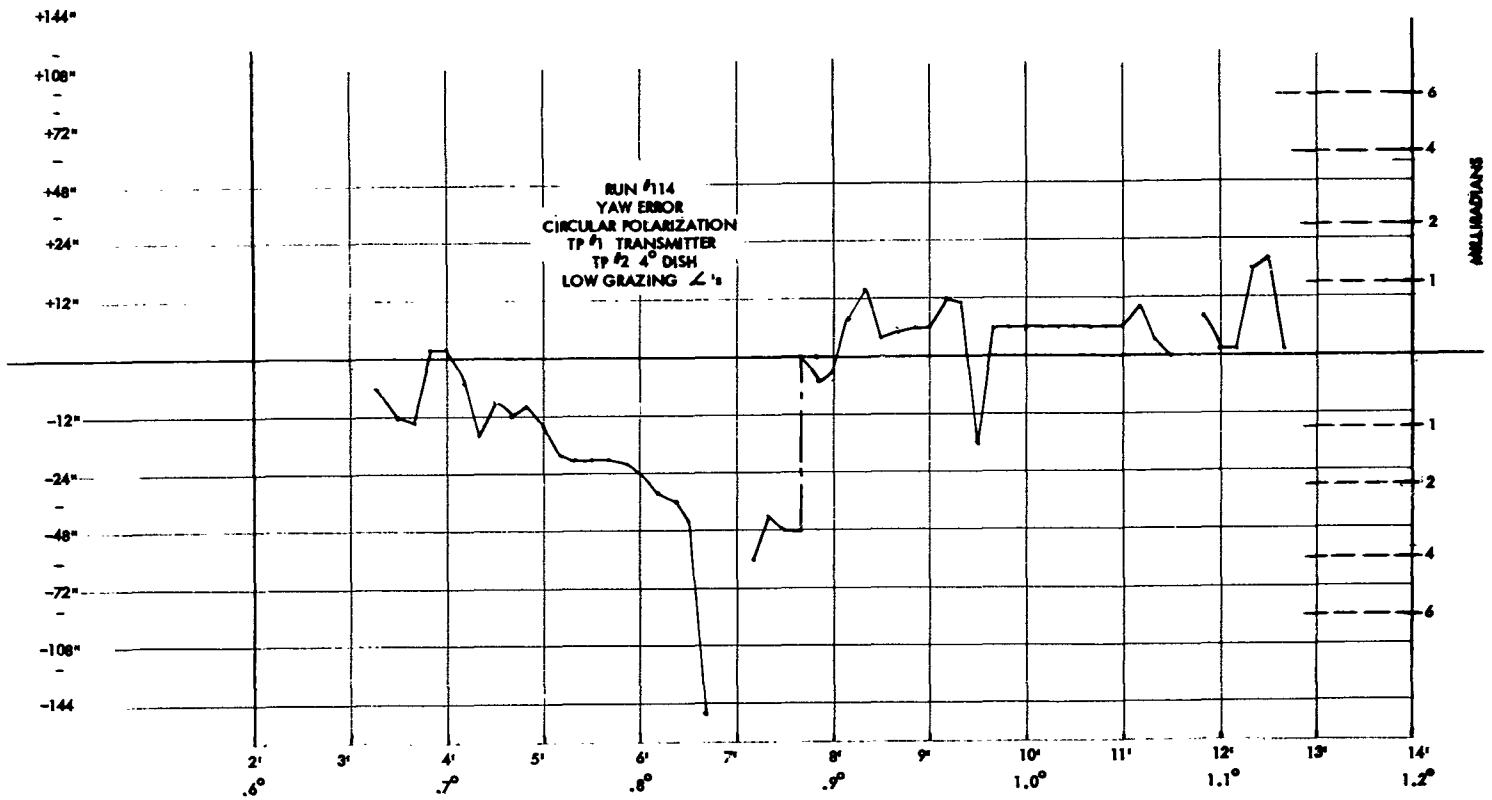

Figure 59. Boresight Error - Yaw - C. P. - 4° - Lower

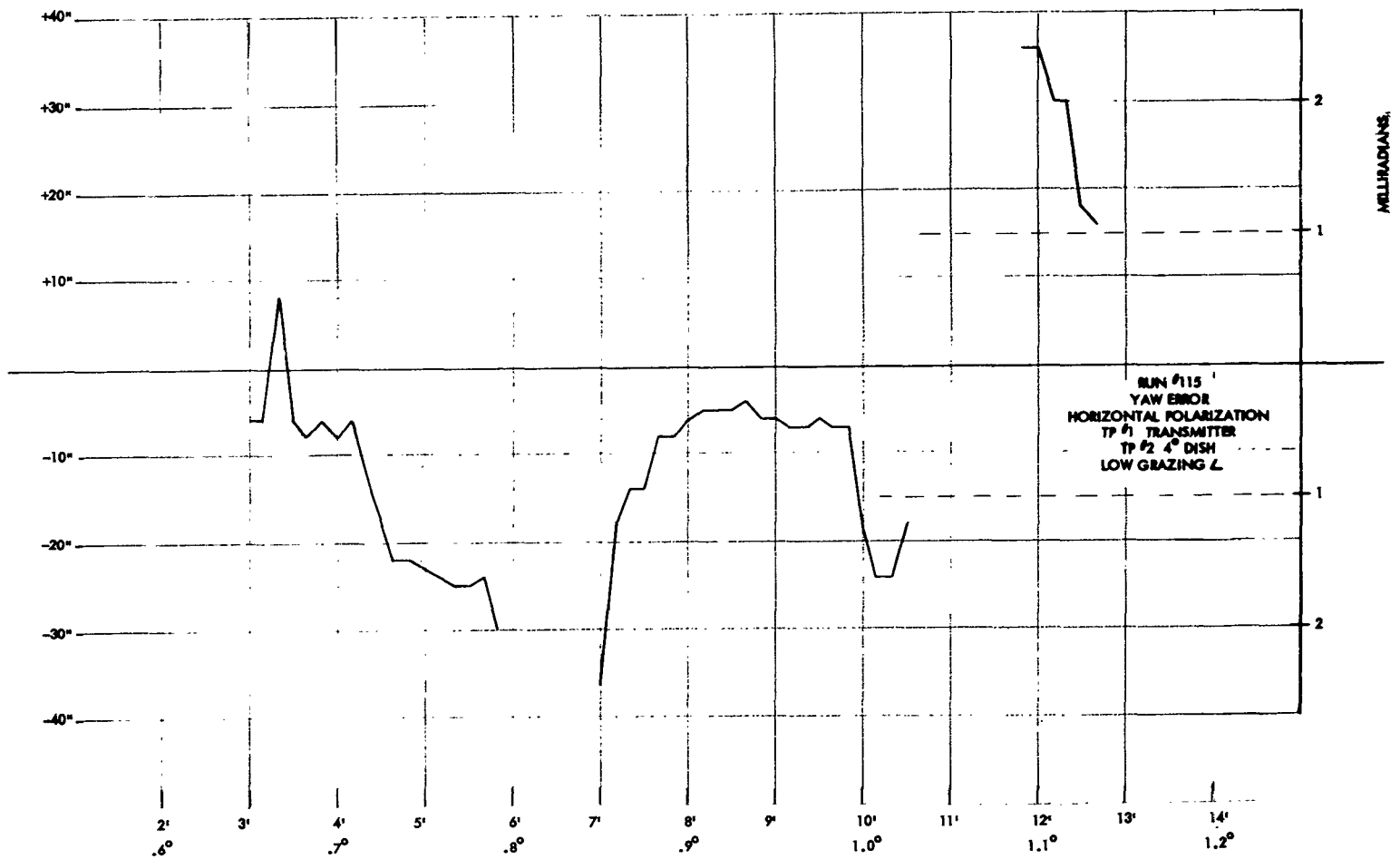

Figure 60. Boresight Error - Yaw - H. P. - 4° - Lower

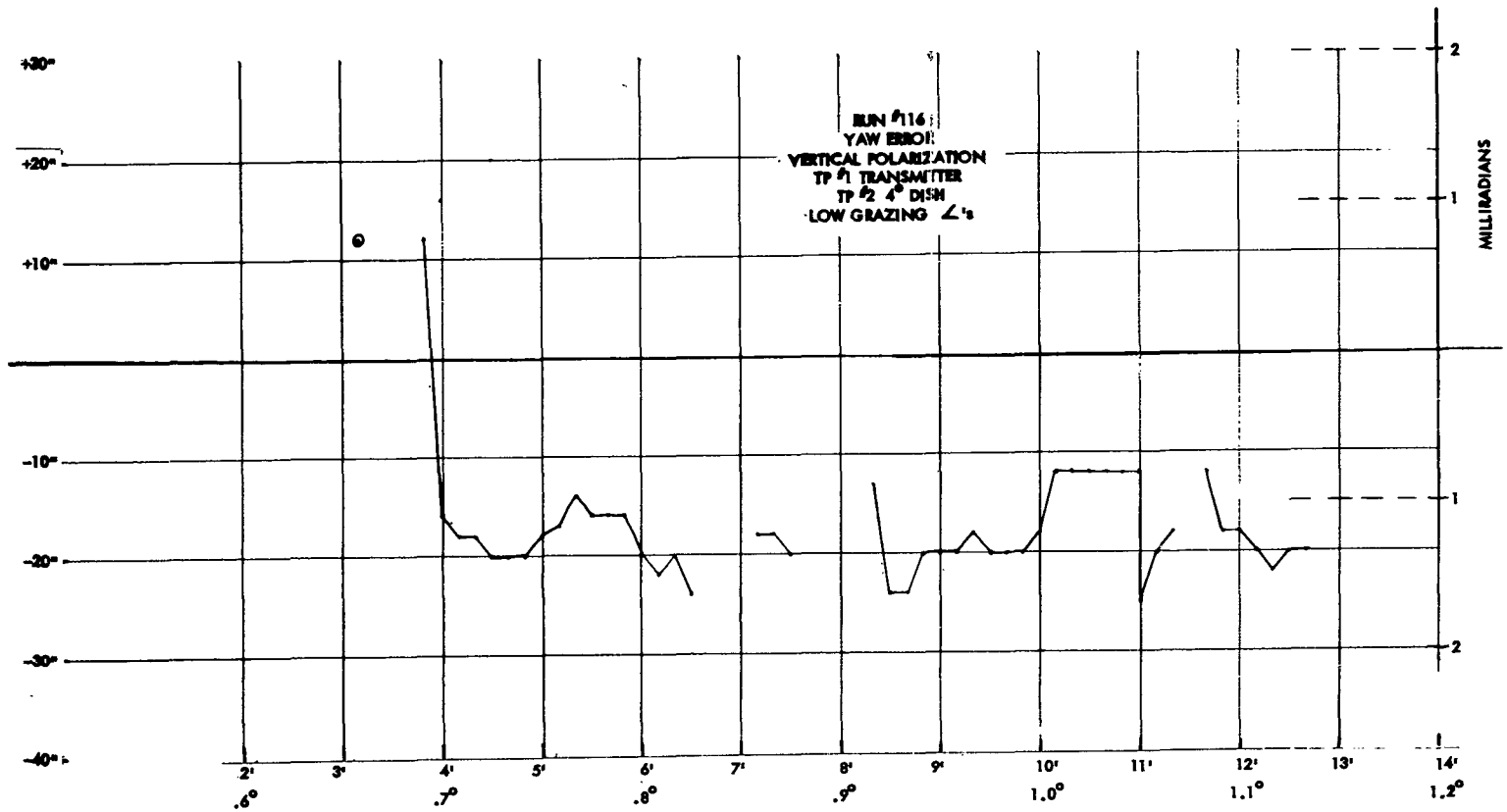

Figure 61. Boresight Error - Yaw - V. P. - 4° - Lower

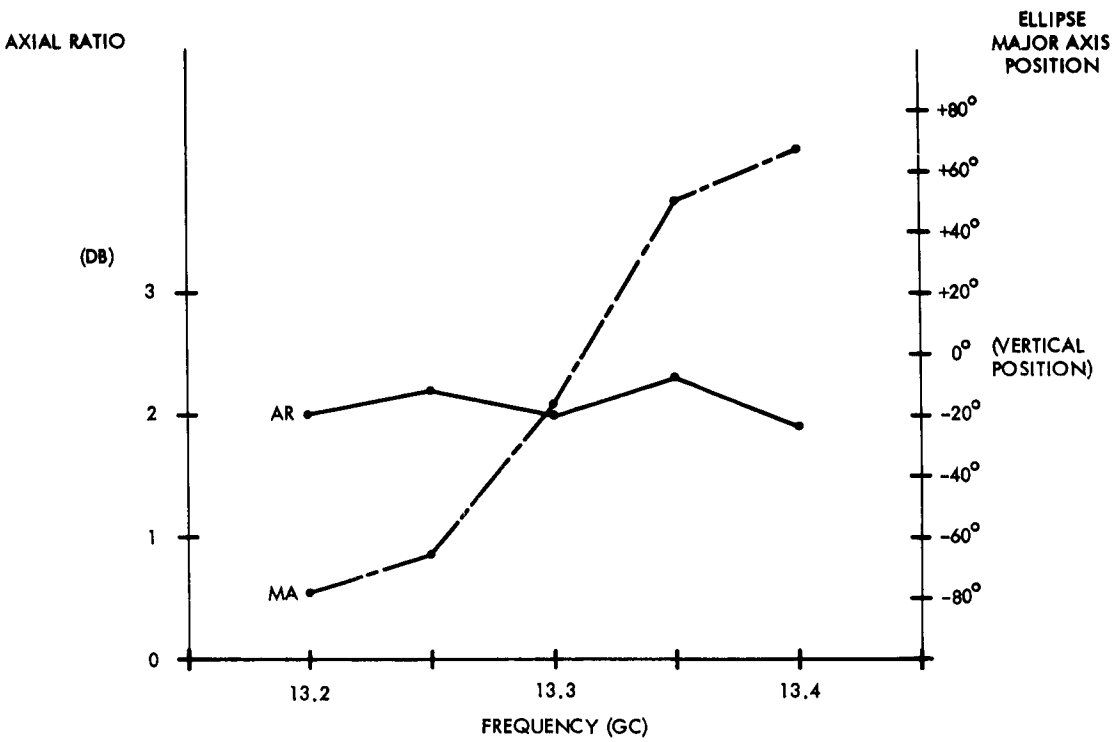

Figure 62. Test Point No. 1 Assembly Axial Ratio vs Frequency

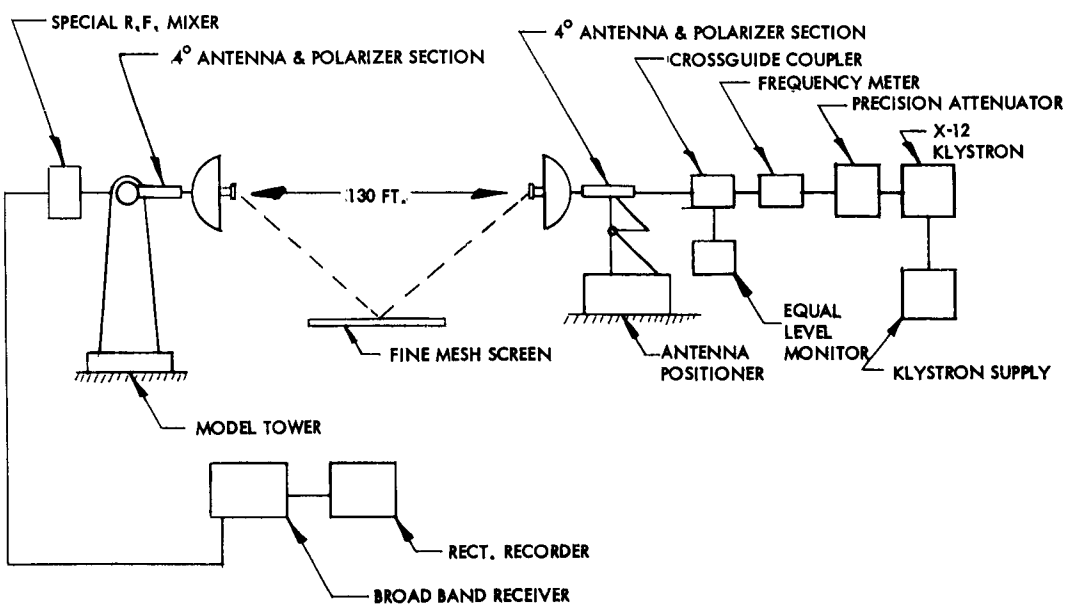

Figure 63. Brewster Angle Test Set-up

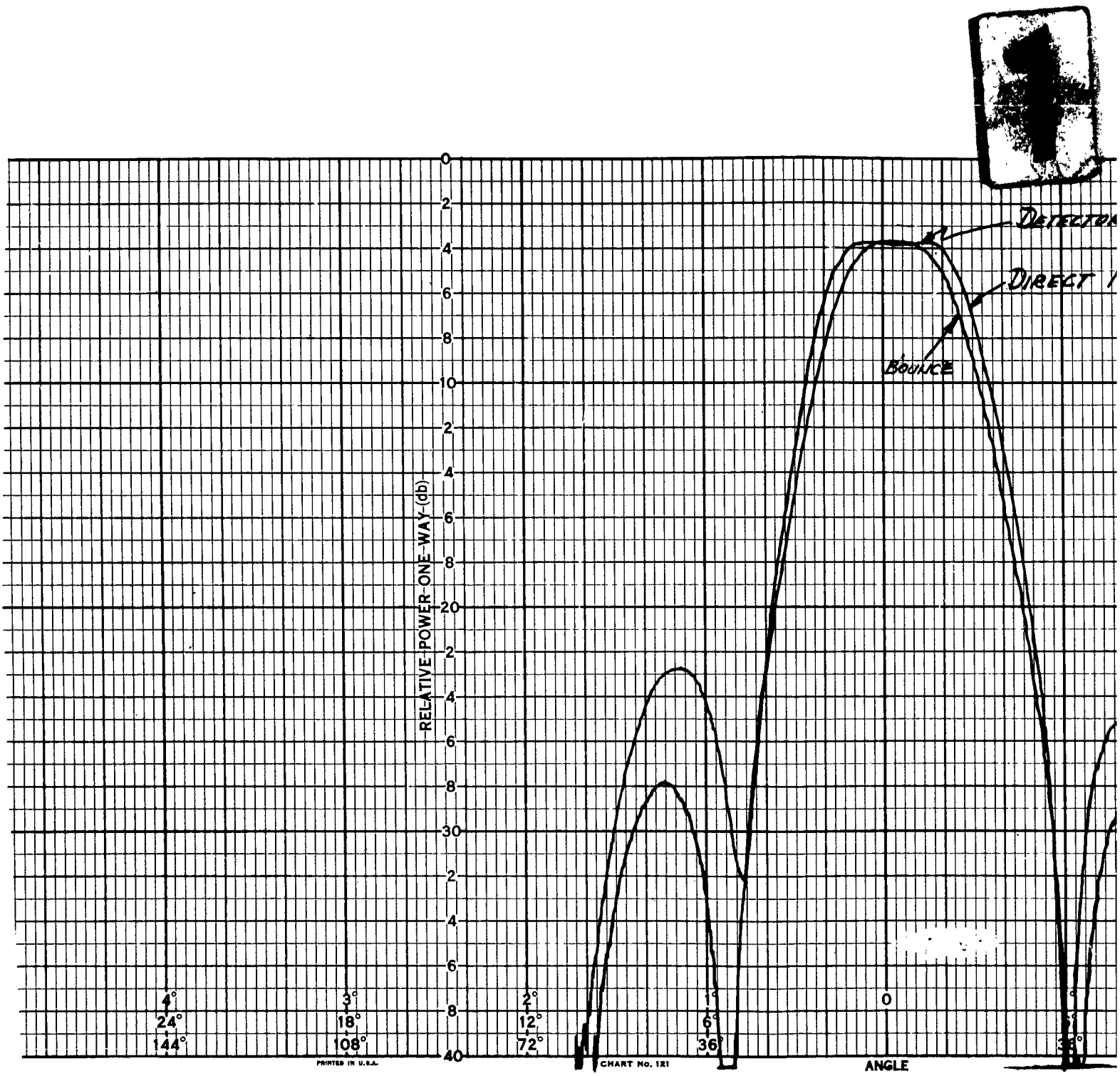
RELATIVE-POWER-ONE-WAY-(db)
0
2
4
6
8
10
2
4
6
8
20
2
4
6
8
30
2
4
6
8
40
4°
24°
144°
3°
18°
108°
2°
12°
72°
1°
6°
36°
0
1°
6°
36°
ANGLE
DIRECT
BOUNCE
PRINTED IN U.S.A.
CHART No. 121

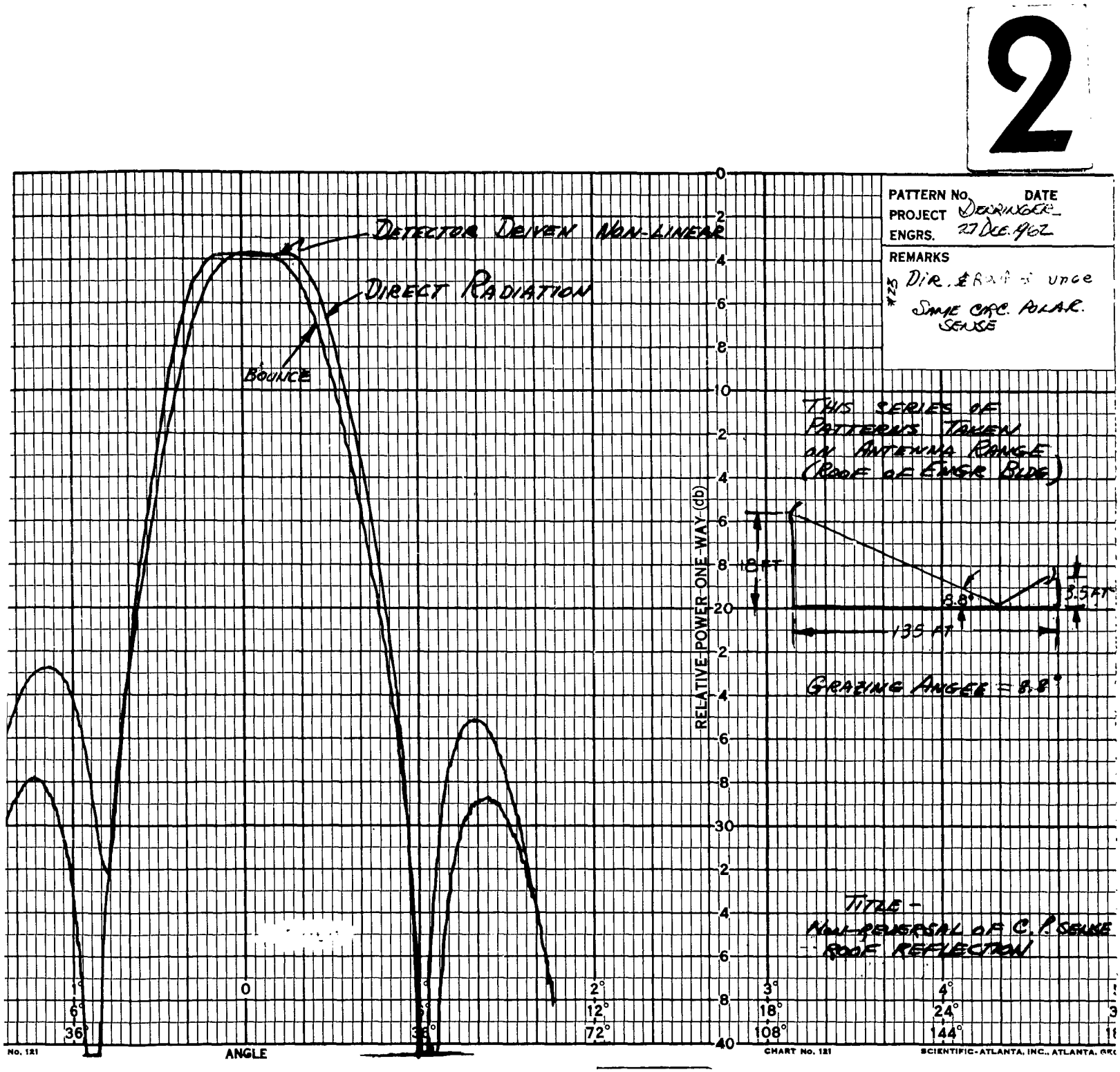

Figure 64. Roof Reflection Tests

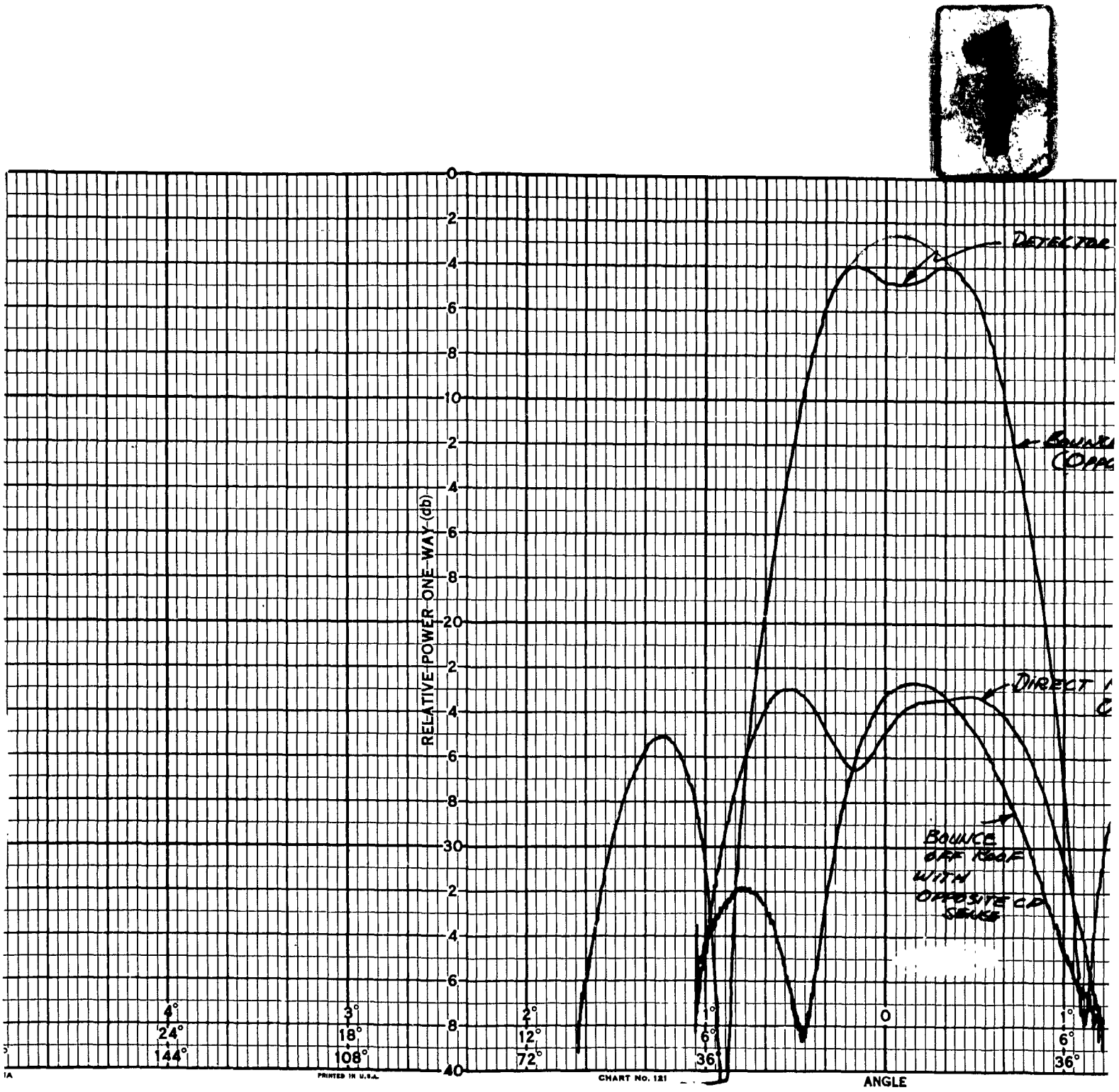
RELATIVE-POWER-ONE-WAY-(db)
0
2
4
6
8
10
2
4
6
8
20
2
4
6
8
30
2
4
6
8
40
4°
24°
144°
3°
18°
108°
2°
12°
72°
1°
6°
36°
0
1°
6°
36°
ANGLE
DIRECT
BOUNCE OFF ROOF WITH OPPOSITE CP SENSE
PRINTED IN U.S.A.
CHART NO. 121

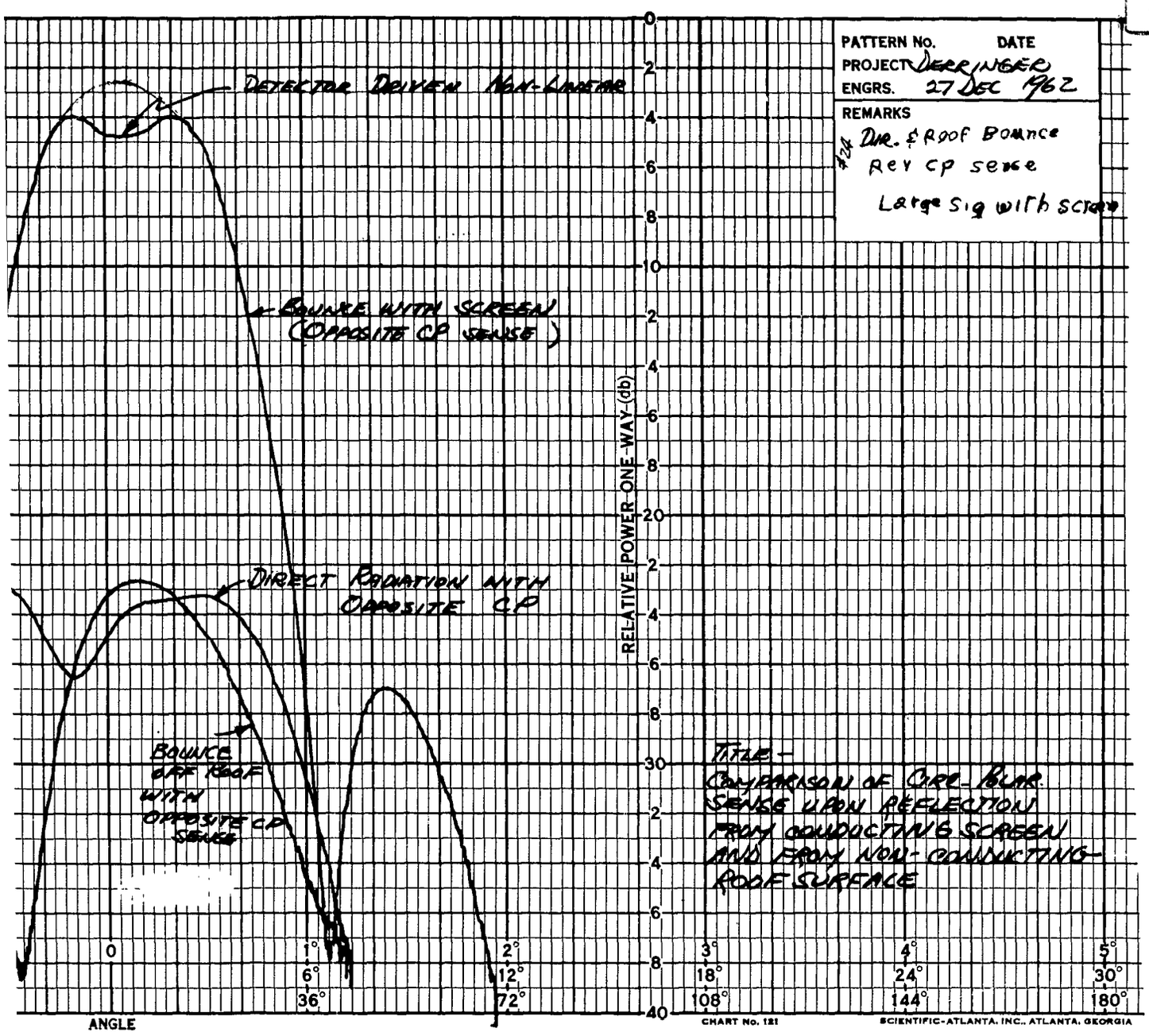

Figure 65. Roof Reflection Tests


Direct Radiation
Trans. & Rec.
Antenna Sample
CP Sensor
RELATIVE-POWER-ONE-WAY-(db)
0
2
4
6
8
10
2
4
6
8
20
2
4
6
8
30
2
4
6
8
40
4°
24°
144°
3°
18°
108°
2°
12°
72°
1°
6°
36°
ANGLE
PRINTED IN U.S.A.
CHART No. 121

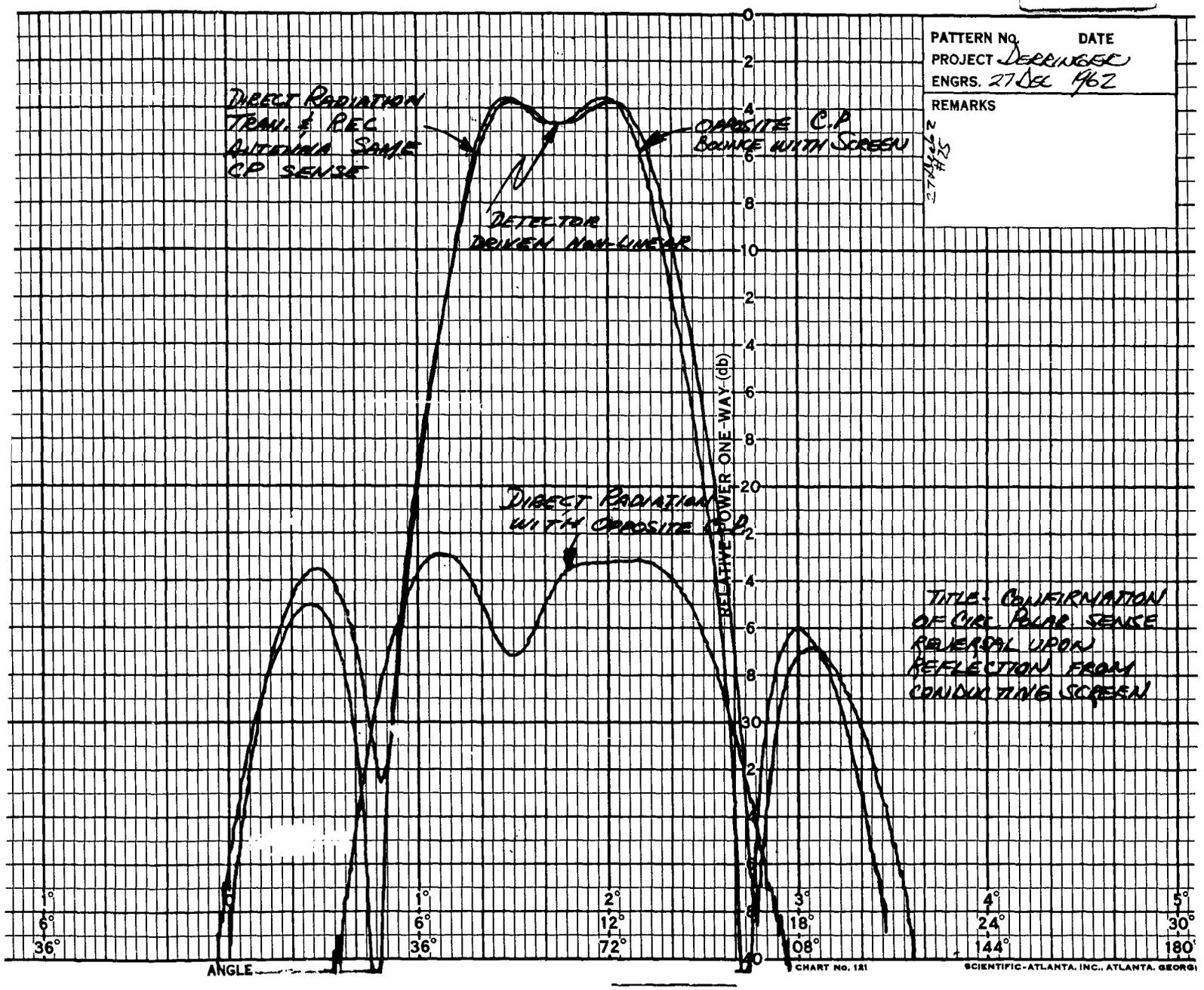

Figure 66. Roof Reflection Tests

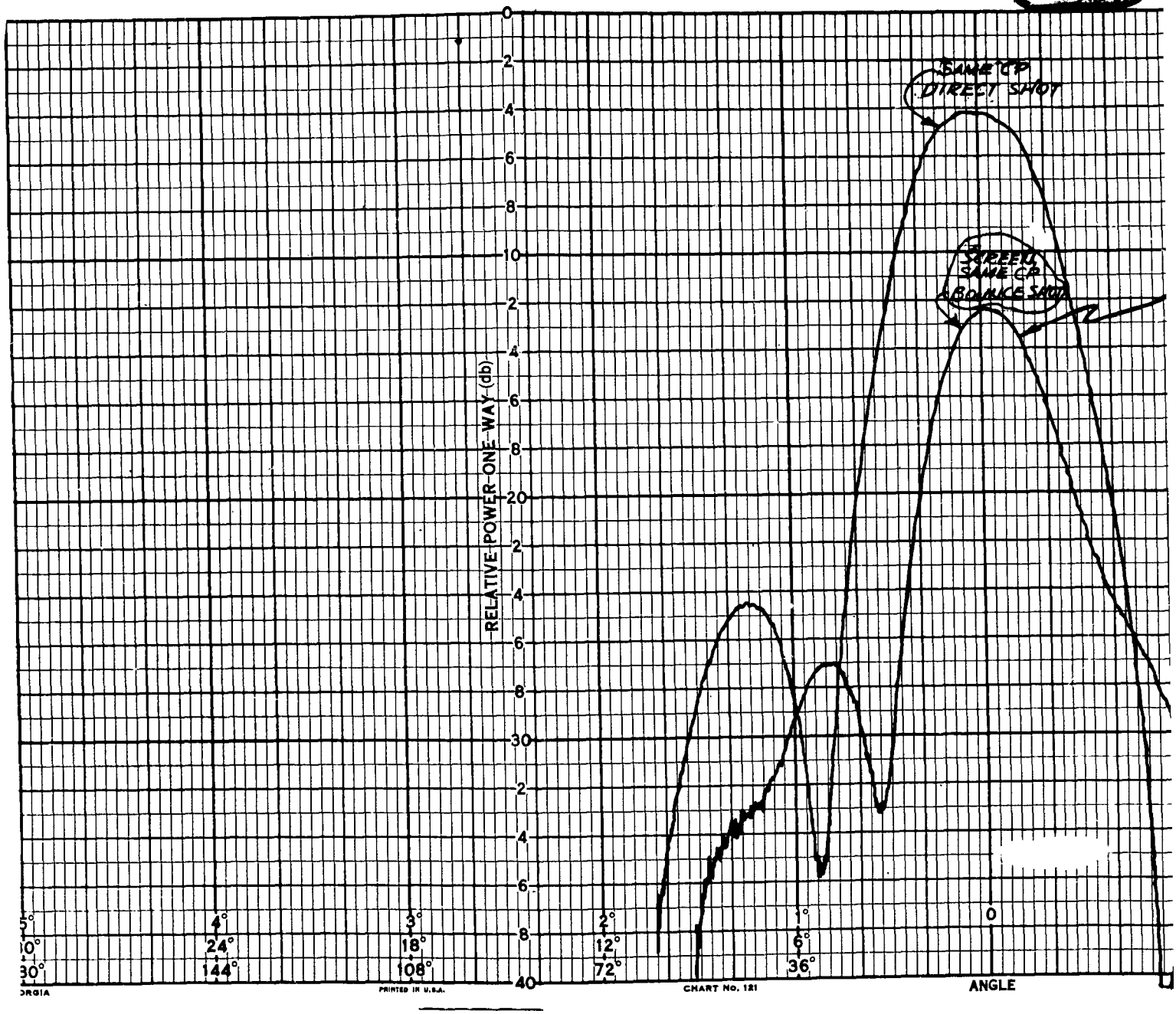
SAME AS DIRECT SHOT
STEELY SAWS CO BOUNCE SHOT
RELATIVE POWER-ONE-WAY (db)
0
2
4
6
8
10
2
4
6
8
20
2
4
6
8
30
2
4
6
8
40
5°
10°
30°
4°
24°
144°
3°
18°
108°
2°
12°
72°
1°
6°
36°
0
ANGLE
ORGIA
PRINTED IN U.S.A.
CHART No. 121

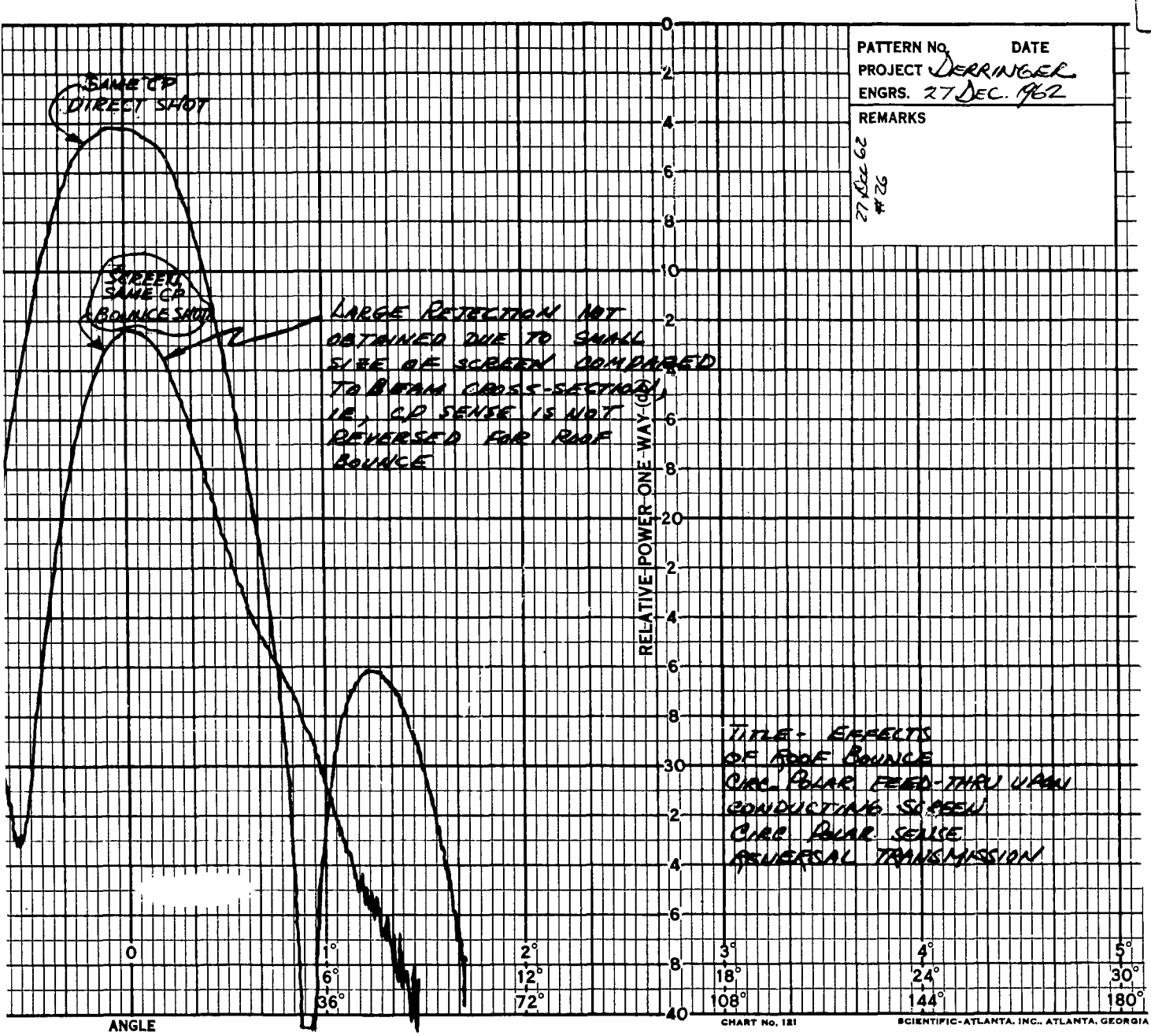

Figure 67. Roof Reflection Tests

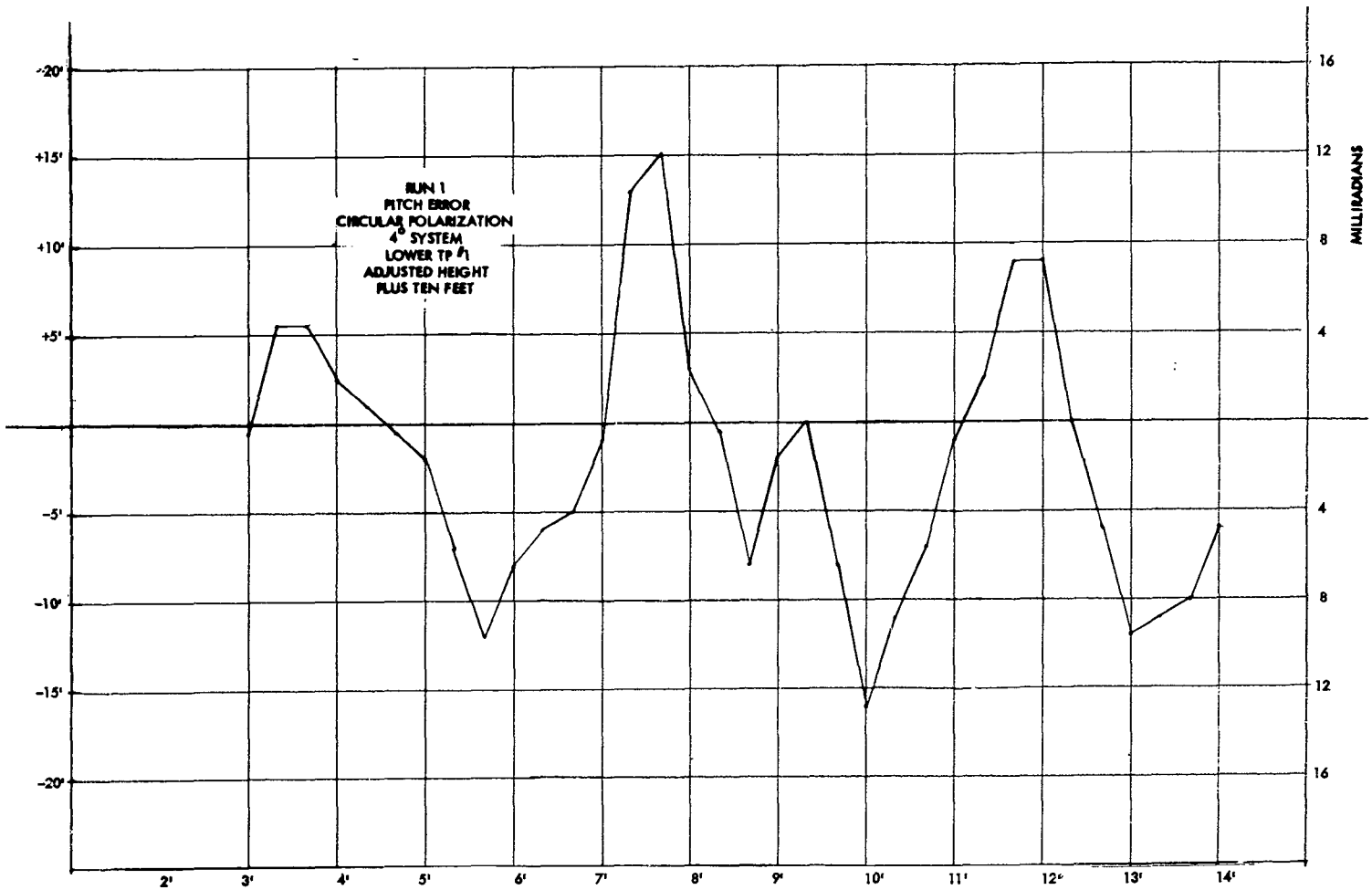

Figure 68. Intermediate Height Boresight Shift

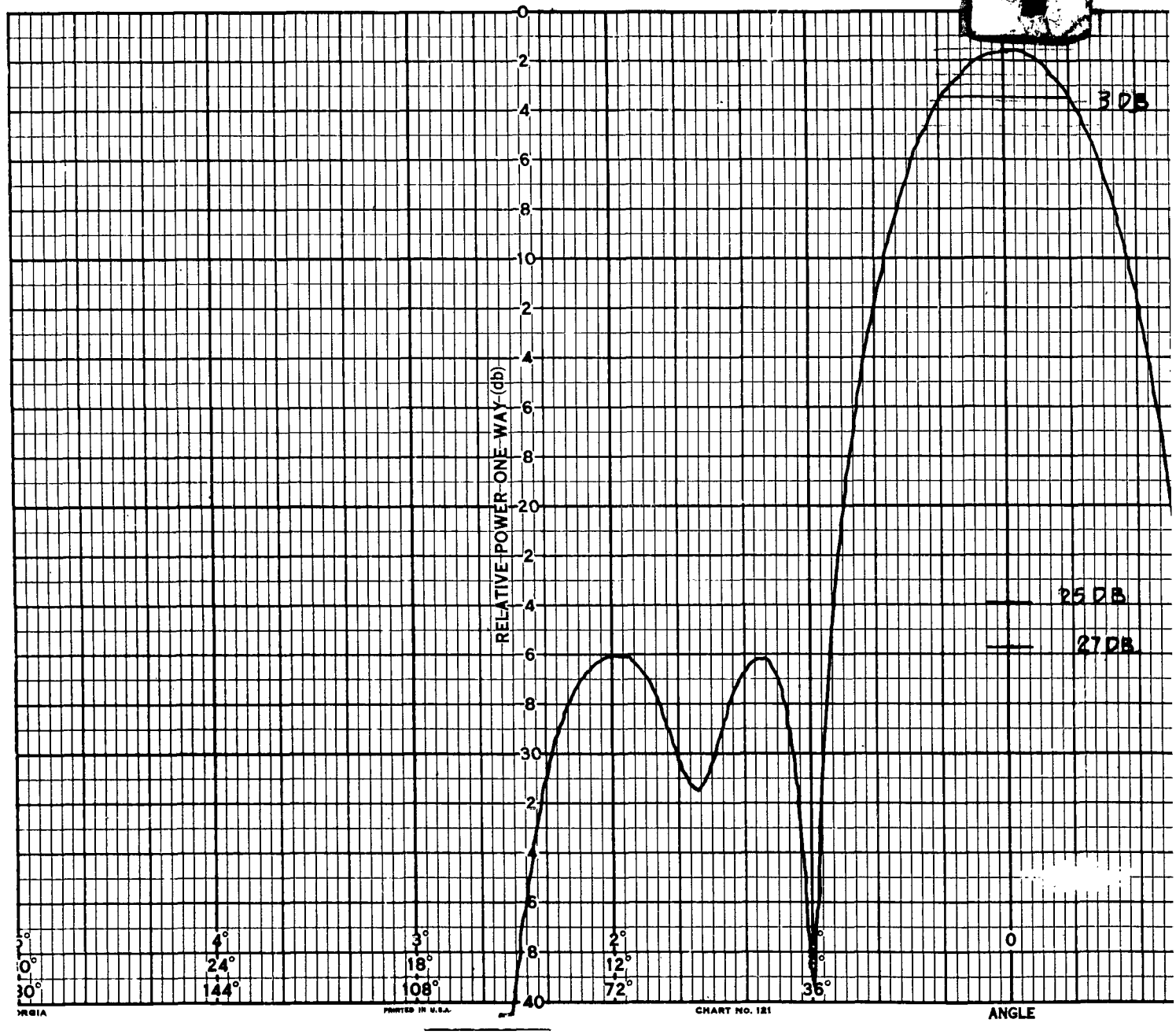
RELATIVE-POWER-ONE-WAY-(db)
0
2
4
6
8
10
2
4
6
8
20
2
4
6
8
30
2
6
8
40
3 DB
25 DB
27 DB
4°
24°
144°
3°
18°
108°
2°
12°
72°
1°
6°
36°
0
ANGLE
PRINTED IN U.S.A.
CHART NO. 121

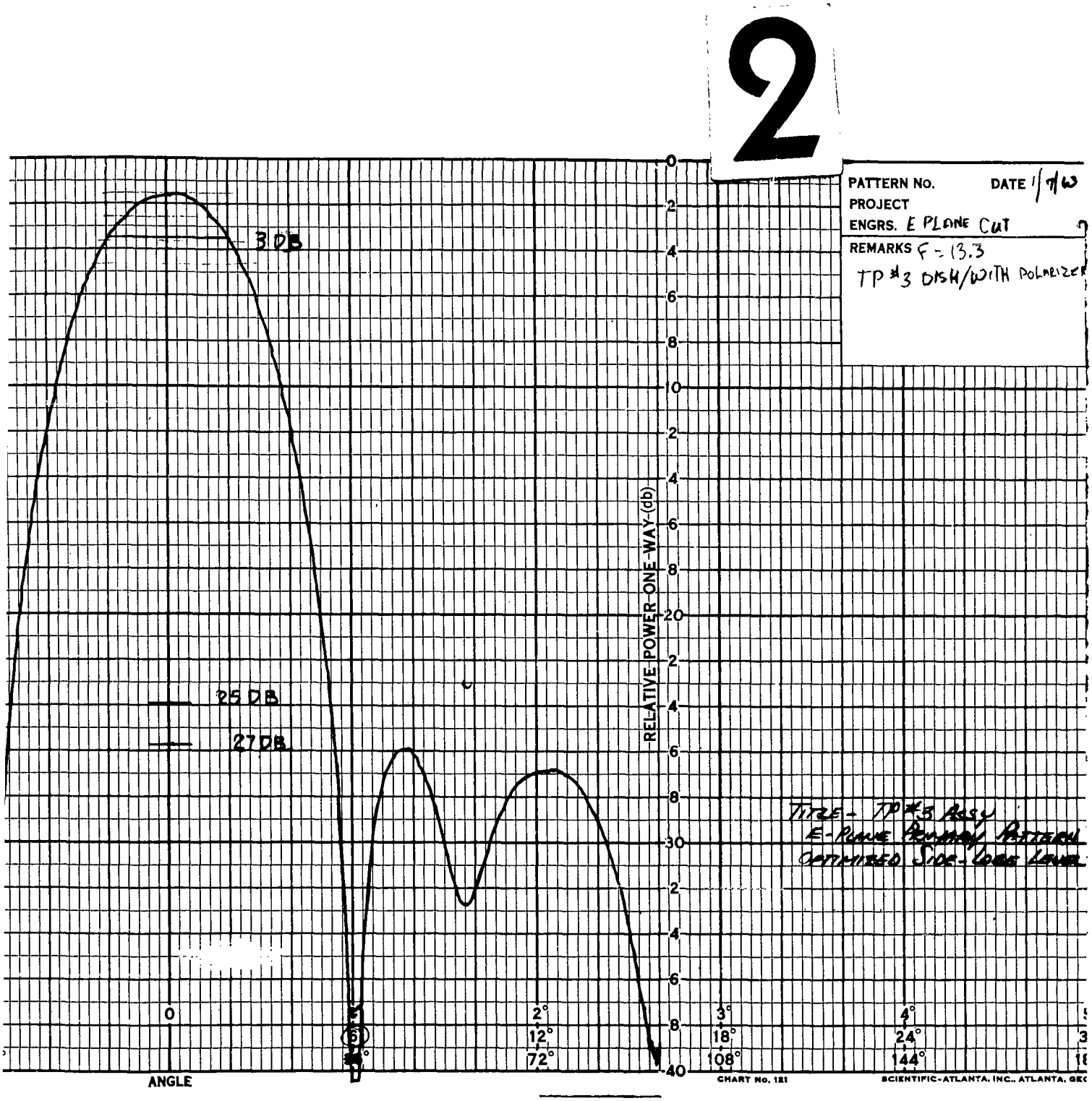

Figure 69. Test Point No. 3 Assembly Optimized Side Lobe Pattern

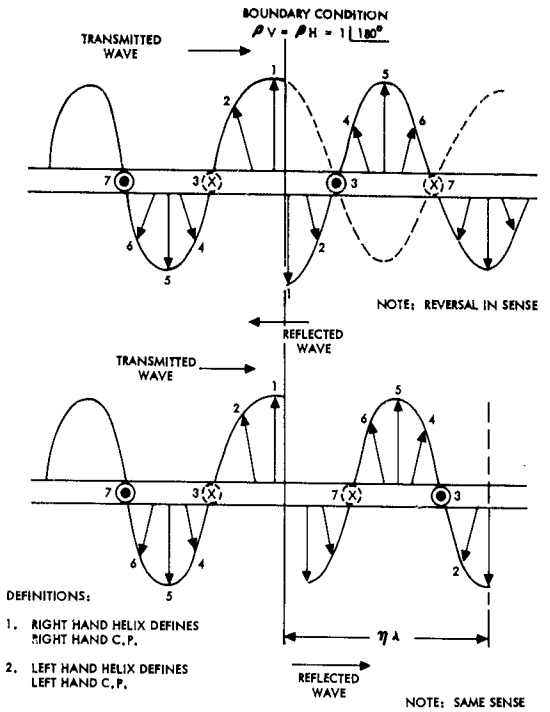

Figure 70. Wave Reflection Diagram

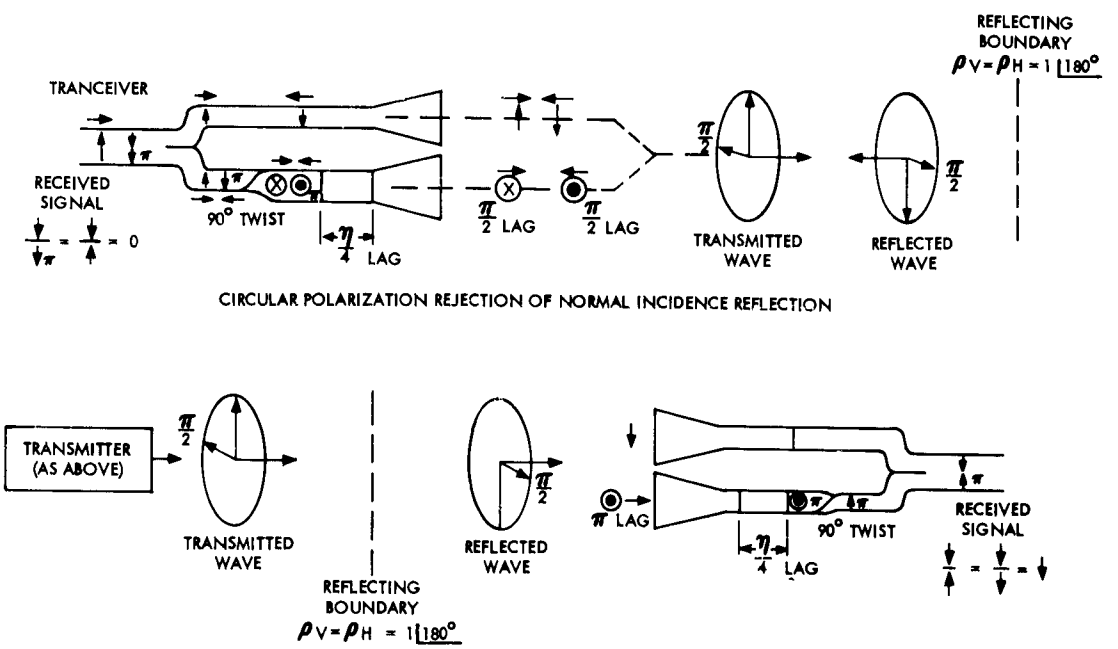

Figure 71. Acceptance and Rejection Diagram

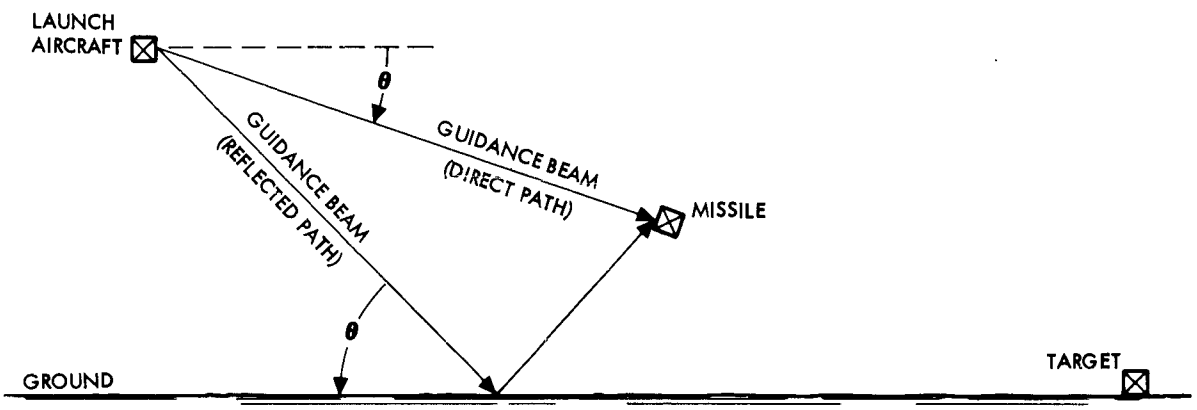

θ_o = LAUNCH ANGLE (APPROXIMATE GRAZING ANGLE AT IMPACT IF θ_o SMALL)

θ = INSTANTANEOUS GRAZING ANGLE

Figure 72. Guidance Geometry

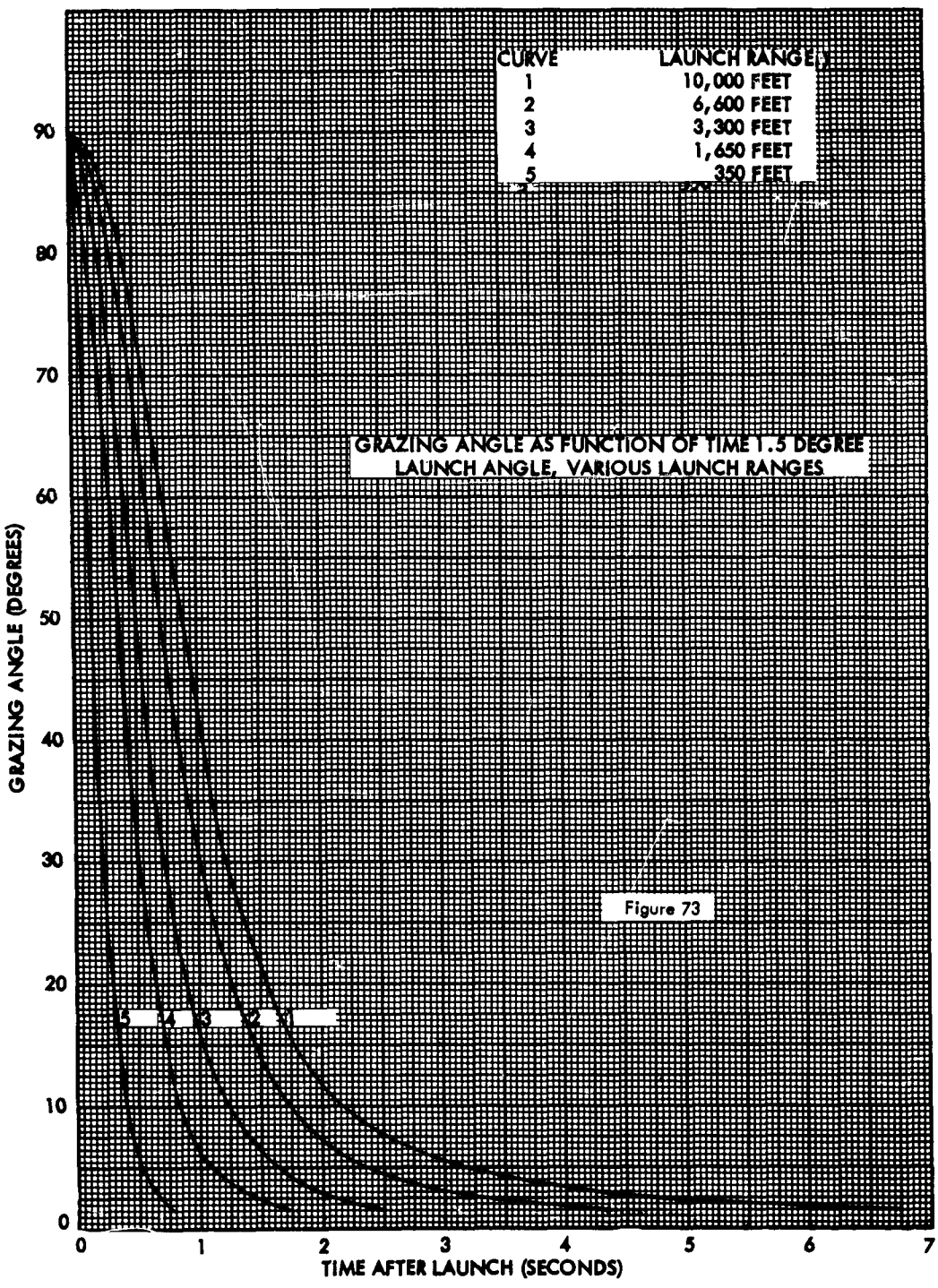

Figure 73. Grazing Angle vs. Time

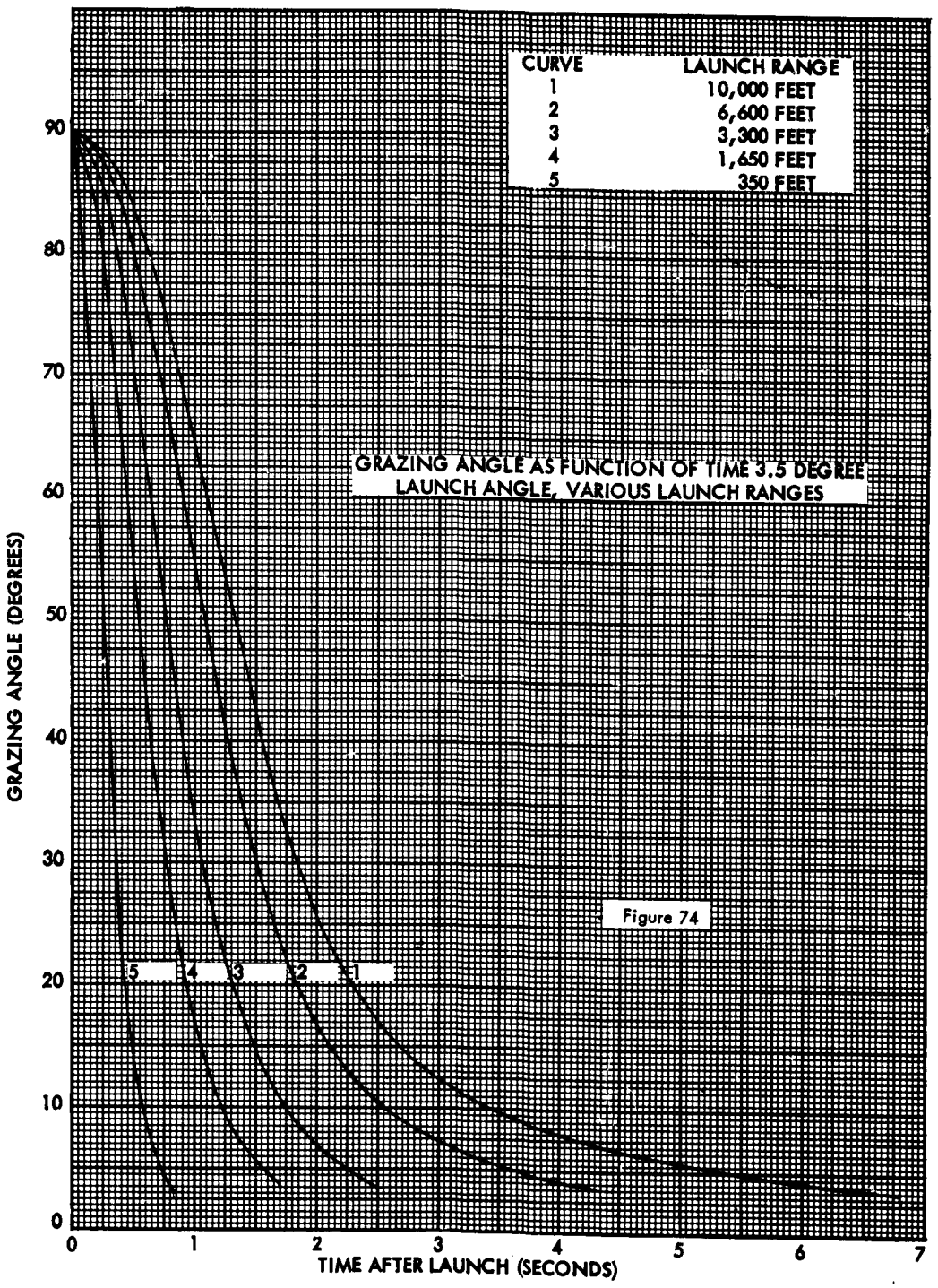

Figure 74. Grazing Angle vs. Time

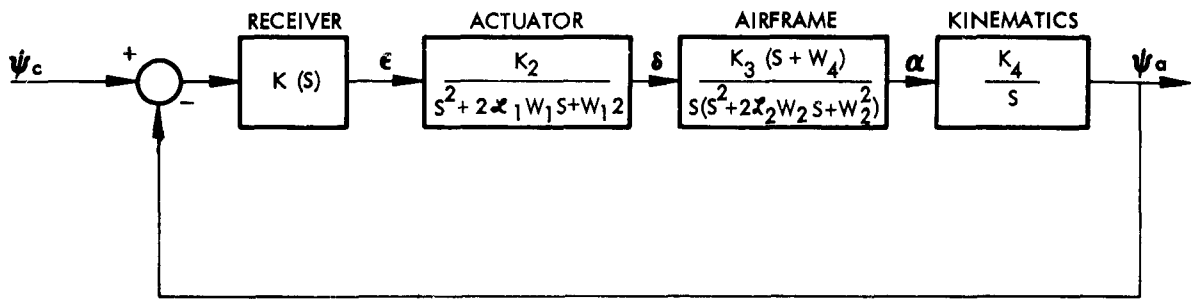

ψ_c = COMMAND ANGULAR POSITION OF MISSILE

ψ_a = ACTUAL ANGULAR POSITION OF MISSILE

ϵ = ERROR VOLTAGE

δ = CONTROL SURFACE DEFLECTION

α = BODY ANGLE OF ATTACK

NOTE: K (s) CONTAINS GUIDANCE LOOP SETTING

Figure 75. Derringer Guidance Loop Pitch Plane